THESIS APPROVAL

GRADUATE SCHOOL, KASETSART UNIVERSITY

Master of Engineering (Chemical Engineering)

DEGREE

Chemical Engineering	Chemical Engineering
FIELD	**DEPARTMENT**

TITLE: A Novel Systematic Approach to Synthesize of Flexible Heat and Mass Exchanger Networks

NAME: Miss Kanokkan Boontom

THIS THESIS HAS BEEN ACCEPTED BY

THESIS ADVISOR

(Associate Professor Thongchai Srinophakun, Ph.D.)

THESIS CO-ADVISOR

(Miss Wongphaka Wongrat, Ph.D.)

THESIS CO-ADVISOR

(Mr. Maythee Saisriyoot, Dr.techn.)

DEPARTMENT HEAD

(Associate Professor Apinya Duangchan, Ph.D.)

APPROVED BY THE GRADUATE SCHOOL ON _____

DEAN

(Associate Professor Gunjana Theeragool, D.Agr.)

THESIS

A NOVEL SYSTEMATIC APPROACH TO SYNTHESIZE OF FLEXIBLE HEAT AND MASS EXCHANGER NETWORKS

KANOKKAN BOONTOM

A Thesis Submitted in Partial Fulfillment of
the Requirements for the Degree of
Master of Engineering (Chemical Engineering)
Graduate School, Kasetsart University
2011

Kanokkan Boontom 2011: A Novel Systematic Approach to Synthesize of Flexible Heat and Mass Exchanger Networks. Master of Engineering (Chemical Engineering), Major Field: Chemical Engineering, Department of Chemical Engineering. Thesis Advisor: Associate Professor Thongchai Srinophakun, Ph.D. 138 pages.

In this research, flexible heat exchanger networks (HENs), mass exchanger networks (MENs), and combined heat and mass exchanger networks (CHAMENs) are focused. The mixed-integer nonlinear programming (MINLP) synthesis combining with nonlinear programming (NLP) feasibility test as a single optimization problem is presented. Furthermore, an optimal control design consisting of five steps is also proposed. The steps are 1) the optimal configuration is generated with a minimum total annual cost (TAC) and minimum slack variables, 2) the optimal configuration is simulated in Aspen Plus to guarantee the optimal target of networks, 3) the active constraint regions are formulated, 4) the optimal split-range control structure is determined by integer linear program (ILP) and 5) the control structure is dynamically tested. Five case studies are illustrated. Case study 1 from Thunyawart (2010) is the heat integration system with 7 process streams. Sweetening of COG process from El-Halwagi and Manousiouthakis (1989) is proposed as case study 2. Case study 3 from Fieg *et al.* (2009) is the large scale heat integration system with 15 process streams. Case study 4 is the sweetening of COG process with external utilities. In this case, hot and cold utilities are added to the process. Sweetening of COG process with simultaneous heat integration is shown in case study 5 where the heat integration system of case 1 is combined with the COG process of case 2. From the results, the proposed approach can obtain the lower total annual cost of the optimal configuration compared with literatures. For dynamics tests, all cases have the control performance structure to maintain all targets of network at the desired values.

/ /

Student's signature Thesis Advisor's signature

ACKNOWLEDGEMENTS

I would like to show appreciation to many people helping and supporting me for performing this thesis research. I would like to express my sincere gratitude to my advisor, Associate Professor Dr. Thongchai Srinophakun for his encouragement and valuable suggestions to this work. Appreciation is also extended to Dr. Wongphaka Wongrat, Dr. Maythee Saisriyoot, Dr. Veerayut Lersbamrungsuk and Assistant Professor Dr. Anusith Thanapimmetha for being my kindly committee and giving me useful recommendations.

Acknowledgement is given to the National Center of Excellence for Petroleum, Petrochemical, and Advanced Material; Center for Advanced Studies in Industrial Technology, for supporting this research.

My sincere thank is also given to my parent and sister for their love and support. Without them, I could not complete this thesis. Thanks also to my friends and team in the Centre of Process Control and Operation (CPCO) at the Department of Chemical Engineering, Kasetsart University for their encouragement.

Kanokkan Boontom

May 2011

TABLE OF CONTENTS

Pages

LIST OF TABLES

LIST OF TABLES (Continued)

LIST OF FIGURES

LIST OF FIGURES (Continued)

LIST OF ABBREVIATIONS

CV	=	controlled variable
CHAMENs	=	combined heat and mass exchanger network(s)
DOF(s)	=	degree(s) of freedom
MENs	=	mass exchanger network(s)
HENs	=	heat exchanger network(s)
ILP	=	integer linear programming
LMTD	=	logarithmic mean temperature difference
NLP	=	nonlinear programming
MINLP	=	mixed-integer nonlinear programming
MPT	=	multi-parametric toolbox
MV	=	manipulated variable
NLP	=	nonlinear programming
RI	=	resilience index
TAC	=	total annual cost

Indices

i, r	=	hot/rich stream
j, s	=	cold/lean stream
k, km	=	superstructure stage
p	=	multi-periods limiting operating conditions

Sets

CP	=	cold process stream
HP	=	hot process stream
LP	=	lean process stream or MSA
LP(t)	=	lean process stream or MSA using tray column
LP(h)	=	lean process stream or MSA using packed column

LIST OF ABBREVIATIONS (Continued)

MP	=	set of a number of operating conditions
RP	=	rich process stream
ST, *STm*	=	superstructure stages

Parameters

b	=	intercept of equilibrium line
C	=	annual operating cost
$C(t)$	=	per stage annual cost of tray column
$C(h)$	=	per height annual cost of packed column
FCp	=	heat capacity flow rate
G	=	flow rate of rich stream
$K_y a$	=	overall mass transfer coefficient
$L^{(up)}$	=	upper bound on mass flow rate of lean stream
m	=	slope of equilibrium line
S	=	cross-sectional area of an exchange unit
$T^{(in)}$	=	inlet temperature of stream
$T^{(out)}$	=	outlet temperature of stream
$\Delta T_{\min}$	=	minimum approach temperature
U	=	overall heat transfer coefficient
$X^{(in)}$	=	inlet composition of lean stream
$X^{(out)}$	=	outlet composition of lean stream
$X^{(up)}$	=	upper bound composition of lean stream
$Y^{(in)}$	=	inlet composition of rich stream
$Y^{(out)}$	=	outlet composition of rich stream
$Y^{(up)}$	=	upper bound composition of rich stream

LIST OF ABBREVIATIONS (Continued)

Greek letters

Λ, Γ	=	large positive values
ε_{ij} , ε_{rs}	=	minimum composition difference between rich stream and lean stream

Variables

dt_{ijk}	=	temperature approach for match *i* and *j* in stage k
$dtcc_{s,km}$	=	temperature approach for matching of lean *s* and cold utility
$dthh_s$	=	temperature approach for matching of lean *s* and hot utility
$dtcu_i$	=	temperature approach for match *i* and cold utility
$dthu_j$	=	temperature approach for match *j* and hot utility
$dtmc_{js,km}$	=	temperature approach for match (*j*,*s*) at temperature location *km*
$dtmh_{is,km}$	=	temperature approach for match (*i*,*s*) at temperature location *km* = 1
g_{ijk}	=	flow rate of rich *i* that is connected to lean *j* in stage *k*
$gg_{rs,km}$	=	flow rate of rich *r* that is connected to lean *s* in stage *km*
H_{ijk}	=	height of in packed column (*i*, *j*, *k*)
$H_{rs,km}$	=	height of in packed column (*r*, *s*, *km*)
l_{ijk}	=	flow rate of lean *j* that is connected to rich *i* in stage *k*
$ll_{rs,km}$	=	flow rate of lean *s* that is connected to rich *r* in stage *km*
L_j	=	flow rate of lean process stream *j*
L_s	=	flow rate of lean process stream *s*
M_{ijk}	=	mass exchanged between rich stream *i* and lean stream *j* in stage *k*
$M_{rs,km}$	=	flow rate of rich *r* that is connected to lean *s* in stage *km*
Nst_{ijk}	=	number of trays in tray column (*i*, *j*, *k*)
$Nst_{rs,km}$	=	number of trays in tray column (*r*, *s*, *km*)
q_{ijk}	=	heat exchanged between streams *i* and *j* in stage *k*

LIST OF ABBREVIATIONS (Continued)

$qcc_{s,km}$	=	heat exchanged between lean stream *s* and cold utility in stage *km*
qcu_i	=	heat exchanged between stream *i* and cold utility
$qhh_{s,km}$	=	heat exchanged between lean stream *s* and hot utility in stage *km* =1
qhu_j	=	heat exchanged between stream *i* and hot utility
$qmh_{is,km}$	=	heat exchanged between hot and lean stream (*i*,*s*) in stage *km* = 1
sx_{ijk}	=	composition of the part of lean *j* that is connected to rich *i* in rich end of an exchanger in stage *k*
sy_{ijk}	=	composition of the part of rich *i* that is connected to lean *j* in lean end of an exchanger in stage *k*
t_{ik}	=	temperature of stream *i* at hot end of stage k
t_{jk}	=	temperature of stream *j* at hot end of stage k
tcc_{jk}	=	temperature of cold stream *j* at the next first stage *k*
$tcinu_j$	=	temperature of cold stream *j* at the first stage *k* =1
$tcoutu_j$	=	temperature of cold stream *j* at the next first stage *k*
thh_{ik}	=	temperature of hot stream *i* at the next last stage *k*
$thinu_i$	=	temperature of hot stream *i* at the last stage *k*
$thoutu_i$	=	temperature of hot stream *i* at the next last stage *k*
$ts_{s,km}$	=	temperature of lean stream *s* between each stage of superstructure
$tss_{s,km}$	=	temperature of lean stream *s* between each stage of superstructure
x_{jk}	=	composition of lean stream *j* in rich end of stage k
$x_{s,km}$	=	composition for lean stream *s* in rich end of stage *km*
$sx_{rs,km}$	=	composition for the part of lean stream *s* that is connected to rich *r* in the rich end of an exchanger in stage *km*
$sy_{rs,km}$	=	composition for the part of rich stream *r* that is connected to lean *s* in the lean end of an exchanger in stage *km*
y_{ik}	=	composition of rich stream *i* in rich end of stage *k*
$y_{r,km}$	=	composition for rich stream *r* in rich end of stage *km*
z_{ijk}	=	binary variable for existence of unit for match *i* and *j* in stage *k*

LIST OF ABBREVIATIONS (Continued)

$zcc_{s,km}$	=	binary variable to denote that cold utility exchanges heat with stream *s* in stage *km*
zcu_i	=	binary variable for existence of unit for match *i* and cold utility
$zhh_{s,km}$	=	binary variable to denote that hot utility exchanges heat with stream *s* in stage *km*
zhu_i	=	binary variable for existence of unit for match *j* and hot utility
$zm_{rs,km}$	=	binary variable to denote existence of match (*r*,*s*) in stage *km*
$zmh_{is,km}$	=	binary variable to denote existence of match (*i*,*s*) in stage *km*
$zmc_{js,km}$	=	binary variable to denote existence of match (*j*,*s*) in stage *km*

A NOVEL SYSTEMATIC APPROACH TO SYNTHESIZE OF FLEXIBLE HEAT AND MASS EXCHANGER NETWORKS

INTRODUCTON

Chemical processes commonly consist of many unit operations to achieve the target of the production. Moreover, for the best performance including cost effectiveness, the yield enhancement, energy efficiency, and pollution prevention of current processes in the chemical plants, hence, processes must be developed. Because the chemical process is an integrated system of interconnected units and streams, the concept of process integration that refers to process design, operation, and retrofitting is a powerful instrument in developing the current processes. The popular technique to integrate the process is the network synthesis e.g. heat exchanger networks (HENs), mass exchanger networks (MENs), and combined heat and mass exchanger networks (CHAMENs). Unfortunately, the network for the large-scale process is difficult to synthesize manually. Hence, this work is to synthesize the above-mentioned network conveniently via the optimization software called GAMS - General Algebraic Modeling System.

In addition, optimal operation for HENs, MENs and CHAMENs can be achieved at input constraint vertices. However, under the changes of operating conditions, optimal vertices could be affected and shifted. Hence, optimal manipulations of inputs are required. A promising procedure based on split-range control technique.

Split-range control is a simple technique that can handle constraint problems on manipulated variables (Marlin, 2000). In split-range control, more than one manipulated variables can be used to adjust one controlled output, that is, when one manipulated variable is saturated, the other will take over task of the saturated one. However, the objective here is focusing on the application of split-range control to implement optimal operation. Glemmestad *et al.* (1996) and Giovanini *et al.* (2003)

pointed out that in most cases optimal operation of HENs can be implemented using split-range control. A systematic procedure for finding an optimal split-range control structure of HENs can be found in Lersbamrungsuk *et al.* (2008).

This work develops a systematic approach of an optimal operation for HENs, MENs and CHAMENs, in a step-by-step as follows. Firstly, flexible HENs, MENs, and CHAMENs are synthesized by MINLP synthesis combining with NLP feasibility test as a single optimization problem to minimize the total annual cost (TAC) and minimum slack variables Secondly, we identify active constraint regions using parametric programming (e.g. with MPT toolbox Kvasnica *et al*. (2004)). Thirdly, an optimal control structure is generated using split-range control. Finally, we check an optimal control structure using Aspen Dynamics.

OBJECTIVES

To synthesize the flexible heat exchanger networks (HENs), mass exchanger networks (MENs), and combined heat and mass exchanger networks (CHAMENs), there are mixed-integer nonlinear programming (MINLP) synthesis combining with nonlinear programming (NLP) feasibility test as a single optimization problem.

Scopes of Work

1. Flexible heat exchanger networks (HENs), mass exchanger networks (MENs), and combined heat and mass exchanger networks (CHAMENs) are focused in this work.

2. Aspen Plus and Aspen Dynamics version 7 are used for validation of the proposed method.

3. The network synthesis is targeted on the minimum total annual cost and minimum slack variables.

Thesis Contributions

1. A systematic method for design and control of heat exchanger networks (HENs), mass exchanger networks (MENs), and combined heat and mass exchanger networks (CHAMENs).

2. To use this knowledge to apply in the other plants.

LITERATURE REVIEW

1. Theories

In this section, we propose the theories there consist of seven parts for using in this research as follows:

1.1 Synthesis of multi-period heat exchanger networks (Chen and Hung, 2007)

The stage-wise superstructure originally proposed by Yee *et al.* (1990) is applied to construct the network structure, for its suitability for formulating the simultaneous solution that involves the consideration of total utility consumption, the total number of matches and the total area of heat exchange units. A two-stage superstructure with two-hot and two-cold streams is illustrated in Figure 1.

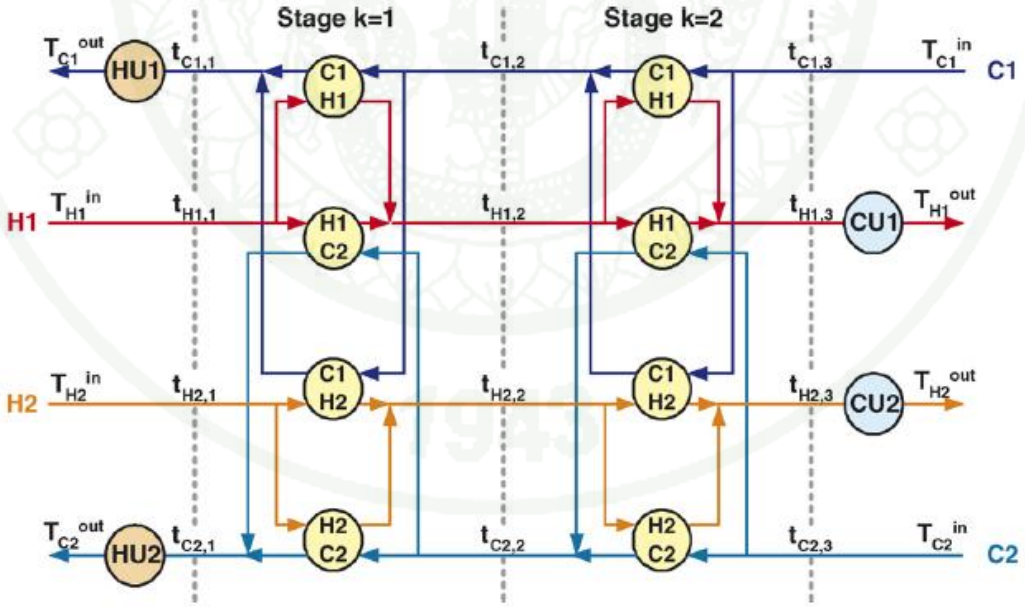

Figure 1 Illustration of two-stage superstructure with two-hot and two-cold streams for HENs synthesis

Source: Chen and Hung (2007)

Instead of directly considering all possible combinations of uncertain input temperatures and heat capacity flow rates for the flexible network synthesis, only a finite number of possible operating conditions are taken into account for network design to reduce the searching space. The mathematical programming formulation as shown in equation 1 for minimizing the total annual cost, TAC, which includes the first term is average costs of the hot and cold utility consumptions over a finite number of operating points and the next three terms are the annual costs of installation and material of the heat exchange units, can be summarized as follows (Biegler *et al*., 1997; Chen and Hung, 2005a; Yee *et al*., 1990):

$$\min TAC = \frac{1}{N_p + 1}\left(\sum_{p \in MP} \sum_{i \in HP} C_{cu} qcu_i^p + \sum_{p \in MP} \sum_{j \in CP} C_{hu} qhu_j^p \right) + \sum_{i \in HP} \sum_{j \in CP} \sum_{k \in ST} C_{ij} A_{ijk}^{\beta_{ij}} + \sum_{i \in HP} C_{i,cu} A_{i,cu}^{\beta_{i,cu}} + \sum_{j \in CP} C_{hu,j} A_{j,hu}^{\beta_{j,hu}} \quad (1)$$

where

$$A_{ijk} \geq \frac{q_{ijk}^p}{U_{ij}\left[dt_{ijk}^p dt_{ij,k+1}^p \left(dt_{ijk}^p + dt_{ij.k+1}^p\right)/2\right]^{1/3}}$$

$$A_{i,cu} \geq \frac{qcu_i^p}{U_{i,cu}\left[dtcu_i^p \left(T_i^{(out)} - T_{cu}^{(in)}\right)\left(dtcu_i^p + T_i^{(out)} - T_{cu}^{(in)}\right)/2\right]^{1/3}}$$

$$A_{hu,j} \geq \frac{qhu_j^p}{U_{hu,j}\left[dthu_j^p \left(T_{hu}^{(in)} - T_j^{(out)}\right)\left(dthu_j^p + T_{hu}^{(in)} - T_j^{(out)}\right)/2\right]^{1/3}}$$

$$A_{ijk}, A_{i,cu}, A_{hu,j} \geq 0$$

Constraint 1: *Overall heat balance for each stream*

This constraint is needed to ensure sufficient heating or cooling of each process stream. The constraints specify that the overall heat transfer requirement of each stream must equal to the sum of the heat it exchanges with other process streams at each stage plus the exchange with the utilities streams.

$$\left(T_i^{(in)p} - T_i^{(out)p}\right) FCp_i^p = \sum_{k \in ST} \sum_{j \in CP} q_{ijk}^p + qcu_i^p \quad (2)$$

$$\left(T_j^{(out)p} - T_j^{(in)p}\right) FCp_j^p = \sum_{k \in STi \in HP} \sum q_{ijk}^p + qhu_j^p \quad (3)$$

$$q_{ijk}^p, qcu_i^p, qhu_j^p \geq 0$$

Constraint 2: *Heat balance at each stage*

An energy balance is also needed at each stage of the superstructure to determine the temperatures. Temperatures for the streams are highest at temperature location k = 1 and lowest at last temperature location k = 3.

$$\left(t_{ik}^p - t_{i,k+1}^p\right) FCp_i^p = \sum_{j \in CP} q_{ijk} \quad (4)$$

$$\left(t_{jk}^p - t_{j,k+1}^p\right) FCp_j^p = \sum_{i \in HP} q_{ijk} \quad (5)$$

$$t_{ik}^p, t_{jk}^p, t_{i,k+1}^p, t_{j,k+1}^p \geq 0$$

Constraint 3: *Assignment of superstructure inlet temperatures*

Fixed supply temperatures of the process streams are assigned as the inlet temperatures to the superstructure. In Figure 1, for hot streams the superstructure inlet corresponds to temperature location k = 1, while the cold streams, the inlet corresponds to location k = 3.

$$t_{i1}^p = T_i^{(in)p}, \; t_{i,N_T+1}^p = T_j^{(in)p} \quad (6)$$

Constraint 4: *Feasibility of temperatures*

Constraints are also needed to specify a monotonic decrease of temperature at each successive stage. In addition, a bound is set for the outlet temperatures of the superstructure at the specific stream's target temperature. Note that the temperature of each stream at its last stage does not necessarily correspond to the stream's target temperature since utility exchanges can occur at the outlet of the superstructure.

$$t_{ik}^{p} \geq t_{i,k+1}^{p} \tag{7}$$

$$t_{jk}^{p} \geq t_{j,k+1}^{p} \tag{8}$$

$$T_{i}^{(out)} \leq t_{i,N_T+1}^{p} \tag{9}$$

$$T_{j}^{(out)} \geq t_{j1}^{p} \tag{10}$$

Constraint 5: *Hot and cold utility load*

Hot and cold utility requirements are determined for each process stream in terms of the outlet temperature in the last stage and the target temperature for that stream. The utility heat load requirements are determined as follows:

$$\left(t_{i,N_T+1}^{p} - T_{i}^{(out)p}\right) FCp_{i}^{p} = qcu_{i}^{p} \tag{11}$$

$$\left(T_{j}^{(out)p} - t_{j1}^{p}\right) FCp_{j}^{p} = qhu_{j}^{p} \tag{12}$$

Constraint 6: *Logical constraints*

Logical constraints and binary variables are needed to determine the existence of process match between streams *i,j* in stage *k* and also any match involving utility streams. The binary variables, 0-1, are represented by z_{ijk} for process stream matches, zcu_i and zhu_j for matches involving cold and hot utility, respectively. An integer value of one for any binary variable designates that the match is presented in the optimal network.

$$q_{ijk}^{p} - \Lambda_{ij} z_{ijk} \leq 0 \tag{13}$$

$$qcu_{i}^{p} - \Lambda_{i} zcu_{i} \leq 0 \tag{14}$$

$$qhu_{j}^{p} - \Lambda_{j} zhu_{j} \leq 0 \tag{15}$$

$$z_{ijk}, zcu_{i}, zhu_{j} \in \{0,1\}$$

Constraint 7: *Calculation of approach temperatures*

The area requirement of each match will be incorporated in the objective function. Calculation of these areas requires that approach temperatures be determined. To ensure feasible driving forces for exchangers that are selected in the optimization procedure, the binary variables are used to activate or deactivate the following constraints. Nevertheless, the approach temperature between the hot and cold streams at any point of any exchangers will be at least $\Delta T_{\min}$.

$$dt_{ijk}^{p} \le t_{ik}^{p} - t_{jk}^{p} + \Gamma_{ij}\left(1 - z_{ijk}\right) \tag{16}$$

$$dt_{ij,k+1}^{p} \le t_{i,k+1}^{p} - t_{j,k+1}^{p} + \Gamma_{ij}\left(1 - z_{ijk}\right) \tag{17}$$

$$dtcu_{i}^{p} \le t_{i,N_T+1}^{p} - T_{cu}^{(out)} + \Gamma_{i}\left(1 - zcu_{i}\right) \tag{18}$$

$$dthu_{j}^{p} \le T_{hu}^{(out)} - t_{j1}^{p} + \Gamma_{j}\left(1 - zhu_{j}\right) \tag{19}$$

$$dt_{ijk}^{p}, dt_{ij,k+1}^{p}, dtcu_{i}^{p}, dthu_{j}^{p} \ge \Delta T_{\min} \tag{20}$$

$$dt_{ijk}^{p}, dt_{ij,k+1}^{p}, dtcu_{i}^{p}, dthu_{j}^{p} \ge 0$$

1.2 Synthesis of multi-period mass exchanger networks (Chen and Hung, 2007)

The stage-wise superstructure for MENs is applied to construct the network structure, for it is also suitable for formulation of the simultaneous solution that involves the consideration of the total consumption of mass separating agents, the total number of stream matches and the total size of mass exchange units (Chen and Hung, 2005b, 2005c; Szitkai *et al.*, 2003). A two-stage superstructure with two-rich and two-lean streams is shown in Figure 2.

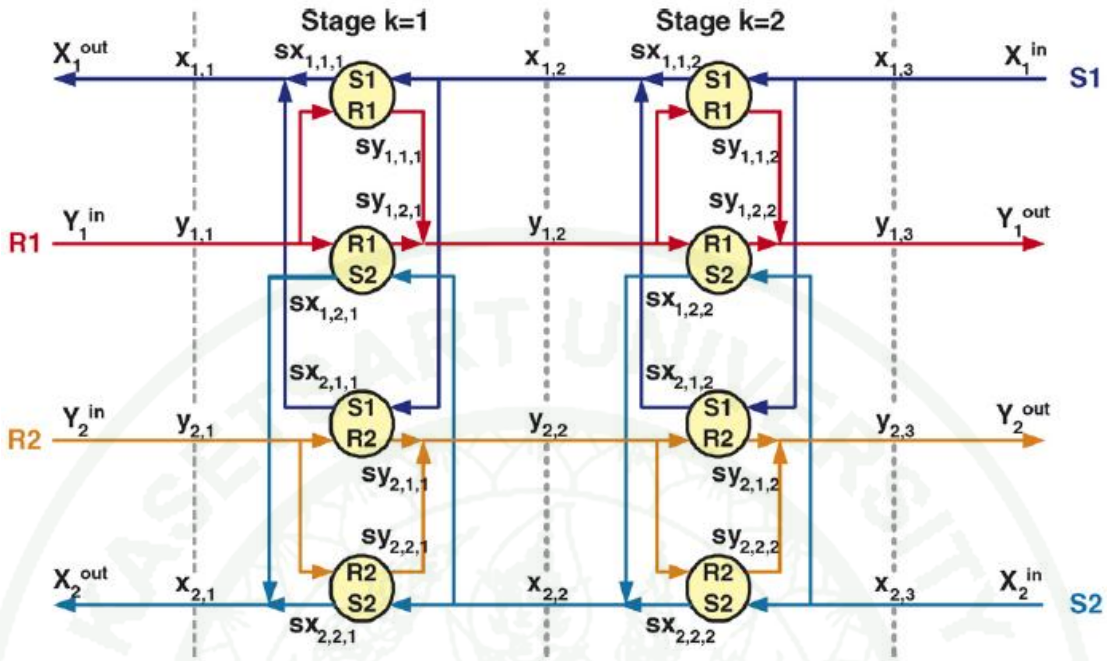

Figure 2 Illustration of two-stage superstructure with two-rich and two-lean streams for MENs synthesis

Source: Chen and Ping (2007)

A finite number of operating points are simultaneously taken into account for MEN synthesis. The mathematical programming formulation to minimize the total annual cost, TAC, that the first term is average costs of external mass separating agents over a finite number of operating points and the next two terms are annual costs of installation and material of the mass exchange units, can be summarized as follows:

$$\min TAC = \frac{1}{N_p + 1} \sum_{j \in LP} C_j L_j^p + \sum_{i \in RP} \sum_{j \in LP^{(t)}} \sum_{k \in ST} C_{ij}^{(t)} Nst_{ijk} + \sum_{i \in RP} \sum_{j \in LP^{(h)}} \sum_{k \in ST} C_{ij}^{(h)} H_{ijk} \quad (21)$$

Mass exchanger can be classified into two main categories: stage-wise exchangers and continuous-contact exchangers. The common types of stage-wise

exchangers are tray or plate columns, and for continuous-contact exchangers are packed towers. When mass exchange takes place in a tray column, the number of required stages must be determined from the Kremser equation. Thus, the log-mean Kremser equation for stage numbers can be formulated as follows:

$$Nst_{ijk} \geq \left[\frac{\left(y_{ik}^{p} - sy_{ijk}^{p}\right)^{0.3275} + \left(sy_{ijk}^{*p} - y_{ij,k+1}^{*p}\right)^{0.3275}}{\left(dyxi_{ijk}^{p}\right)^{0.3275} + \left(dyxo_{ijk}^{p}\right)^{0.3275}} \right]^{1/0.3275}$$

When absorption or stripping takes place, a continuous-contact packed towers is suggested for mass exchange. The required packed height for *i*,*j* match in stage *k* for separation is characterized by a number of imaginary transfer units, Nst_{ijk}, and the overall height of a transfer unit, H_{ijk}. The overall packed height is given by the following equation, where the log-mean calculation is also applied from Chen's approximation and the smooth approximation method.

$$H_{ijk} \geq \frac{M_{ijk}^{p}}{k_y aS} \times \left[\frac{\left(dyxi_{ijk}^{p}\right)^{0.3275} + \left(dyxo_{ijk}^{p}\right)^{0.3275}}{2} \right]^{1/0.3275}$$

$$Nst_{ijk}, H_{ijk} \geq 0$$

where $y_{ij,k+1}^{*p} = m_{ij} x^{p}{}_{j,k+1} + b_{ij}$ and $sy_{ij,k+1}^{*p} = m_{ij} sx^{p}{}_{ijk} + b_{ij}$ are equilibrium composition

Constraint 1*: Overall mass balance over the whole network*

An overall mass balance is needed to ensure sufficient exchange of any transferred components for all rich streams. The constraints specify that the overall mass transferable requirement of each rich stream must be equal to the sum of mass which is exchanged with other lean process streams or MSAs at each stage. Similar constraints also apply for all lean streams, as stated in the following.

$$\left(y_{i1}^{p} - y_{i,N_s+1}^{p}\right) G_i^{p} = \sum_{k \in ST} \sum_{j \in LP} M_{ijk}^{p} \qquad (22)$$

$$\left(x_{j1}^{p} - X_{j,N_s+1}^{p}\right)L_j^p = \sum_{k\in ST}\sum_{i\in RP} M_{ijk}^{p} \tag{23}$$

$$y_{ik}^{p}, x_{jk}^{p}, G_i^p, L_j^p, M_{ijk}^{p} \geq 0$$

Constraint 2*: Mass balance in each stage*

These constraints are also needed to determine the composition of the transferable component as well as partition of flow rates for all parallel units. The composition location $k = 1$ involves the highest composition. The component and total mass balance for each stream in each stage are as follows:

$$\left(y_{ik}^{p} - y_{i,k+1}^{p}\right)G_i^p = \sum_{j\in LP} M_{ijk}^{p} \tag{24}$$

$$\left(x_{jk}^{p} - X_{j,k+1}^{p}\right)L_j^p = \sum_{ij\in RP} M_{ijk}^{p} \tag{25}$$

$$G_i^p = \sum_{j\in LP} g_{ijk}^{p} \tag{26}$$

$$L_j^p = \sum_{j\in RP} \ell_{ijk}^{p} \tag{27}$$

$$g_{ijk}^{p}, \ell_{ijk}^{p} \geq 0$$

Constraint 3*: Mass balance in each exchange unit*

For the exchange unit between rich stream i and lean stream j in stage k, the compositions before mixers, sy_{ijk}^{p} and sx_{ijk}^{p} are defined. A component mass balance is needed for each local exchange unit, where g_{ijk}^{p} and ℓ_{ijk}^{p} are split mass flow rates.

$$g_{ijk}^{p}\left(y_{ik}^{p} - sy_{ijk}^{p}\right) = M_{ijk}^{p} \tag{28}$$

$$\ell_{ijk}^{p}\left(sx_{ijk}^{p} - x_{j,k+1}^{p}\right) = M_{ijk}^{p} \tag{29}$$

$$y_{i,k+1}^{p}, x_{j,k+1}^{p}, sy_{ijk}^{p}, sx_{ijk}^{p} \geq 0$$

Constraint 4*: Assignment of superstructure inlet/outlet compositions*

The given inlet/outlet compositions of the rich and lean streams are assigned as the inlet/outlet compositions to the superstructure. For rich streams, the superstructure inlet corresponds to composition location $k = 1$. While for lean streams, the inlet corresponds to location $k = N_S + 1$.

$$Y_i^{p(in)} = y_{i1}^p,\ X_j^{p(in)} = x_{j,N_s+1}^p \tag{30}$$

$$Y_i^{p(out)} = y_{i,N_s+1}^p,\ x_{j1}^p \le X_j^{(up)} \tag{31}$$

$$X_j^{p(out)} = x_{j1}^p,\ y_{i,N_s+1}^p \le Y_i^{(up)} \tag{32}$$

$$L_j^p \le L_j^{(up)} \tag{33}$$

Constraint 5*: Feasibility of the transferable component*

Constraints are also needed to guarantee monotonic decrease of all compositions at successive stages.

$$y_{ik}^p \ge y_{i,k+1}^p \tag{34}$$

$$x_{jk}^p \ge x_{j,k+1}^p \tag{35}$$

Constraint 6*: Logical constraints*

Logical constraints and binary variables, z_{ijk}, are needed to determine the existence of process match between streams *i*,*j* in stage *k*. An integer value of 1 for binary variable z_{ijk} designates that the match between rich stream *i* and lean stream *j* in stage *k* is presented in the optimal network. z_{ijk} is zero if the match (*i*, *j*) in stage *k* is absent, and thus the mass load M_{ijk}^p also becomes zero.

$$M_{ijk}^p - U_{ij}^p z_{ijk} \le 0 \tag{36}$$

$$z_{ijk} \in \{0,1\}$$

Constraint 7*: Feasibility constraints of the equilibrium relationships*

The feasibility constraints of the equilibrium relationships ensure positive driving forces for the potential process exchange units. Binary variables are used to

activate or deactivate the following constraints. If a match does not occur, the associated binary variable equals zero and the large positive upper bound Γ_{ij}^{p} is remained. In these equations, a minimum composition approach ε_{ij} is also chosen so that feasible mass transfer in a finite number of equilibrium stages or finite area can be achieved in each transfer unit.

$$dyxi_{ijk}^{p} \le y_{ik}^{p} - m_{ij} sx_{ijk}^{p} - b_{ij} + \Gamma_{ij}^{p}\left(1 - z_{ijk}\right) \tag{37}$$

$$dyxo_{ijk}^{p} \le sy_{ijk}^{p} - m_{ij} sx_{j,k+1}^{p} - b_{ij} + \Gamma_{ij}^{p}\left(1 - z_{ijk}\right) \tag{38}$$

$$dyxi_{ijk}^{p}, dyxo_{ijk}^{p} \ge m_{ij}\varepsilon_{ij}$$

$$dyxi_{ijk}^{p}, dyxo_{ijk}^{p} \ge 0$$

1.3 Flexibility test for heat exchanger networks (Chen and Hung, 2007)

According to the resulting multi-period heat exchange network configuration from Section 1.1, the calculation of temperature difference around all matched units in each period is examined to ensure feasible driving force for all units. They apply binary parameters z_{ijk}^{p}, zcu_{i}^{p} and zhu_{j}^{p} to denote the existence of units in the superstructure for current network when executing the simplified flexibility analysis. Then, the z_{ijk}^{p} value is assigned to be one when the (i, j) match at stage k is existing, otherwise the value is zero. The relations concerned with approach temperatures are, respectively, multiplied with the given binary parameters z_{ijk}^{p}, zcu_{i}^{p} and zhu_{j}^{p} for relaxing the equality constraints for those units that are not existent in the candidate network. A lot of testing points $p \in MP$ randomly distributed within the uncertain parametric domain are then applied to examine if the current network structure can be accepted. For those existing units, slack variables, sdt_{ijk}^{p}, $sdtcu_{i}^{p}$ and $sdthu_{j}^{p}$ are used for measuring the violation of approach temperatures (Aaltola, 2003), where the units area are not considered temporarily to simplify the flexibility test.

$$z_{ijk}^{p}\left(dt_{ijk}^{p}-\left(t_{ik}^{p}-t_{jk}^{p}+sdt_{ijk}^{p}\right)\right)=0 \quad (39)$$

$$z_{ij,k+1}^{p}\left(dt_{ij,k+1}^{p}-\left(t_{i,k+1}^{p}-t_{j,k+1}^{p}+sdt_{ij,k+1}^{p}\right)\right)=0 \quad (40)$$

$$zcu_{i}^{p}\left(dtcu_{i}^{p}-\left(t_{i,N_T+1}^{p}-T_{cu}^{p(out)}+sdcu_{i}^{p}\right)\right)=0 \quad (41)$$

$$zhu_{j}^{p}\left(dthu_{j}^{p}-\left(T_{hu}^{p(out)}-t_{j,1}^{p}+sdhu_{j}^{p}\right)\right)=0 \quad (42)$$

After this, the simplified flexibility testing problem can be written as the following linear programming (LP) to minimize the summation of these slack variables for each testing point.

$$\min J_{H'}^{p}=\sum_{i\in HP}\sum_{j\in CP}\sum_{k\in ST}\left(z_{ijk}^{p}sdt_{ijk}^{p}+z_{ij,k+1}^{p}sdt_{ij,k+1}^{p}\right)+\sum_{i\in HP}zcu_{i}^{p}sdtcu_{i}^{p}+\sum_{j\in CP}zhu_{j}^{p}sdthu_{j}^{p} \quad (43)$$

The idea of this formulation is to minimize the overall violation of temperature approaches for each set of testing data. The most violating point, i.e., the testing point with maximum positive $J_{H'}^{p}$, value over all $p \in MP$, can be taken as an additional period for subsequent network synthesis. That is, when at least one testing point fails to pass the simplified LP flexibility test, then the multi-periods MINLP model is resolved for network synthesis with this additional period included. The loop, including the MINLP synthesis step and the LP flexibility test as shown in Figure 1, should be repeated until the resulting network is feasible for all test points in the whole specified range of parametric variations.

1.4 Flexibility test for mass exchanger networks (Chen and Hung, 2007)

To identify the feasibility of each testing point without considering the restraints on unit size, slack variables $sdyxi_{ijk}^{p}$ and $sdyxo_{ijk}^{p}$ are used to measure the violation of feasible driving forces for existing mass exchange units. The fixed binary parameters z_{ijk}^{p} are used to define whether the constraint of specific composition difference is involved or not.

$$z_{ijk}^{p}\left(dyxi_{ijk}^{p}-\left(y_{ik}^{p}-m_{ij}sx_{ijk}^{p}-b_{ij}+sdyxi_{ijk}^{p}\right)\right)=0 \quad (44)$$

$$z_{ijk}^{p}\left(dyxo_{ijk}^{p}-\left(sy_{ijk}^{p}-m_{ij}sx_{j,k+1}^{p}-b_{ij}+sdyxo_{ijk}^{p}\right)\right)=0 \quad (45)$$

The problem of measuring the overall violation of each testing point $p \in MP$ can be formulated as the following nonlinear program.

$$\min J_{M'}^{p}=\sum_{i\in HP}\sum_{j\in CP}\sum_{k\in ST}z_{ijk}^{p}\left(sdyxi_{ijk}^{p}+sdyxo_{ijk}^{p}\right) \quad (46)$$

A positive $J_{M',\min}^{p}$ value implies the infeasible MENs structure for the testing point. The most violated testing point(s) can be appended as new period(s) for the synthesis of new MENs candidate. One can proceed the flexibility test considering units area restraints when all testing points have zero violation measure.

1.5 Synthesis of multi-period combined heat and mass exchanger network (Turnprakiat, 2007)

In his work, he adapts the stage-wise superstructure for modeling the synthesis problem of combined heat and mass exchanger networks optimization. Figure 3 shows the two-stage superstructure for the combined heat and mass exchanger networks (CHAMENs) in case of both high temperature favorable equilibrium relation for MSA, S1, and low temperature favorable equilibrium relation for MSA, S2, are used. The external hot and cold utilities are taken into account to use with both lean streams, S1 and S2, and we assume no waste heat in the process.

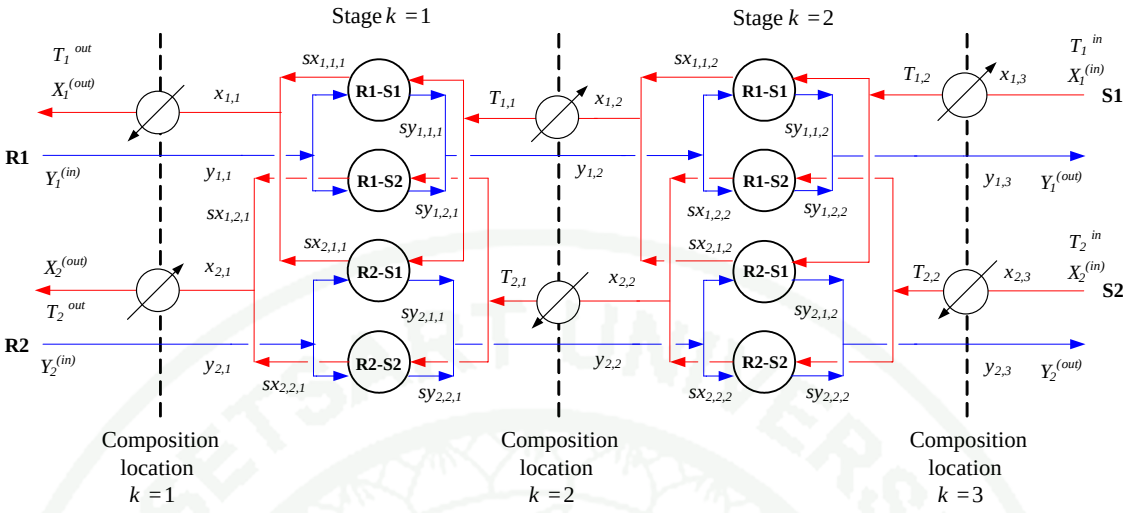

Figure 3 Two-stage superstructure for combined heat and mass exchanger networks

Source: Turnprakiat (2007)

The synthesis of combined heat and mass exchanger network must concern about the trade off between investment cost of mass exchangers and the total cost for heat exchangers - utilities and investment cost. The main factor in trading off these costs is the equilibrium relation for each MSAs. We classify the type of equilibrium relation into two types which are high temperature favorable equilibrium relation and low temperature favorable equilibrium relation.

For the principle of high temperature favorable equilibrium relation, if we increase the temperature to the MSAs, lean stream, the mass exchange performance of those MSAs on the rich stream will increase. Consequently, the size of the mass exchanger will decrease. The MSAs that suitable for this equilibrium relation is a stripping agent for a stripper. In contrast, for the low temperature favorable equilibrium relation, the decreasing of the MSAs' temperature will impact in reducing the size of the mass transfer equipment. MSAs that is classified to this equilibrium type, normally, is a solvent for gas absorption.

Within each stage of the superstructure, mass exchanges between any pair of rich and lean streams can occur. In each stage, the rich (lean) process stream can

split and direct to an exchanger in order to match with each lean (rich) stream. Obviously, the two-stage superstructure for the problem containing two rich and two lean streams involved eight mass exchangers with four possible matches in each stage e.g. in stage k = 1, possible matches are R1 - S1, R1 - S2, R2 - S1, and R2 - S2. Moreover, in each stage of superstructure, MSA, S1, is assumed to be heated up to the favorable temperature in order to enhance the mass exchange performance before fed to the mass exchanger and finally must be cooled down to the initial temperature of that MSA. Conversely, MSA, S2, is assumed to be cooled down to the favorable temperature in order to enhance the mass exchange performance before fed to the mass exchanger and must be heated up to the initial temperature of that MSA at the first composition location of superstructure.

The objective function is the minimum total annualized cost of the network which is subjected to the following constraints. The derived constraints are divided into two parts in which dependent upon the temperature favorable of MSAs used.

Constraint 1: *Overall mass balance over the whole network*

An overall mass balance is needed to ensure sufficient exchange of any transferred component for all rich streams. The constraints specify that the overall mass transferable requirement of each rich stream must be equal to the sum of mass which exchanged with other lean process streams or MSAs at each stage.

$$\left(y_{i1}^{p} - y_{i,N_s+1}^{p}\right)G_i^{p} = \sum_{k\in ST}\sum_{j\in LP} M_{ijk}^{p} \tag{47}$$

$$\left(x_{j1}^{p} - X_{j,N_s+1}^{p}\right)L_j^{p} = \sum_{k\in ST}\sum_{i\in RP} M_{ijk}^{p} \tag{48}$$

Constraint 2: *Mass balance in each stage*

These constraints are also needed to determine the composition of the transferable component as well as partition of flow rates for all parallel units. The composition location k = 1 involves the highest composition whereas $k = N_S + 1$ involves the lowest composition.

$$\left(y_{ik}^{p} - y_{i,k+1}^{p}\right)G_i^{p} = \sum_{j \in LP} M_{ijk}^{p} \tag{49}$$

$$\left(x_{jk}^{p} - X_{j,k+1}^{p}\right)L_j^{p} = \sum_{ij \in RP} M_{ijk}^{p} \tag{50}$$

$$G_i^{p} = \sum_{j \in LP} g_{ijk}^{p} \tag{51}$$

$$L_j^{p} = \sum_{j \in RP} \ell_{ijk}^{p} \tag{52}$$

Constraint 3: *Mass balance in each exchange unit*

A component mass balance is required for each local exchange unit. The new variables include of split mass flow rates g_{ijk}^{p} and ℓ_{ijk}^{p}, and composition before mixer, sy_{ijk}^{p} and sx_{ijk}^{p}, as depicted in Figure 3.

$$g_{ijk}^{p}\left(y_{ik}^{p} - sy_{ijk}^{p}\right) = M_{ijk}^{p} \tag{53}$$

$$\ell_{ijk}^{p}\left(sx_{ijk}^{p} - x_{j,k+1}^{p}\right) = M_{ijk}^{p} \tag{54}$$

Constraint 4: *Assignment of superstructure inlet/outlet compositions*

The given inlet/outlet compositions of rich and lean streams are assigned as the inlet/outlet compositions to the superstructure. For rich streams, the superstructure inlet corresponds to composition location $k = 1$. While for lean streams, the inlet corresponds to location $k = N_S + 1$.

$$Y_i^{p(in)} = y_{i1}^{p},\ Y_i^{p(out)} = y_{i,N_s+1}^{p} \tag{55}$$

$$X_j^{p(in)} = x_{j,N_s+1}^{p},\ X_j^{p(out)} = x_{j1}^{p} \tag{56}$$

Constraint 5: *Feasibility of the transferable component*

Constraints are also needed to guarantee monotonic decrease of all compositions at successive stages.

$$y_{ik}^{p} \geq y_{i,k+1}^{p},\ x_{jk}^{p} \geq x_{j,k+1}^{p} \tag{57}$$

Constraint 6: *Logical constraints for mass exchange system*

Logical constraints and binary variables are needed to determine the existence of process match between streams *i*,*j* in stage *k*. An integer value of one for binary variable z_{ijk} designates that the match between rich stream *i* and lean stream *j* in stage *k* is presented in the optimal network.

$$M_{ijk}^{p} - U_{ij}^{p} z_{ijk} \leq 0 \tag{58}$$

Constraint 7: *Feasibility constraints of the equilibrium relationships*

The feasibility constraints of the equilibrium relationships ensure positive driving forces for the potential process exchange units. Binary variables are used to activate or deactivate the following constraints.

$$y_{ijk}^{p} - m_{ij}\left(t_{jk}^{p}\right)\left(sx_{ijk}^{p} + \varepsilon_{ij}\right) - b_{ij} + \Gamma_{ij}^{p}\left(1 - z_{ijk}\right) \geq 0 \tag{59}$$

$$sy_{ijk}^{p} - m_{ij}\left(t_{jk}^{p}\right)\left(x_{ijk}^{p} + \varepsilon_{ij}\right) - b_{ij} + \Gamma_{ij}^{p}\left(1 - z_{ijk}\right) \geq 0 \tag{60}$$

As mentioned about two cases of equilibrium relations, the constraints used in each case are different. If a stripping agent is selected as a MSAs used in the process, the case of high temperature favorable equilibrium relation must be investigated. The constraints are defined as follows:

Constraint 8: *Hot and cold utilities load*

Hot and cold utility requirements are determined for each lean stream in term of the outlet temperature in the last stage and the target temperature for that stream. The utility heat load requirements are determined as follows:

$$\left(t_{jk}^{p} - Ts_{j}^{(out)p}\right) L_{j} Cp_{j}^{p} = qcu_{jk}^{p} \tag{61}$$

$$\left(t_{jk}^{p} - t_{j,k+1}^{p}\right) L_{j} Cp_{j}^{p} = qhu_{j,k+1}^{p} \tag{62}$$

Constraint 9: *Assignment of superstructure inlet temperature*

Fixed supply temperatures ($Ts_j^{p(in)}$) of the lean streams are assigned as the inlet temperatures to the superstructure. In Figure 3, the lean streams inlet temperature corresponds to the last composition location, $k = 3$.

$$Ts_j^{p(in)} = t_{j,N_s+1}^{p} \tag{63}$$

Constraint 10: *Feasibility of temperatures*

Constraints are also needed to specify a monotonic increase of temperature at the first composition location, and monotonic decrease for the following successive stage of superstructure.

$$Ts_j^{(out)} \le t_{jk}^{p} \tag{65}$$

$$t_{jk}^{p} \ge t_{j,k+1}^{p} \tag{66}$$

$$Ts_j^{(up)} \ge t_{jk}^{p} \tag{67}$$

Constraint 11: *Logical constraints for heat exchange system*

Logical constraints and binary variables are needed to determine the existence of utility match between lean streams and external utility in stage *k*. The binary variables, 0-1, are represented by zcu_{jk} and zhu_{jk} for matches involving cold and hot utility, respectively. An integer value of one for any binary variable designates that the match is presented in the optimal network.

$$qcu_{jk}^{p} - \Lambda_j zcu_{jk} \le 0 \tag{68}$$

$$qhu_{j,k+1}^{p} - \Lambda_j zhu_{j,k+1} \le 0 \tag{69}$$

Constraint 12: *Calculation of approach temperatures*

The area requirement of each match will be incorporated in the objective function. Calculation of these areas requires that approach temperatures be

determined. Nevertheless, the approach temperature between the lean stream and hot/cold utilities at any point of any exchangers will be at least $\Delta T_{\min}$.

$$\Delta T_{\min} \geq t_{jk}^{p} - TIN_{hu} \tag{70}$$

$$dtcu_{jk} \leq t_{jk}^{p} - TOUT_{cu} \tag{71}$$

$$dthu_{jk} \leq TOUT_{hu} - t_{j,k+1} \tag{72}$$

In case of MSAs is a solvent for gas absorption, it implies that low temperature is more thermodynamically favorable for mass exchange than high temperature. For this scenario, generally, constraints numbers 1 to 7 and 9 e.g. mass balances, feasibility of the transferable component etc., are exactly the same. The additional constraints for low temperature equilibrium relation are performed as follows:

Constraint 13: *Hot and cold utilities load*

Hot and cold utility requirements are determined for each lean stream in term of the outlet temperature in the last stage and the target temperature for that stream. The utility heat load requirements are determined as follows:

$$\left(Ts_{j}^{(out)p} - t_{jk}^{p}\right)L_{j}Cp_{j}^{p} = qhu_{jk}^{p} \tag{73}$$

$$\left(t_{j,k+1}^{p} - t_{jk}^{p}\right)L_{j}Cp_{j}^{p} = qcu_{j,k+1}^{p} \tag{74}$$

Constraint 14: *Feasibility of temperatures*

Constraints are also needed to specify a monotonic decrease of temperature at the first composition location, and monotonic increase for the following successive stage of superstructure.

$$Ts_{j}^{(out)} \geq t_{jk}^{p} \tag{75}$$

$$t_{jk}^{p} \leq t_{j,k+1}^{p} \tag{76}$$

$$Ts_j^{(lo)} \le t_{jk}^p \tag{77}$$

Constraint 15: *Logical constraints for heat exchange system*

Logical constraints and binary variables are needed to determine the existence of utility match between lean streams and external utility in stage *k*. The binary variables, 0-1, are represented by zcu_{jk} and zhu_{jk} for matches involving cold and hot utility, respectively. An integer value of one for any binary variable designates that the match is presented in the optimal network.

$$qhu_{jk}^p - \Lambda_j zhu_{jk} \le 0 \tag{78}$$

$$qcu_{j,k+1}^p - \Lambda_j zcu_{j,k+1} \le 0 \tag{79}$$

Constraint 16: *Calculation of approach temperatures*

The area requirement of each match will be incorporated in the objective function. Calculation of these areas requires that approach temperatures be determined. Nevertheless, the approach temperature between the lean stream and hot/cold utilities at any point of any exchangers will be at least $\Delta T_{\min}$.

$$\Delta T_{\min} \ge TIN_{cu} - t_{jk}^p \tag{80}$$

$$dthu_{jk} \le TOUT_{hu} - t_{jk}^p \tag{81}$$

$$dtcu_{jk} \le t_{j,k+1} - TOUT_{cu} \tag{82}$$

Objective Function: *Minimum total annualized cost*

In the synthesis of CHAMENs, The objective function consists of four main terms i.e. MSAs cost and the annualized equipment cost for mass exchange system, and utilities cost and the annualized equipment cost for heat exchange system. The equation for this objective is derived as follow:

In the synthesis of CHAMENs, The objective function consists of five main terms i.e. the average costs of external mass separating agents over a finite number of operating points; the annual costs of installation and material of the mass

exchange units; the average costs of the hot and cold utility consumptions over a finite number of operating points; the annual costs of installation and material of the heat exchange units. The equation for this objective is derived as follow:

$$\min TAC = \frac{1}{N_p + 1}\sum_{j\in LP} C_j L_j^p + \sum_{i\in RP}\sum_{j\in LP^{(t)}}\sum_{k\in ST} C_{ij}^{(t)} Nst_{ijk} + \sum_{i\in RP}\sum_{j\in LP^{(h)}}\sum_{k\in ST} C_{ij}^{(h)} H_{ijk}$$
$$+ \frac{1}{N_p + 1}\left(\sum_{p\in MP}\sum_{j\in LP} C_{cu} qcu_j^p + \sum_{p\in MP}\sum_{j\in LP} C_{hu} qhu_j^p\right)$$
$$+ \sum_{p\in MP}\sum_{j\in LP} C_{j,cu} A_{j,cu}^p + \sum_{p\in MP}\sum_{j\in LP} C_{hu,j} A_{hu,j}^p \qquad (83)$$

where

$$A_{j,cu} \geq \frac{qcu_j^p}{U_{j,cu}\left[dtcu_j^p \left(T_j^{(out)} - T_{cu}^{(in)}\right)\left(dtcu_j^p + T_j^{(out)} - T_{cu}^{(in)}\right)/2\right]^{1/3}}$$

$$A_{hu,j} \geq \frac{qhu_j^p}{U_{hu,j}\left[dthu_j^p \left(T_{hu}^{(in)} - T_j^{(out)}\right)\left(dthu_j^p + T_{hu}^{(in)} - T_j^{(out)}\right)/2\right]^{1/3}}$$

$$A_{j,cu}, A_{hu,j} \geq 0$$

$$Nst_{ijk} \geq \left[\frac{\left(y_{ik}^p - sy_{ijk}^p\right)^{0.3275} + \left(sy_{ijk}^{*p} - y_{ij,k+1}^{*p}\right)^{0.3275}}{\left(dyxi_{ijk}^p\right)^{0.3275} + \left(dyxo_{ijk}^p\right)^{0.3275}}\right]^{1/0.3275}$$

$$H_{ijk} \geq \frac{M_{ijk}^p}{k_y aS} \times \left[\frac{\left(dyxi_{ijk}^p\right)^{0.3275} + \left(dyxo_{ijk}^p\right)^{0.3275}}{2}\right]^{1/0.3275}$$

$$Nst_{ijk}, H_{ijk} \geq 0$$

Synthesizing the special case of CHAMENs is carried out using the modified stage-wise superstructure as demonstrated in Figure 4. The superstructure contains two main configurations, one for HENs superstructure and another for MENs superstructure.

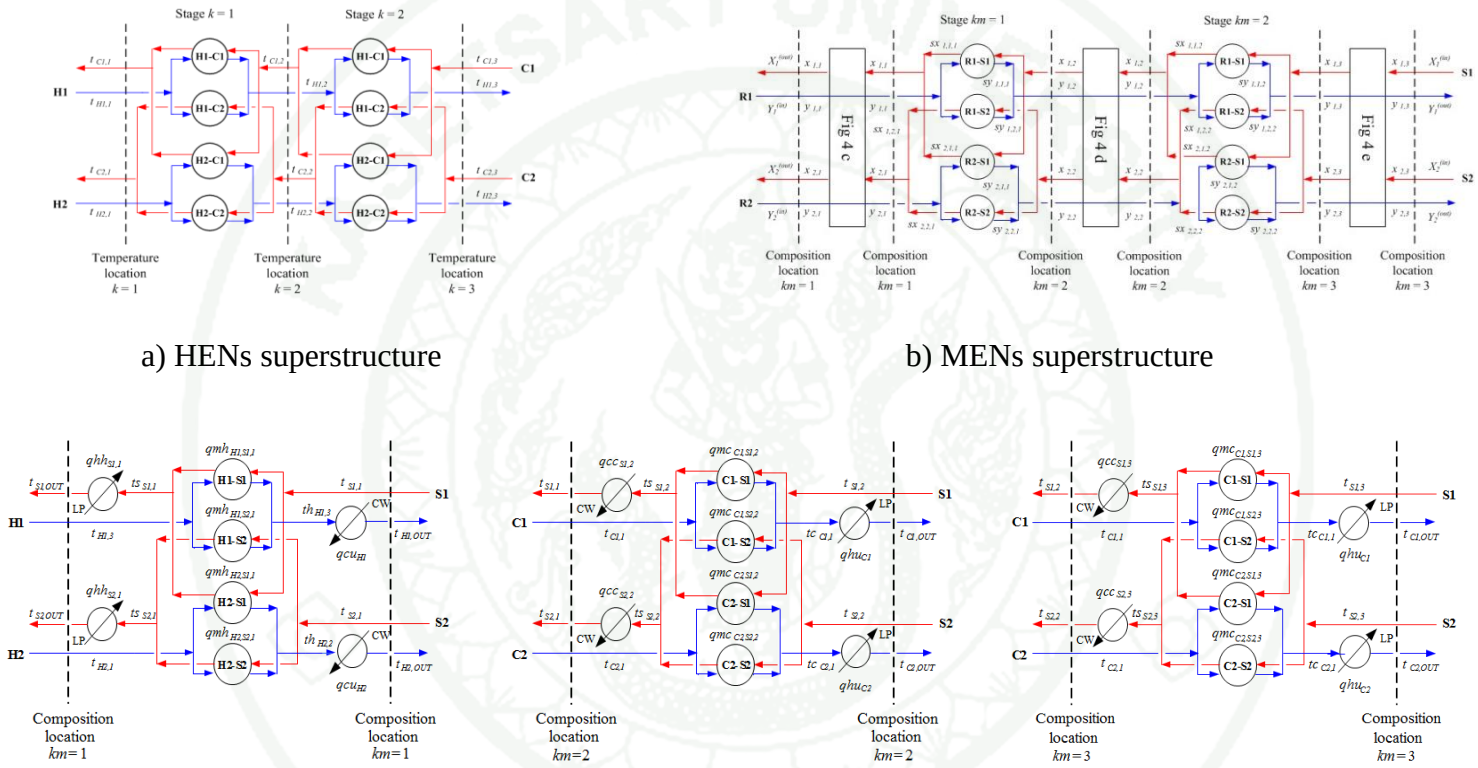

a) HENs superstructure

b) MENs superstructure

c) First-stage superstructure

d) Second-stage superstructure

e) Third-stage superstructure

Figure 4 Stage-wise superstructure for a special case of CHAMENs: a) HENs superstructure, b) MENs superstructure, c) First-stage superstructure, d) Second-stage superstructure and e) Third-stage superstructure

Source: Turnprakiat (2007)

In this figure, the low temperature favorable equilibrium MSAs is examined. The main of this superstructure is almost the same as the structure for HENs and MENs. The differences are all cold streams in the first stage of HENs superstructure, before fed to the heater, are taken into account as a source to cool down MSAs in each stage of MENs superstructure. All hot streams in the last stage of HENs superstructure are joined to heat up MSAs in the first stage of MENs superstructure before fed to the heater. The following part derives the constraints and objective function used in this special case of CHAMENs.

The objective function of this section is to minimize total annualized cost of the network which is subjected to the following constraints. The derived constraints are divided into two parts which are the constraint for heat integration, and the constraints for mass integration. Furthermore, some essential constraints which are used to calculate the energy balance in the MENs superstructure are also included.

Constraint 1: *Overall heat balance for each stream*

This constraint is needed to ensure sufficient heating or cooling of each process stream. The constraints specify that the overall heat transfer requirement of each stream must equal to the sum of the heat it exchanges with other process streams at each stage plus the exchange with the utilities streams

$$\left(T_i^{(in)p} - T_i^{(out)p}\right)FCp_i^p = \sum_{k\in ST}\sum_{j\in CP} q_{ijk}^p + \sum_{s\in LP} qmh_{is,1} + qcu_i^p \tag{84}$$

$$\left(T_j^{(out)p} - T_j^{(in)p}\right)FCp_j^p = \sum_{k\in ST}\sum_{i\in HP} q_{ijk}^p + \sum_{km}\sum_{s\in LP} qmc_{js,km} + qhu_j^p \tag{85}$$

Constraint 2: *Heat balance at each stage*

An energy balance is also needed at each stage of HENs and MENs superstructure to determine the temperatures. For HENs, streams temperature are the highest at location k = 1 and the lowest at last temperature location. For MENs, the highest temperature locates at the inlet and outlet of that lean stream whereas the lowest is at the first stage km =1

$$\left(t_{ik}^{p} - t_{i,k+1}^{p}\right) FCp_{i}^{p} = \sum_{j \in CP} q_{ijk} \tag{86}$$

$$\left(t_{jk}^{p} - t_{j,k+1}^{p}\right) FCp_{j}^{p} = \sum_{i \in HP} q_{ijk} \tag{87}$$

$$\left(thinu_{i}^{p} - thoutu_{i}^{p}\right) FCp_{i}^{p} = \sum_{s \in LP} qmh_{is,1} \tag{88}$$

$$\left(tcoutu_{j}^{p} - tcinu_{j}^{p}\right) FCp_{j}^{p} = \sum_{km} \sum_{s \in LP} qmc_{js,km} \tag{89}$$

$$\left(tss_{s,1}^{p} - ts_{s,1}^{p}\right) L_{s} Cp_{s}^{p} = \sum_{i \in HP} qmh_{is,1} \tag{90}$$

$$\left(ts_{s,km+1}^{p} - tss_{s,km+1}^{p}\right) L_{s} Cp_{s}^{p} = \sum_{j \in CP} qmc_{js,km+1} \tag{91}$$

Constraint 3: *Assignment of superstructure inlet and outlet temperatures*

Fixed supply temperatures of the process streams are assigned as the inlet temperatures to the superstructure. In Figure 4a, for hot streams the inlet corresponds to temperature location $k = 1$, while the cold streams, the inlet corresponds to location $k = 3$ and for Figure 4e, the inlet temperature of each lean streams is located at the last composition location ($km = 3$). In addition, the constraints for the inlet/outlet temperature at the first and the last stage of HENs superstructure are also derived as follow;

$$t_{i1}^{p} = T_{i}^{(in)p} \;, t_{i,N_s+1}^{p} = T_{j}^{(in)p} \;, ts_{s,NS_m+1}^{p} = T_{s}^{(in)p} \tag{92}$$

$$t_{i,N_s+1}^{p} = thinu_{i}^{p} \;, thh_{i,N_s+1}^{p} = thout_{i}^{p} \tag{93}$$

$$t_{j,1}^{p} = tcinu_{j}^{p} \;, tcc_{j,1}^{p} = tcout_{j}^{p} \tag{94}$$

Constraint 4: *Feasibility of temperatures*

Constraints are also needed to specify a monotonic decrease of temperature at each successive stage. In addition, a bound is set for the outlet temperatures of the superstructure at the specific stream target temperature. Note that in HENs and MENs superstructure, the temperature of each stream at its last stage does not necessarily correspond to the stream target temperature since utility exchanges can occur at the outlet of this superstructure.

$$t_{ik}^{p} \geq t_{i,k+1}^{p} \tag{95}$$

$$t_{jk}^{p} \geq t_{j,k+1}^{p} \tag{96}$$

$$T_{i}^{(out)} \leq thh_{i,N_s+1}^{p},\ t_{i,N_s+1}^{p} \geq thh_{i,N_s+1}^{p} \tag{97}$$

$$T_{j}^{(out)} \geq tcc_{j,1}^{p},\ tcc_{j,1}^{p} \geq tc_{j,1}^{p} \tag{98}$$

$$T_{s}^{(out)} \geq tss_{s,1}^{p},\ tss_{s,1}^{p} \geq ts_{s,1}^{p} \tag{99}$$

$$ts_{s,km+1} \geq tss_{s,km+1}^{p},\ tss_{s,km+1}^{p} \geq ts_{s,km}^{p} \tag{100}$$

Constraint 5: *Hot and cold utility load*

Hot and cold utility requirements are determined for each process stream in term of the outlet temperature in the last stage and the target temperature for that stream. The utility heat load requirements are determined as follows:

$$\left(t_{i,N_s+1}^{p} - T_{i}^{(out)p}\right)FCp_{i}^{p} = qcu_{i}^{p} \tag{101}$$

$$\left(T_{j}^{(out)p} - tcc_{j,1}^{p}\right)FCp_{j}^{p} = qhu_{j}^{p} \tag{102}$$

$$\left(T_{s}^{(out)p} - tss_{s,1}^{p}\right)L_{s}Cp_{s}^{p} = qhh_{s,1}^{p} \tag{103}$$

$$\left(tss_{s,km+1}^{p} - ts_{s,km}^{p}\right)L_{s}Cp_{s}^{p} = qcc_{s,km+1}^{p} \tag{104}$$

Constraint 6: *Logical constraints*

Logical constraints and binary variables are needed to determine the existence of process match between streams *i*,*j* in stage *k* and also any match involving utility streams. The binary variables, 0-1, are represented by z_{ijk} for process stream matches, and zcu_i and zhu_j for matches involving cold and hot utility, respectively. An integer value of one for any binary variable designates that the match is presented in the optimal network.

$$q_{ijk}^{p} - \Lambda_{ij} z_{ijk} \leq 0 \tag{105}$$

$$qmh_{is,1}^{p} - \Lambda_{is} zmh_{is,1} \leq 0 \tag{106}$$

$$qmc_{js,km+1}^{p} - \Lambda_{js} zmc_{js,km+1} \leq 0 \tag{107}$$

$$qcu_i^p - \Lambda_i zcu_k \le 0 \tag{108}$$

$$qhu_j^p - \Lambda_j zhu_j \le 0 \tag{109}$$

$$qcc_{s,km+1}^p - \Lambda_s zcc_{s,km+1} \le 0 \tag{110}$$

$$qhh_{s,1}^p - \Lambda_s zhh_{s,1} \le 0 \tag{111}$$

Constraint 7: *Calculation of approach temperatures*

The area requirement of each match will be incorporated in the objective function. Calculation of these areas requires that approach temperatures are determined. To ensure feasible driving forces for exchangers that are selected in the optimization procedure, the binary variables are used to activate or deactivate the following constraints. Nevertheless, the approach temperature between the hot and cold streams at any point of any exchangers will be at least $\Delta T_{\min}$.

$$dt_{ijk}^p \le t_{ik}^p - t_{jk}^p + \Gamma_{ij}\left(1 - z_{ijk}\right) \tag{112}$$

$$dt_{ij,k+1}^p \le t_{i,k+1}^p - t_{j,k+1}^p + \Gamma_{ij}\left(1 - z_{ijk}\right) \tag{113}$$

$$dtmhi_{is,km}^p \le thinu_i^p - tss_{s,km}^p + \Gamma m_{is}\left(1 - zmh_{is,km}\right) \tag{114}$$

$$dtmho_{is,km}^p \le thoutu_i^p - ts_{s,km}^p + \Gamma m_{is}\left(1 - zmh_{is,km}\right) \tag{115}$$

$$dtmci_{js,km}^p \le ts_{s,km}^p - tcoutu_j + \Gamma m_{js}\left(1 - zmc_{js,km}\right) \tag{116}$$

$$dtmco_{js,km}^p \le tss_{s,km}^p - tcinu_j + \Gamma m_{js}\left(1 - zmc_{js,km}\right) \tag{117}$$

$$dthu^p{}_j \le T_{hu}^{out} - tcc^p{}_{j,1} \tag{118}$$

$$dtcu^p{}_i \le thh^p{}_{i,N_s+1} - T_{cu}^{out} \tag{119}$$

$$dthh^p{}_s \le T_{hu}^{out} - tss^p{}_{s,1} \tag{120}$$

$$dtcc^p{}_{s,km+1} \le tss_{s,km+1}^p - T_{cu}^{out} \tag{121}$$

The second part is the constraints derived to use in the section of MENs design. The constraints described in chapter two about MENs superstructure are employed to synthesize this special case of CHAMENs.

Constraint 8: *Overall mass balance over the whole network*

An overall mass balance is needed to ensure sufficient exchange of any transferred component for all rich streams. The constraints specify that the overall mass transferable requirement of each rich stream must be equal to the sum of mass which exchanged with other lean process streams or MSAs at each stage.

$$\left(Y_r^{(in)p} - Y_r^{(out)p}\right)G_r^p = \sum_{km \in STm} \sum_{s \in LP} M_{rs,km}^p \tag{122}$$

$$\left(X_s^{(out)p} - X_s^{(in)p}\right)L_s^p = \sum_{km \in STm} \sum_{r \in RP} M_{rs,km}^p \tag{123}$$

Constraint 9: *Mass balance in each stage*

These constraints are also needed to determine the composition of the transferable component as well as partition of flow rates for all parallel units. The composition location $km = 1$ involves the highest composition whereas $km = NS_m + 1$ involves the lowest composition.

$$\left(y_{r,km}^p - y_{r,km+1}^p\right)G_r^p = \sum_{s \in LP} M_{rs,km}^p \tag{124}$$

$$\left(x_{s,km}^p - x_{s,km+1}^p\right)L_s^p = \sum_{s \in RP} M_{rs,km}^p \tag{125}$$

$$G_r^p = \sum_{s \in LP} gg_{rs,km}^p \tag{126}$$

$$L_s^p = \sum_{r \in RP} ll_{rs,km}^p \tag{127}$$

Constraint 10: *Mass balance in each exchange unit*

A component mass balance is required for each local exchange unit. The new variables include of split mass flow rates, $gg_{rs,km}$ and $ll_{rs,km}$, and composition before mixer, $sy_{rs,km}$ and $sx_{rs,km}$, as depicted in Figure 4b.

$$gg_{rs,km}^p \left(y_{r,km}^p - sy_{rs,km}^p\right) = M_{rs,km}^p \tag{128}$$

$$ll_{rs,km}^p \left(sx_{rs,km}^p - x_{s,km+1}^p\right) = M_{rs,km}^p \tag{129}$$

Constraint 11: *Assignment of superstructure inlet/outlet compositions*

The given inlet/outlet compositions of rich and lean streams are assigned as the inlet/outlet compositions to the superstructure. For rich streams, the superstructure inlet corresponds to composition location *km* = 1. For lean streams, the inlet corresponds to location $km = NS_m + 1$.

$$Y_r^{p(in)} = y_{r,1}^p,\ Y_r^{p(out)} = y_{r,NS_m+1}^p \tag{130}$$

$$X_s^{p(in)} = x_{s,NS_s+1}^p,\ X_s^{p(out)} = x_{s,1}^p \tag{131}$$

Constraint 12: *Feasibility of the transferable component*

Constraints are also needed to guarantee monotonic decrease of all compositions at successive stages.

$$y_{r,km}^p \geq y_{r,km+1}^p,\ x_{s,km}^p \geq x_{s,km+1}^p \tag{132}$$

Constraint 13: *Logical constraints for mass exchange system*

Logical constraints and binary variables are needed to determine the existence of process match between streams *r,s* in stage *km*. An integer value of one for binary variable $zm_{rs,km}$ designates that the match between rich stream *r* and lean stream *s* in stage *km* is presented in the optimal network.

$$M_{rs,km}^p - Um_{rs}^p zm_{rs,km} \leq 0 \tag{133}$$

Constraint 14: *Feasibility constraints of the equilibrium relationships*

The feasibility constraints of the equilibrium relationships ensure positive driving forces for the potential process exchange units. Binary variables are used to activate or deactivate the following constraints.

$$y_{r,km}^p - m_{rs}\left(t_{s,km}^p\right)\left(sx_{r,km}^p + \varepsilon_{rs}\right) - b_{rs} + \Gamma_{rs}^p\left(1 - zm_{rs,km}\right) \geq 0 \tag{134}$$

$$sy_{rs,km}^p - m_{rs}\left(t_{s,km}^p\right)\left(x_{s,km+1}^p + \varepsilon_{rs}\right) - b_{rs} + \Gamma_{rs}^p\left(1 - zm_{rs,km}\right) \geq 0 \tag{135}$$

Objective Function: *Minimum total annualized cost*

In the synthesis of special CHAMENs, we attempt to minimize the total annualized cost of the system. The objective function in this task, thus, consists of four main terms i.e. MSAs cost and the annualized equipment cost for mass exchange system, and utilities cost and the annualized equipment cost for heat exchange system. The equation for this objective is derived as follow:

$$\begin{aligned}\min TAC = {} & \frac{1}{N_p+1}\sum_{s\in LP} C_s L_s^p + \sum_{r\in RP}\sum_{s\in LP^{(t)}}\sum_{km\in STm} C_{rs}^{(t)} Nst_{rs,km} + \sum_{r\in RP}\sum_{s\in LP^{(h)}}\sum_{km\in STm} C_{rs}^{(h)} H_{rs,km} \\ & + \frac{1}{N_p+1}\left(\sum_{p\in MP}\sum_{i\in HP} C_{cu} qcu_i^p + \sum_{p\in MP}\sum_{j\in CP} C_{hu} qhu_j^p\right) \\ & + \frac{1}{N_p+1}\left(\sum_{p\in MP}\sum_{s\in LP} C_{hu} qhh_{s,1}^p + \sum_{p\in MP}\sum_{s\in LP} C_{cu} qcc_{s,km}^p\right) \\ & + \sum_{i\in HP}\sum_{j\in CP}\sum_{k\in ST} C_{ij} A_{ijk}^{\beta_{ij}} + \sum_{i\in HP} C_{i,cu} A_{i,cu}^{\beta_{i,cu}} + \sum_{j\in CP} C_{hu,j} A_{j,hu}^{\beta_{j,hu}} + \sum_{i\in HP}\sum_{s\in LP} A_{is,1}^{\beta_{is}} \\ & + \sum_{j\in CP}\sum_{s\in LP}\sum_{km\in STm} C_{js} A_{js,km}^{\beta_{js}} + \sum_{s\in LP} C_s A_{s,1}^{\beta_s} + \sum_{s\in LP}\sum_{km} C_s A_{s,km}^{\beta_{s,}} \end{aligned} \quad (136)$$

where

$$Nst_{rs,km} \geq \left[\frac{\left(y_{r,km}^p - sy_{rs,km}^p\right)^{0.3275} + \left(sy_{rs,km}^{*p} - y_{rs,km+1}^{*p}\right)^{0.3275}}{\left(dyxi_{rs,km}^p\right)^{0.3275} + \left(dyxo_{rs,km}^p\right)^{0.3275}}\right]^{1/0.3275}$$

$$H_{rs,km} \geq \frac{M_{rs,km}^p}{k_y aS} \times \left[\frac{\left(dyxi_{rs,km}^p\right)^{0.3275} + \left(dyxo_{rs,km}^p\right)^{0.3275}}{2}\right]^{1/0.3275}$$

$$A_{ijk} \geq \frac{q_{ijk}^p}{U_{ij}\left[dt_{ijk}^p dt_{ij,k+1}^p \left(dt_{ijk}^p + dt_{ij.k+1}^p\right)/2\right]^{1/3}}$$

$$A_{j,cu} \geq \frac{qcu_j^p}{U_{j,cu}\left[dtcu_j^p \left(T_j^{(out)} - T_{cu}^{(in)}\right)\left(dtcu_j^p + T_j^{(out)} - T_{cu}^{(in)}\right)/2\right]^{1/3}}$$

$$A_{hu,j} \geq \frac{qhu_j^p}{U_{hu,j}\left[dthu_j^p \left(T_{hu}^{(in)} - T_j^{(out)}\right)\left(dthu_j^p + T_{hu}^{(in)} - T_j^{(out)}\right)/2\right]^{1/3}}$$

$$A_{is,1} \geq \frac{q^{p}_{is,1}}{U_{is}\left[dtmhi^{p}_{is,1} dtmho^{p}_{is,1}\left(dtmhi^{p}_{is,1} + dtmho^{p}_{is.1}\right)/2\right]^{1/3}}$$

$$A_{js,km} \geq \frac{q^{p}_{js,km}}{U_{js}\left[dtmci^{p}_{js,km} dtmco^{p}_{js,km}\left(dtmci^{p}_{js,km} + dtmco^{p}_{js.km}\right)/2\right]^{1/3}}$$

$$A_{s,1} \geq \frac{q^{p}_{s,1}}{U_{s,1}\left[dthh^{p}_{s}\left(T^{(out)}_{hu} - tss_{s,1}\right)\left(dthh^{p}_{s} + T^{(out)}_{hu} - T^{(in)}_{hu}\right)/2\right]^{1/3}}$$

$$A_{s,km+1} \geq \frac{q^{p}_{s,km+1}}{U_{s,km+1}\left[dtcc^{p}_{s,km+1}\left(tss_{s,km+1} - T^{(in)}_{cu}\right)\left(dtcc^{p}_{s,km+1} + T^{(in)}_{cu} - T^{(out)}_{cu}\right)/2\right]^{1/3}}$$

1.6 Parametric programming

In an optimization framework, where the objective is to minimize or maximize a performance criterion subject to a given set of constraints and where some of the parameters in the optimization problem vary between specified lower and upper bounds, parametric programming is a technique for obtaining (i) the objective function and the optimization variables as a function of these parameters and (ii) the regions in the space of the parameters where these functions are valid (Fiacco, 1983; Gal, 1995; Acevedo and Pistikopoulos, 1996, 1997; Pertsinidis *et al.*, 1998; Papalexandri, 1998; Acevedo, 1999; Dua and Pistikopoulos, 1999)

The main advantage of using the parametric programming techniques to address such problems is that for problems pertaining to plant operations, such as for process planning Pistikopoulos *et al.* (1998) and scheduling, one can obtain a complete map of all the optimal solutions. Moreover, as the operating conditions fluctuate, one does not have to re-optimize for the new set of conditions since the optimal solution as a function of parameters (or the new set of conditions) is already available. Mathematically, such problems can be posed as multi-parametric mixed-integer nonlinear programming problems of the following form:

$$z(\theta) = \min d^T y + f(x) \tag{137}$$

subject to $Ey + g(x) \le b + F\theta$

$$\theta_{\min} \le \theta \le \theta_{\max}$$

$$x \in X \subseteq \Re^n$$

$$y \in Y = \{0,1\}^m$$

$$\theta \in \Theta \subseteq \Re^s$$

where y is vector of 0–1 binary variables, x is a vector of continuous variables, f is a scalar, continuously differentiable and convex function of x, g is a vector of continuously differentiable and convex functions of x, b and d are constant vectors, E and F are constant matrices, θ is a vector of parameters, $\theta_{\min}$ and $\theta_{\max}$ are the vectors of lower and upper bounds on θ, and X and Θ are compact and convex polyhedral sets of dimensions n and s, respectively. While the detailed theory and algorithms for solving equation 137 were proposed by Dua *et al.*, (1999, 2000), the engineering significance of solving equation 137 by using parametric programming.

1.7 Degrees of freedom of networks

To operate the plant in an optimal manner, one should first answer the two questions: (Q1) are there enough degrees of freedom (DOFs, or manipulated variables) for control? and (Q2) are there extra degrees of freedom for an optimization? The question (Q1) is used to check the possibility to control each controlled variable independently, while the question (Q2) is used to check whether except the control design for setpoint satisfaction, we also need to consider the economic objective or not. For heat exchanger networks, Marselle *et al.* (1982) proposed the definition of the number of degrees of freedom (N_{DOF}) by

$$N_{DOF} = N_{units} - N_t \tag{138}$$

where N_{units} is the number of exchanger units or manipulated variables (degrees of freedom) and N_t is the number of target temperatures.

The condition $N_{DOF} > 0$ is necessary for the operation to be feasible and utility cost optimizable. However, this is not enough to answer the questions (Q1) and (Q2). The more precise definition of the number of degrees of freedom with respect to utility cost optimization ($N_{DOF,U}$) that was sufficient to answer the two questions was proposed by Glemmestad (1997) as shown in the following:

$$N_{DOF,U} = DS + N_U - N_t \tag{139}$$

where DS is the dimensional space spanned by the manipulated variables in the inner exchanger to the outer exchanger and N_U is the number of utility types.

The implication of $N_{DOF,U}$ can be summarized as shown in Table 1. The operation will be structurally feasible (question Q1) if and only if the condition $N_{DOF,U} \geq 0$ can be satisfied. Furthermore, there will be extra degrees of freedom for utility cost optimization (question Q2) if and only if $N_{DOF,U} > 0$.

Table 1 The implication of $N_{DOF,U}$

Case	(Q1)	(Q2)
$N_{DOF,U}<0$	No	No
$N_{DOF,U}=0$	Yes	No
$N_{DOF,U}>0$	Yes	Yes

It is obvious that the operation of networks will be more challenging when $N_{DOF,U} > 0$ because aside from the set-point satisfaction, the utility cost should also be minimized. This means that a common heuristic rule for the control design such as manipulating the last exchanger on a stream for a direct effect (Marselle *et al.*, 1982; Calandranis and Stephanopoulos, 1988; Mathisen, 1994) may not be preferred from an energy point of view.

Several strategies were proposed to handle optimal operation of networks. The early researches were techniques based on structural information. Marselle *et al.* (1982) applied a graph theory to suggest a control structure and developed a control policy to adjust flow distributions in networks to meet target with minimum utility usage. Calandranis and Stephanopoulos (1988) used the structural characteristics of networks to identify routes to allocate loads to available sinks and developed a knowledge-based concept to select the best route. The methods based on structural information using a sign matrix (directional effect among manipulated variables and controlled variables) were proposed by Mathisen (1994) and Glemmestad *et al.* (1996).

However, the control design based on structural information cannot guarantee the optimality in some cases; hence a conventional online-optimization may be recommended. The researches based on online and periodic optimizations for optimal operation of networks can be found in Aguilera and Marchetti (1998), Glemmestad *et al.* (1999) and González *et al.* (2006). Nevertheless, online-optimization requires a rather complex approach for the implementation. Hence, some recent researches for the optimal operation have been devoted to simple ways of implementing (economic) optimal operation. For example, Skogestad (2000) proposed a concept of 'self-optimizing control' that is, finding a magic variable to keep constant and then resulting in optimality. Pistikopoulos *et al.* (2002) used offline parametric optimization to simplify the task of online optimization.

1.8 Optimal split-range control structure (Lersbamrungsuk, 2007)

In general problems, with a large number of manipulated variables and regions of active constraints, this is not a trivial task. Hence, a systematic method of determining this pairing is needed. Lersbamrungsuk (2007) proposes two approaches for determining optimal split-range control structure. In the first approach, one first identifies the set of nominal active constraints and then uses the information of directional effect (arithmetic sign) between a manipulated variable and a controlled variable to determine optimal split-range control structure. However, the control

structure cannot guarantee optimality in some cases such as when a sign is unclear. Hence, the second approach based on an optimization formulation to determine an optimal split-range control structure is further developed. However, the further information of all active constraint regions in a given disturbance space is required. An integer linear programming (ILP) formulation for the design of an optimal split-range control structure is as follows:

Definition 1: *Set of controlled and manipulated variables*

CV: set of controlled variables**, CV** = $\{ CV_1, CV_2, \ldots, CV_{N_{CV}-1}, CV_{N_{CV}} \}$

MV: set of manipulated variables, **MV** = $\{ MV_1, MV_2, \ldots, MV_{N_m-1}, MV_{N_m} \}$

MVAAT: subset of **MV** with manipulated variables which are always active constraints (saturated at upper or lower bounds)

MVINAT: subset of **MV** with manipulated variables which are always inactive constraints (never saturated)

MVAT: subset of **MV** with manipulated variables which change between being active and inactive constraints

Definition 2 *Primary and secondary manipulated variables*

Primary manipulated variable: A manipulated variable that is used for controlling an output (target), except when it is saturated.

Secondary manipulated variable: A manipulated variable that is used to take over the task of a saturated primary manipulated variable.

Definition 3 *Relationship between primary and secondary manipulated variables*

Let $x_{i,j}$ (where i,j $\in$ **MV**) be a binary variable which represents the relationship between manipulated variable MV_i and manipulated variable MV_j

for i=j, $x_{i,i}$ = 1 implies MV_i is a primary manipulated variable

$x_{i,i}$ = 0 implies MV_i is a secondary manipulated variable or unused

for i≠ j, $x_{i,j}$ = 1 implies MV_j is a secondary manipulated variable for MV_i

$x_{i,j}$ = 0 implies MV_j is not a secondary manipulated variable for MV_i

Definition 4*: Relative order between manipulated variables and controlled variables*

Let $r_{k,j}$ be a relative order between controlled variable CV_k and manipulated variable MV_j. Relative order is a structural measure of how direct an effect an input has on an output (i.e. physical closeness) (Daoutidis and Kravaris, 1992). However, for simplicity we assume $r_{k,j}$ as a number of exchanger units between controlled variable CV_k and manipulated variable MV_j

Definition 5: *Relationship between controlled variables and manipulated variables*

Let $z_{k,j}$ (where k $\in$ **CV**, j $\in$ **MV**) be a binary variable that represents the relationship between controlled variable CV_k and manipulated variable MV_j

$z_{k,j}$ = 1 implies controlled variable CV_k is paired with manipulated variable MV_j

$z_{k,j}$ = 0 implies controlled variable CV_k is not paired with manipulated variable MV_j

Objective function I: *Minimizing the number of "inter-connection" or "complexity" of control structure (unnecessary relationships between primary and secondary manipulated variables)*

$$\min J_I = \sum_i \sum_{j \neq i} x_{i,j} \qquad \text{i, j} \in \mathbf{MV} \tag{140}$$

Constraint 1: *Assign one primary manipulated variable to each control objective*

Number of primary manipulated variable is equal to number of controlled variables (N_{CV})

$$\sum_{i} x_{i,i} = N_{CV} \qquad \text{i} \in \mathbf{MV} \qquad (141)$$

Constraint 2: *A manipulated variable MV_i that always is an active constraint should not be used for other purposes*

Manipulated variable MV_i is not used for control

$$x_{i,i} = 0 \qquad \text{i} \in \mathbf{MVAAT} \qquad (142)$$

Manipulated variable MV_i has no need of a secondary manipulated variable

$$\sum_{j \neq i} x_{i,j} = 0 \qquad \in \mathbf{MVAAT}, \text{j} \in \mathbf{MV} \qquad (143)$$

Manipulated variable MV_i is not used as a secondary manipulated variable

$$\sum_{j \neq i} x_{j,i} = 0 \qquad \text{i} \in \mathbf{MVAAT}, \text{j} \in \mathbf{MV} \qquad (144)$$

Constraint 3*: A manipulated variable MV_i that is never an active constraint is used as a primary manipulated variable with no need of a secondary manipulated variable*

Manipulated variable MV_i is a primary manipulated variable

$$x_{i,i} = 1 \qquad \text{i} \in \mathbf{MVINAT} \qquad (145)$$

Manipulated variable MV_i has no need of a secondary manipulated variable

$$\sum_{j \neq i} x_{i,j} = 0 \qquad \text{i} \in \mathbf{MVINAT}, \text{j} \in \mathbf{MV} \qquad (146)$$

Manipulated variable MV_i is not used as a secondary manipulated variable

$$\sum_{j \neq i} x_{j,i} = 0 \qquad \text{i} \in \textbf{MVINAT}, \text{j} \in \textbf{MV} \qquad (147)$$

Constraint 4: *A manipulated variable MV_i that changes between being an active and inactive constraint may be a primary or secondary manipulated variable.*

- MV_i may have a need or no need of a secondary manipulated variable

if MV_i is chosen to be a primary manipulated variable that can be saturated (active constraint), then a secondary manipulated variable is needed

$$\text{if } x_{i,i} = 1 \text{ then } \sum_{j \neq i} x_{i,j} = 1 \qquad \text{i, j} \in \textbf{MVAT}$$

if MV_i is not chosen to be a primary manipulated variable, then it has no need of a secondary manipulated variable

$$\text{if } x_{i,i} = 0 \text{ then } \sum_{j \neq i} x_{i,j} = 0 \qquad \text{i, j} \in \textbf{MVAT}$$

the above two statements can be written as equation (148)

$$-x_{i,i} + \sum_{j \neq i} x_{i,j} = 0 \qquad \text{i, j} \in \textbf{MVAT} \qquad (148)$$

- MV_i can be or cannot be used as a secondary manipulated variable

if MV_j is chosen to be a primary manipulated variable, then it is not used as a secondary manipulated variable for the other manipulated variables

$$\text{if } x_{j,j} = 1 \text{ then } \sum_{i \neq j} x_{i,j} = 0 \qquad \text{i, j} \in \textbf{MVAT}$$

if MV_j is chosen to be a secondary manipulated variable, then it is used for at least one primary manipulated variable

$$\text{if } x_{j,j} = 0 \text{ then } \sum_{i \neq j} x_{i,j} \geq 1 \qquad \text{i, j} \in \textbf{MVAT}$$

the above two statements can be written as equation (149) and (150)

$$x_{j,j} + \sum_{i \neq j} x_{i,j} \geq 1 \qquad \text{i, j} \in \textbf{MVAT} \qquad (149)$$

and $$M(x_{j,j} - 1) + \sum_{i \neq j} x_{i,j} \leq 0 \qquad \text{i, j} \in \textbf{MVAT} \qquad (150)$$

where M = a positive integer which is greater than the number of members in **MVAT**

Constraint 5: *Possible and impossible split-range combination of manipulated variables (these constraints are obtained from the information of active constraint regions)*

Constraint 5A: Impossible split-range combination of manipulated variables

"Impossible pair: two manipulated variables which are active constraints (saturated) at the same time cannot be combined as a split-range pair"

For an active constraint region R, we have

$$\sum_{i} \sum_{j \neq i} x_{i,j} = 0 \qquad \text{i, j} \in \textbf{MVAT}^{\textbf{A,R}} \qquad (151)$$

where $\textbf{MVAT}^{\textbf{A,R}}$ is the subset of **MVAT** with manipulated variables being active constraints in region R.

Constraint 5B: Possible split-range combination of manipulated variables

"Possible pair: two manipulated variables which are not active (inactive) constraint at the same time may be combined as a split-range pair"

For an active constraint region R, we have

$$x_{j,j} + \sum_{i \neq j} x_{i,j} \geq 1 \qquad \text{i} \in \textbf{MVAT}^{\textbf{I,R}}, \text{j} \in \textbf{MVAT}^{\textbf{A,R}} \qquad (152)$$

$$x_{i,i} + \sum_{j \neq i} x_{j,i} \geq 1 \qquad \text{i} \in \textbf{MVAT}^{\textbf{I,R}}, \text{j} \in \textbf{MVAT}^{\textbf{A,R}} \qquad (153)$$

where $\textbf{MVAT}^{\textbf{I,R}}$ is the subset of **MVAT** with manipulated variables being inactive constraints in region R

Combining objective function I and constraints 1-5, Problem P1 can be written,

Problem P1

$$\min J_I = \sum_i \sum_{j \neq i} x_{i,j} \qquad \text{i, j} \in \textbf{MV}$$

subject to equations (141) - (153)

By solving the problem P1, one obtains split-range pairs that can provide optimal switching between active constraint regions. However, the solution of problem P1 may be not unique. Hence, relative orders are introduced as an additional criterion for screening the set of poorly controllable structure solutions. The additional objective function and constraints are as follows:

Objective function II: *Minimizing the sum of relative order of the control pairs*

$$\min J_{II} = \sum_k \sum_j r_{k,j} z_{k,j} \qquad \text{k} \in \textbf{CV}, \text{j} \in \textbf{MV} \qquad (154)$$

Constraint 6*: Assign one manipulated variable to each control objective*

$$\sum_j z_{k,j} = 1 \qquad \text{k} \in \textbf{CV}, \text{j} \in \textbf{MV} \qquad (155)$$

Constraint 7*: Only primary manipulated variables are paired with controlled variables.*

If MV_j is a primary manipulated variable, it must be paired with a controlled variable

$$\text{If } x_{j,j} = 1 \text{ then } \sum_k z_{k,j} = 1 \qquad \text{k} \in \textbf{CV}, \text{j} \in \textbf{MV}$$

If MV_j is not a primary manipulated variable, it must not be paired

If $x_{j,j} = 0$ then $\sum_k z_{k,j} = 0$ k ∈ **CV**, j ∈ **MV**

therefore,

$$-x_{j,j} + \sum_k z_{k,j} = 0 \qquad \text{k} \in \mathbf{CV}, \text{j} \in \mathbf{MV} \qquad (156)$$

The ILP problem now concerns with two objective functions that can be solved using lexicographic optimization. In lexicographic optimization, the objectives are arranged in a decreasing order of preference and objectives with a higher preference are considered to be infinitely more important than those with lower orders. Among solutions that are optimal with respect to the first objective, solutions that are optimal with respect to the second objective are chosen.

Using the idea of lexicographic optimization, we first solve P1:

$$J_I^* = \min_x J_I(x), \qquad x \in S$$

where S is the feasible set and then solve an associated problem P1′:

$$\min_x J_{II}(x) \qquad x \in S,\ J_I = J_I^*(x)$$

which ensures that among minimized J_I solutions, the minimized J_{II} solutions are chosen. In principle, we need to solve 2 optimization problems in sequence. However, it is possible to solve P1 and P1′ as a single optimization problem by minimizing a weighted objective function $wJ_I + J_{II}$, where w is a sufficiently large positive number chosen appropriately. Suggestions for choice of w are given in Sherali (1982), and Sherali and Soyster (1983). Hence, we solve the following problem P2:

Problem P2

$$J = \min(wJ_I + J_{II}) \qquad \text{i, j} \in \mathbf{MV}, \text{k} \in \mathbf{CV}$$

$$J_I = \sum_i \sum_{j \neq i} x_{i,j}\ ,\ J_{II} = \sum_k \sum_j r_{k,j} z_{k,j}$$

subject to equations (141) - (153) and (155) - (156)

It can be seen that constraints 6 and 7 (equations 155 and 156) do not alter the feasible set for P1. The ILP problem P2 consists of two objective functions with a weighting factor (*w*) between the two. The first objective is used to minimize complexity when changing between active constraints whereas the second objective (controllability) is used to select the most controllable control structure. A large value of *w* will imply that the second objective (controllability) will only be considered when there are multiple solutions.

2. Literature Review

The simultaneous synthesis of flexible heat exchanger network was presented by Aaltola (2002) for generating flexible heat exchanger networks (HENs) over a specified range of variations in the flow rates and temperatures of the streams, so that the total annual costs (TAC) as a result of utility charges, exchanger areas and selection of matches are minimized. His work includes a multi-period simultaneous MINLP model to synthesize a flexible HENs configuration and a search algorithm involving multi-period LP/NLP model to overcome limitations related to the MINLP model. The result of work showed HENs which can work in varying conditions without losing stream temperature targets and can keep economically optimal energy integration.

In 1989, El-Halwagi and Manousiouthakis introduced the notion of synthesizing mass exchange networks (MENs). A two-stage used to find cost of MENs. In first stage, a thermodynamic procedure was used to identify the

thermodynamic bottleneck (pinch points) that limits the extent of mass exchanged between rich and lean process streams. Beginning networks are generated at this stage. In the second stage developed the beginning networks are developed to a final configuration of the MENs that satisfied the assigned exchange duty at minimum venture cost. Their methods could apply to the synthesis of MENs with single-component targets or multi-component compatible target.

Srinivas and El-Halwagi (1994) introduced the problem of synthesizing combined heat and reactive mass exchange networks (CHARMENs) that can simultaneously separate a certain pollutant from a set of rich streams to a set of mass-separating agents and perform the specified heat transfer task in a cost-effective way. The proposed work introduces a systematic and generally applicable procedure to trade-off the two objectives and synthesize a CHARMENs. The first target is to minimize the cost of MSAs and heating/cooling utilities. The minimum operating cost (MOC) solution of the network is identified via a mixed-integer nonlinear program (MINLP). In the second stage, the minimum number of heat and reactive mass-exchange units which can realize the MOC solution will be generated. This target aims at minimizing the fixed cost of the network. In addition, they present a method for synthesizing near-optimal CHARMENs. Finally, an example problem is solved to elucidate the various aspects of the proposed synthesis procedure.

A simple strategy for the synthesis of flexible heat exchange networks (HENs) or mass exchange networks (MENs) was proposed by Chen and Ping (2007) that involves expected disturbance range in the flow rates and temperatures (for HENs) or compositions (for MENs) of the inlet process streams. Several numerical examples were supplied to demonstrate the applicability of the proposed strategy for the synthesis of flexible heat exchange networks or mass exchange networks. The problem of optimization is done based on the stage-wise superstructure in order to get a minimum total annual cost (TAC).

Porsom (2008) developed a systematic approach of an optimal operation for heat exchanger networks (HENs). In his work, HENs are synthesized by mixed-

integer non-linear programming (MINLP) from given hot and cold stream data to minimize the total annual cost (TAC). Linear programming (LP) is used to propose the final flexible HENs for design of control structure. Next, an optimal split-range control structure is determined by integer linear program (ILP). Finally, the proposed configurations are verified by dynamics simulation.

Lersbamrungsuk (2007) proposed a new simple technique to implement optimal operation of HENs. For certain HENs that only single bypasses and utility duties are considered as manipulated variables. The optimal operation of HENs can be formulated as a linear programming (LP) problem. The LP formulation implies that optimal solutions will always lie at some input constraint vertices.

MATERIALS AND METHODS

Materials

1. Laptop
   (a) CPU (Intel Core2Duo CPU 1.66 GHz)
   (b) 2.00 GB of RAM
   (c) 160 GB of hard disk
2. Operating System: Microsoft Window XP
3. Software
   (a) GAMS (General Algebraic Modeling System) versions 22.8 Beta
   (b) MATLAB version 2009a
   (c) Aspen Plus version 7.0
   (d) Aspen Dynamics version 7.0

Methods

1. Overall Methodology

An approach of simultaneous MINLP superstructure and NLP feasibility models for synthesizing flexible HENs, MENs and CHAMENs is proposed in this work. The main steps are represented in this work as follows:

1.1 The flexible HENs, MENs and CHAMENs are generated.

1.2 The active constraint regions can be formulated.

1.3 The optimal split-range control structure can be determined.

1.4 The control structure is dynamically tested.

2. Synthesis of flexible HENs, MENs and CHAMENs

In the past research (Chen and Hung, 2007; Porsom, 2008; Thunyawart 2010), there formulate the optimum configuration of HENs, MENs and CHAMENs by individual step by step (Figure 5). The first step is synthesis configuration for minimizing the total annual cost. The HENs, MENs and CHAMENs can be synthesized by means of any existing mixed-integer nonlinear optimization algorithm (MINLP model). The second step is feasibility test for minimizing slack variables by nonlinear optimization algorithm (NLP model). This step uses a lot of testing conditions generated randomly within the possible operating ranges to examine the flexibility of the network resulting from pervious synthesis step. The flexibility is determined by using the random points simulation in order to take into account the possibility of nonextreme critical points. If the resulting flexibility does not accepted, then a new network candidate with improved operational flexibility must be found.

For this work, there formulate the optimum configuration of HENs, MENs and CHAMENs by one step (Figure 6). That is the flexibility requirement is directly taken into account in the synthesis step to reduce the times step. The new approach is simultaneous MINLP model and NLP model to synthesizing a superstructure and the optimal configuration are proposed. There is optimizing to find the answer by the objective function is the minimizing annual cost and the minimizing slack variables.

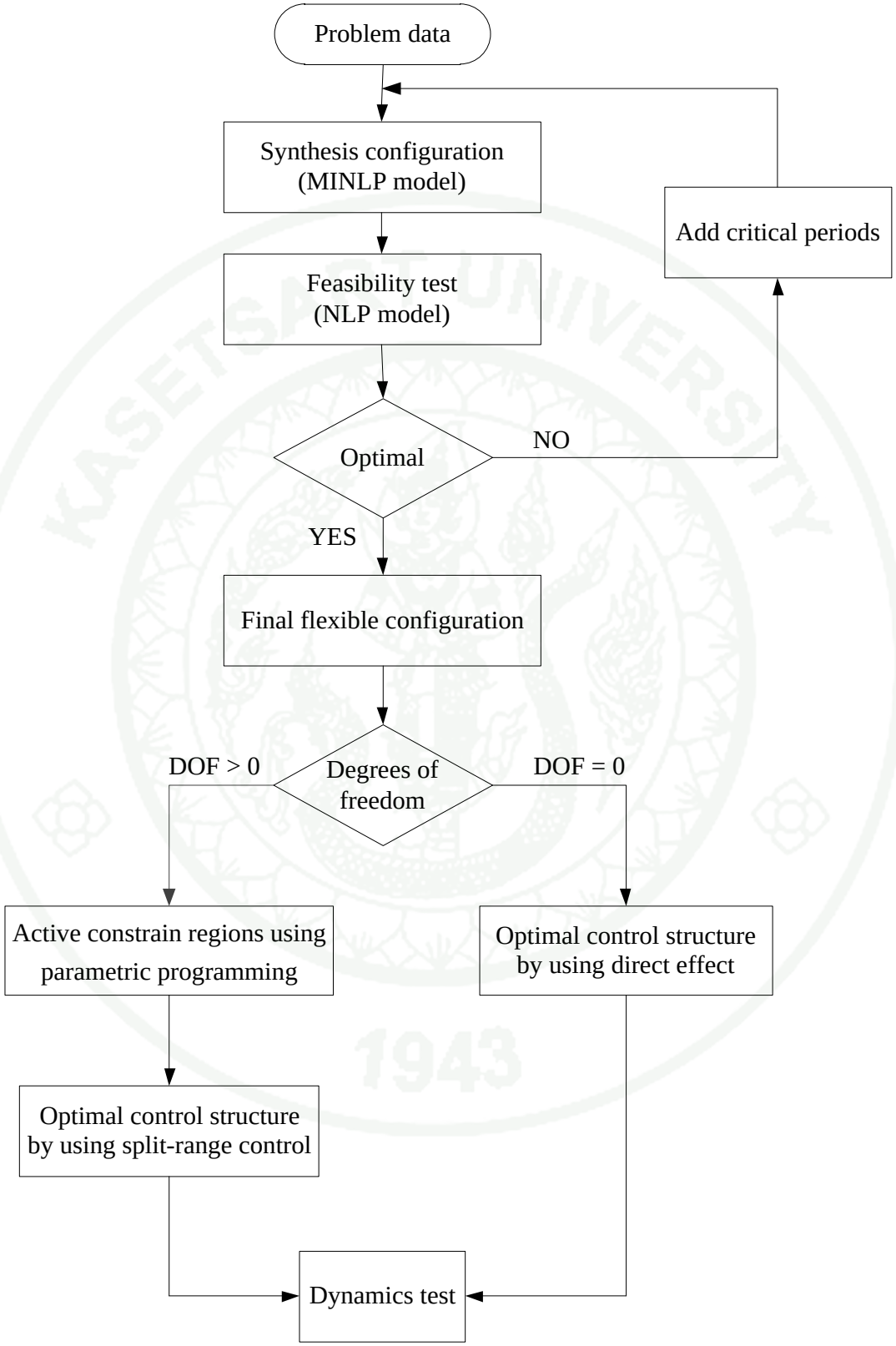

Figure 5 Systematic procedure in the past research

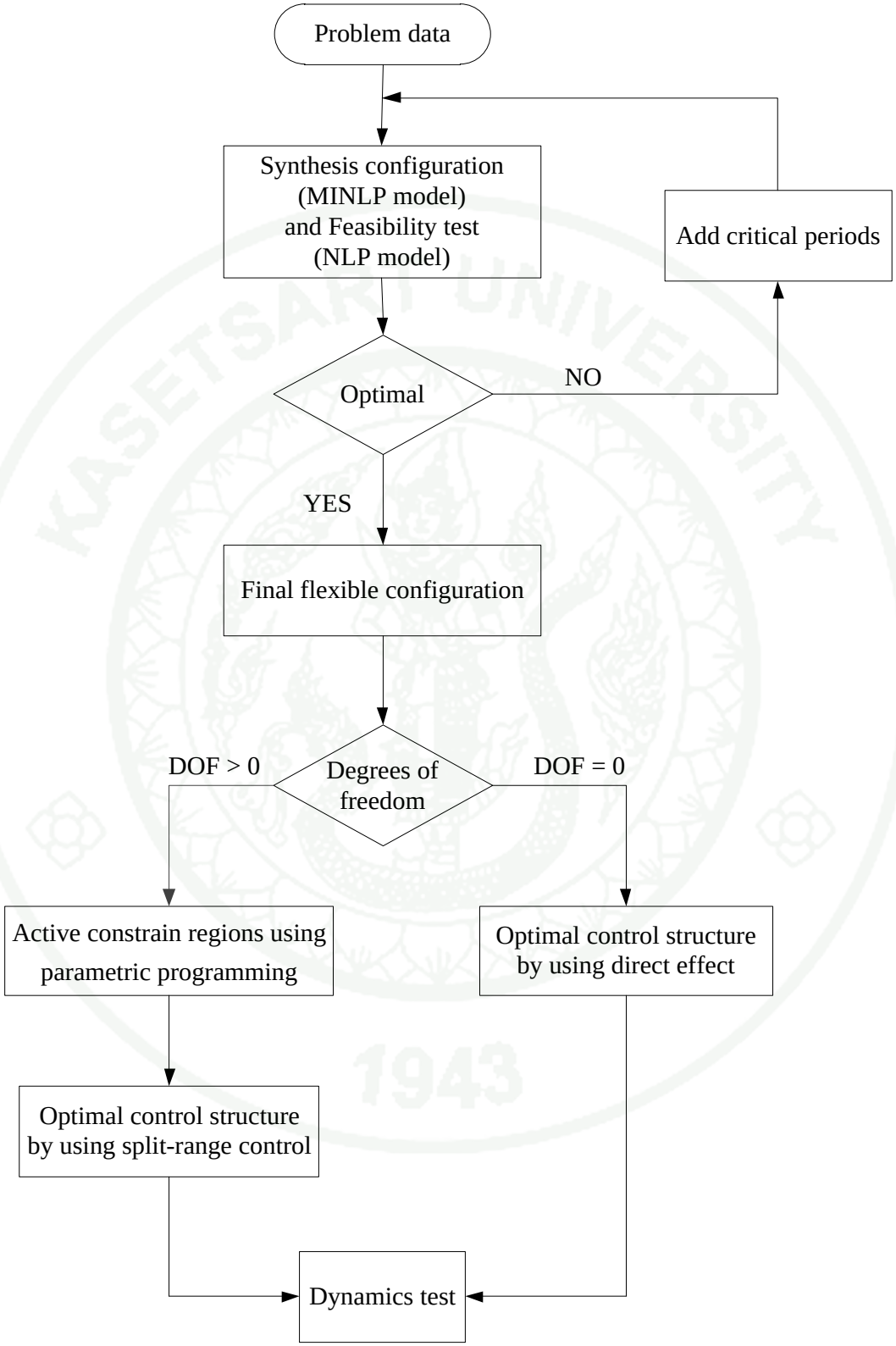

Figure 6 Systematic procedure approach in this work

3. Switching between active constraints

In this research, we design the control structure for network by applying the spilt-range control to keep target of HENs, MENs and CHAMENs.

Split-range controllers are commonly used to adjust two or more manipulated variables to keep target of process with a single controller. A technique using structural information (sign matrix) to find a control structure was proposed by Mathisen (1994) and Glemmestad *et al.* (1996). They commented that in most cases the resulting control structure can be implemented in a split-range control manner. When two manipulated variables are used in a split-range controller, one of them is referred as primary manipulated variable and the other as a secondary manipulated variable. The primary manipulated variable can be thought of as the manipulated variable that is used to control a target under the nominal condition. However, the final choice of primary and secondary manipulated variables can be based on other considerations also. This flexibility will be exploited in the final control structure design.

Hence, we must find the active constraint regions before design the spilt-range control. This section describes methods to implement the optimal policy by tracking the changing set of active constraints. The assumptions are:

- Target of networks are feasible for the given disturbance window (output constraints do not change).

- The output constraints do not change and are always active. The optimal point is a vertex, i.e., at the intersection of constraints, and hence a certain number of inputs are at the constraints.

The optimal solution has the following properties:

a) The set of active constraints remains constant in a certain region of the disturbance space. The largest region in the disturbance space where the set of active constraints remains the same is known as critical region. Critical regions are polyhedral in shape for a linear programming (LP) and can be determined using off-line optimization or parametric programming tools (Kvasnica *et al.*, 2004).

b) If there are two or more critical regions in the given disturbance window, from the definition of critical region, it follows that the set of constraints are different. Since the output constraints do not change, it follows that the set of input constraints are different in each critical region. At the interface between two neighboring critical regions, constraints corresponding to both critical regions are active (which is a degenerate LP solution). However, since this constitutes a set of measure zero (i.e., the probability of being exactly on the boundary is zero), it does not affect the controllability properties of the network on the whole.

Using these properties of the optimal solution, it is possible to operate the networks optimally using the following procedure:

a) In a given critical region R_o, it is possible to operate the networks optimally using a decentralized control structure where some manipulated variables are used to control the output constraints using SISO control loops with zero steady state error, for example, PI controllers. The remaining manipulated variables are maintained at the constraints.

b) If the disturbances are such that we have moved from R_o to a different region R_1, it is possible to implement the optimal policy in R_1 by tracking the transition or change in active constraints.

Supposing that a system comprises of 3 manipulated variables and 2 controlled variables. Hence, 2 manipulated variables are needed for control.

Furthermore, since one optimal solution is always at input constraints, the remaining manipulated variables may be at constraints (saturated). For a given operating window, active constraint regions can be found by parametric programming and the results are summarized as shown in Table 2 and Figure 2.

Table 2 Set of active constraints for example process

Region	MV_1	MV_2	MV_3
1	S	U	U
2	U	U	S
3	U	S	U

U - Unsaturated manipulated variable (inactive constraint) to be used for control

S - Saturated manipulated variable (active constraint)

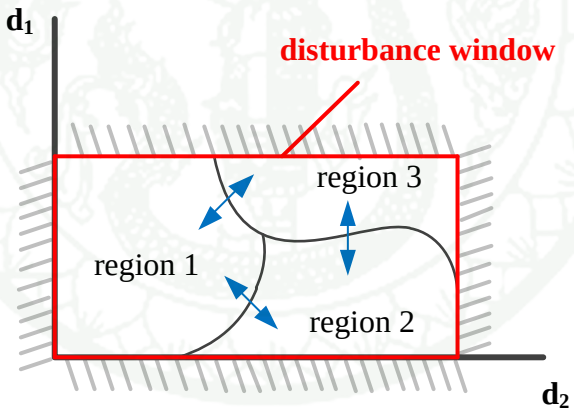

Figure 7 Active constraint regions

Thus, in region 1, it is optimal to use MV_2 and MV_3 to control the outputs T1 and T2 respectively using SISO PI control loops and keep MV_1 at constraint. When moving into region 2, MV_3 saturates and so, the optimal policy is to keep MV_3 at the constraint and instead use MV_1 as a manipulated variable for control. Thus MV_1 and MV_2 are used for control in region 2. Likewise, in region 3, the optimal policy is to control T1 and T2 using MV_1 and MV_3 and keep MV_2 at constraint. It is possible to keep tracking the regions under the changes in active constraints. When the new

region is determined, the optimal policy corresponding to the new region is implemented.

To extend the application of split-range control to implement optimal operation of chemical processes, let us show a motivation example on a scrubber as shown in Figure 8. There are two types of MSA (MSA A and MSA B) for using in the scrubber. Assume that MSA A is cheaper than MSA B. Hence, to operate the scrubber in an optimal manner (minimizing MSA cost), MSA A should be used in the nominal condition while MSA B should be a supplementary (e.g. the flow of MSA A reaches the upper limit). When MSA A is in use, the flow of MSA B presents the active constraint (saturated) at the lower bound. And when MSA B is in use (i.e. the flow of MSA A reaches the maximum limit), the flow of MSA A present at the active constraint (saturated) at the upper bound. This optimal operation can be implemented using split-range control.

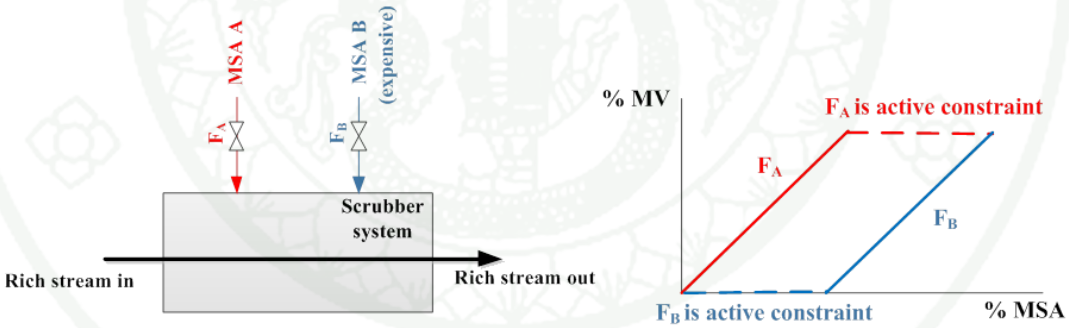

Figure 8 A scrubber system

For this scrubber system in Figure 8, suppose that optimal operation always lies at the constraints of F_A or F_B depending on the variation of the desired outlet mass fraction. Hence, the active constraint regions can be divided to two regions as summarized in Table 3. In the two regions, F_A and F_B switch alternately as active constraint. For this example, the set of active constraints can be found obviously by inspection. However, for more complicated systems, a systematic method is required.

In general, parametric programming (Kvasnica *et al.*, 2004) can be served for this task.

Table 3 Set of active constraints for furnace system

Region	F_A	F_B
1	U	S
2	S	U

U - Unsaturated manipulated variable (inactive constraint) to be used for control

S - Saturated manipulated variable (active constraint)

4. Design of optimal split-range control structure

The optimal split-range control structure design consisting of three steps which are

Step 1: The number of degrees of freedom with respect to utility cost optimization ($N_{DOF,U}$) are checked because only the system with some degrees of freedom for optimization will be considered. (Glemmestad, 1997)

- For systems in which no degree of freedom is available for optimization, the optimal operation can be reduced as control problems. (e.g. control pairing problems that can be handled using direct effect or RGA input saturation problem or input constraint problems (Giovanini *et al.*,2003))

- For systems in which some degrees of freedom are available for optimization, go further to step 2.

Step 2: Find active constraint regions using parametric programming. (e.g. with MPT toolbox (Kvasnica *et al.*,2004))

Step 3: An optimal split-range control structure can be found using Problem P2. (Lersbamrungsuk, 2007)

RESULTS AND DISCUSSION

The results can be divided into four parts. The first part shows simultaneous MINLP model and NLP model for feasibility test to get a superstructure of five examples adapted from literatures. The second part is the simulation of the synthesized networks using Aspen Plus to ensure the optimal target approach. The third part, we find optimal control structure. And, the last section is the test of dynamics response for all control design In this work, five case studies are implemented; case study 1 is HENs problem from Thunyawart (2010), case study 2 is MENs problem from by El-Halwagi and Manousiouthakis (1989), case study 3 is large scale HENs from Fieg *et al*. (2009), case study 4 is MENs combining with external utilities (CHAMENs) and case study 5 is the special case of MENs with simultaneous integration of the heat system (CHAMENs).

Case study 1: Heat integration system for 7 process streams

The HENs information was from Thunyawart (2010). This example consists of three hot and four cold process streams, with one hot and one cold utility. The problem data is given in Table 4. The disturbances are the inlet temperatures of all hot streams with the expected variation ±10 °C. The cost equation for an exchanger is \$700 + 175 (Area) $^{0.8}$ (Area unit in m^2) and the minimum approach temperature equal to 10 °C.

Table 4 Problem data for the case study 1

Stream	*TIN* (°C)	*TOUT* (°C)	*FCp* (kW/°C)	*h* (kW/m^2°C)	Cost ($/kW-yr)
H1	650	370	10	1	-
H2	590	370	20	1	-
H3	190	30	15	1	-
C1	410	650	15	1	-
C2	353	500	13	1	-
C3	80	167	5	1	-
C4	20	160	5	1	-
S1	800	800	-	3.4	80
W1	20	30	-	1.7	15

The stage-wise superstructure approach is applied to synthesize the problem. To solve the multi-period simultaneous MINLP synthesis model incorporating with NLP feasibility test model. General Algebraic Modeling System (GAMS) is used as the main solution tool. The solvers used are "DICOPT" for MINLP, "MINOS" for NLP and "CPLEX" for mixed-integer programming (MIP).

Results for this case are illustrated in Table 5 and Figure 9. We find that in addition to the five periods uncertain parameters that allowing the inlet temperature to change ±10%. It has five heat exchangers in four stages and the total annual cost is 262,225 $/year, which included the cost for cooling and heating utilities is 150,562 $/year. Figure 9 shows the optimal network.

Table 5 Result data (Multi-period) for the case study 1

Period	Stream	*TIN* (°C)	*TOUT* (°C)	*FCp* (kW/°C)	*h* (kW/m^2 °C)	Cost ($/kW-yr)
1	H1	650	370	10	1	-
	H2	590	370	20	1	-
	H3	190	30	15	1	-
	C1	410	650	15	1	-
	C2	353	500	13	1	-
	C3	80	167	5	1	-
	C4	20	160	5	1	-
2	H1	645	370	10	1	-
	H2	587	370	20	1	-
	H3	200	30	15	1	-
	C1	410	650	15	1	-
	C2	353	500	13	1	-
	C3	80	167	5	1	-
	C4	20	160	5	1	-
3	H1	660	370	10	1	-
	H2	580	370	20	1	-
	H3	180	30	15	1	-
	C1	410	650	15	1	-
	C2	353	500	13	1	-
	C3	80	167	5	1	-
	C4	20	160	5	1	-

Table 5 (Continued)

Period	Stream	*TIN* (°C)	*TOUT* (°C)	*FCp* (kW/°C)	*h* (kW/m^2 °C)	Cost ($/kW-yr)
4	H1	648	370	10	1	-
	H2	595	370	20	1	-
	H3	196	30	15	1	-
	C1	410	650	15	1	-
	C2	353	500	13	1	-
	C3	80	167	5	1	-
	C4	20	160	5	1	-
5	H1	640	370	10	1	-
	H2	600	370	20	1	-
	H3	184	30	15	1	-
	C1	410	650	15	1	-
	C2	353	500	13	1	-
	C3	80	167	5	1	-
	C4	20	160	5	1	-
	S1	800	800	-	3.4	80
	W1	20	30	-	1.7	15

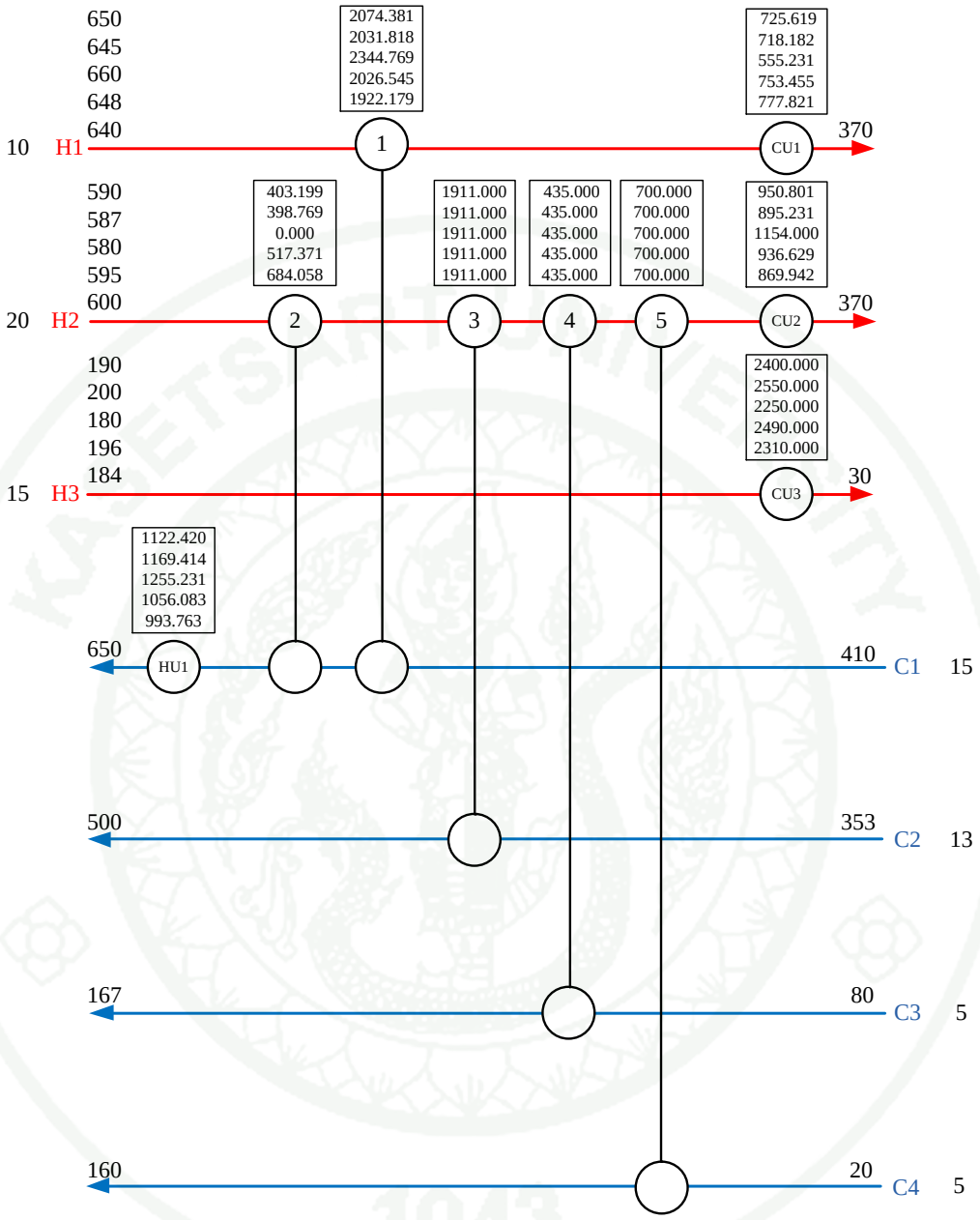

Figure 9 Optimal network configurations for case study 1

To ensure the overall heat balance and the thermal specification of the synthesis problem, we simulate using Aspen Plus as shown in Figure 10. The result is shown in Table 6 which indicates that the heat duty of utilities and area of heat exchanger. We found that the results given by GAMS and Aspen Plus are not much difference. The difference may be from the assumptions used in the synthesis model

(e.g. the constant pressure, constant heat capacity). From the result, we can conclude that the optimal HENs obtained from GAMS acceptable. In addition, the total annual cost obtained from this work is lower than the result of Thunyawart (2010).

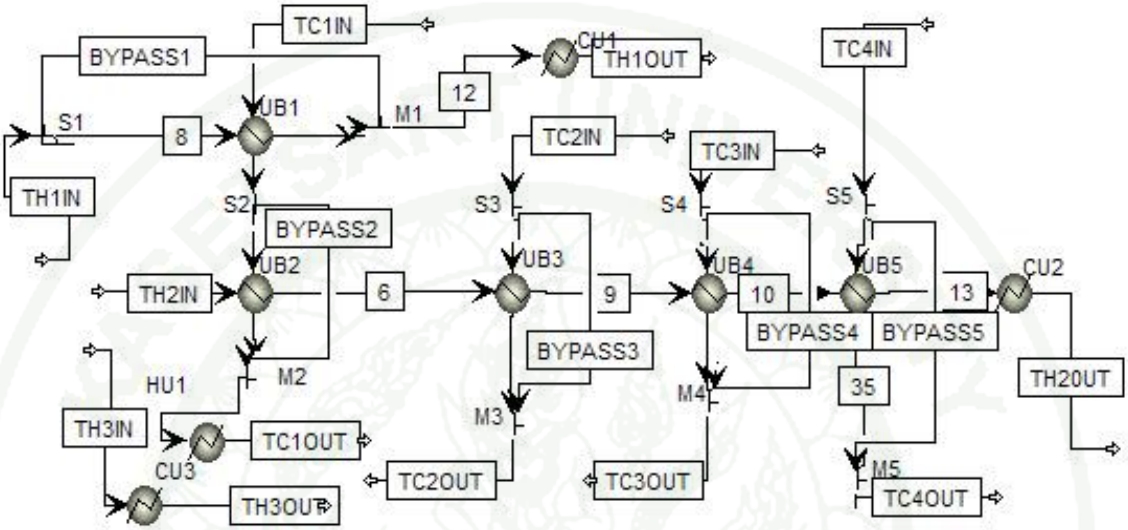

Figure 10 Optimal network configurations for case study 1 on Aspen Plus

Table 6 Targets verification on Aspen Plus for case study 1

Targets	GAMS result	Aspen result	% Relative Difference
Heating utility (kW)	1255.23	1208.57	3.72
Cooling utility (kW)	4481.82	4581.46	2.17
Total Area (m^2)	237.73	302.04	21.29

After that, degrees of freedom (DOFs) are checked. The manipulated variables in the inner HENs to the outer HENs are 5. Number of utility are 4 and number of target temperatures are 7. We can obtain $N_{DOF,U}$ = 5+4-7 = 2. This case have two degree of freedom for utility cost optimization. Therefore, a strategy for optimal operation is needed.

And then, the information set of active constraints will be used to design optimal split-range control structure. The multi-parametric toolbox (Kvasnica *et al.*, 2004) is used to find active constraint regions as shown in Table 7.

Table 7 Set of active constraints in case study 1

Region	Manipulated variables								
	Q_{c1}	Q_{c2}	Q_{c3}	Q_{h1}	u_{b1}	u_{b2}	u_{b3}	u_{b4}	u_{b5}
1	U	U	U	S_U	S_L	U	U	U	U
2	U	U	U	U	S_L	S_L	U	U	U

U - Unsaturated manipulated variable (inactive constraint)

S_L - Saturated manipulated variable (active constraint) at the lower bound

S_U - Saturated manipulated variable (active constraint) at the upper bound

Table 7 demonstrates that the manipulated variables Q_{h1} and u_{b2} switch alternately to become active constraints when they are combined as a split-range pair. Since the manipulated variables u_{b1} is always saturated; therefore, it is not used for control. Furthermore, the manipulated variables Q_{c1}, Q_{c2}, Q_{c3}, u_{b3}, u_{b4} and u_{b5} have never saturated, so there is no need of split-range combinations.

Relative orders show relationship between manipulate variables and controller outputs. In Table 8, relative order equal to 1 represents that controller output is extremely changed when a manipulated variable is adjusted. If relative order is increased, controller output will be slightly changed when manipulated variable is adjusted. Moreover, relative order at ∞ represents that controller output cannot change (no effect) that manipulated variable is adjusted. This implies that manipulated variable adjustment has increasingly less effect on controller output change as relative order approaches ∞.

Table 8 Relative orders of the HENs in the case study 1

MV / CV	Q_{c1}	Q_{c2}	Q_{c3}	Q_{h1}	u_{b1}	u_{b2}	u_{b3}	u_{b4}	u_{b5}
TH_1^{out}	1	∞	∞	∞	2	∞	∞	∞	∞
TH_2^{out}	∞	1	∞	∞	∞	5	4	3	2
TH_3^{out}	∞	∞	1	∞	∞	∞	∞	∞	∞
TC_1^{out}	∞	∞	∞	1	3	2	∞	∞	∞
TC_2^{out}	∞	∞	∞	∞	∞	2	1	∞	∞
TC_3^{out}	∞	∞	∞	∞	∞	3	2	1	∞
TC_4^{out}	∞	∞	∞	∞	∞	∞	∞	2	1

Then, the GAMS software is used to solve the ILP problem. The results are optimal split-range control structure. The values of binary variables $x_{i,j}$ and $z_{k,j}$ from solving problem are shown in Tables 9 and 10, respectively. In Table 9, there are primary manipulated variables (Q_{c1}, Q_{c2}, Q_{c3}, u_{b2}, u_{b3}, u_{b4} and u_{b5}) and the secondary manipulated variable (Q_{h1} for u_{b2}). If the primary manipulated variable, u_{b2}, is saturated, the secondary manipulated variable, Q_{h1}, is used to control output. Table 10 shows the control pairing, the direct effect, which are TH_1^{out} - Q_{c1}, TH_2^{out} - Q_{c2} , TH_3^{out} - Q_{c3} , TC_1^{out} - u_{b2}, TC_2^{out} - u_{b3} , TC_3^{out} - u_{b4} and TC_4^{out} - u_{b5}. The resulting control structure is shown in Figure 11.

Table 9 The value of $x_{i,j}$ after solving problem for the case study 1

Pri MV \ Sec MV	Q_{c1}	Q_{c2}	Q_{c3}	Q_{h1}	u_{b2}	u_{b3}	u_{b4}	u_{b5}
Q_{c1}	1							
Q_{c2}		1						
Q_{c3}			1					
u_{b2}				1	1			
u_{b3}						1		
u_{b4}							1	
u_{b5}								1

(the remaining entries are zero)

Table 10 The value of $z_{k,j}$ after solving problem for the case study 1

CV \ MV	Q_{c1}	Q_{c2}	Q_{c3}	u_{b2}	u_{b3}	u_{b4}	u_{b5}
TH_1^{out}	1						
TH_2^{out}		1					
TH_3^{out}			1				
TC_1^{out}				1			
TC_2^{out}					1		
TC_3^{out}						1	
TC_4^{out}							1

(the remaining entries are zero)

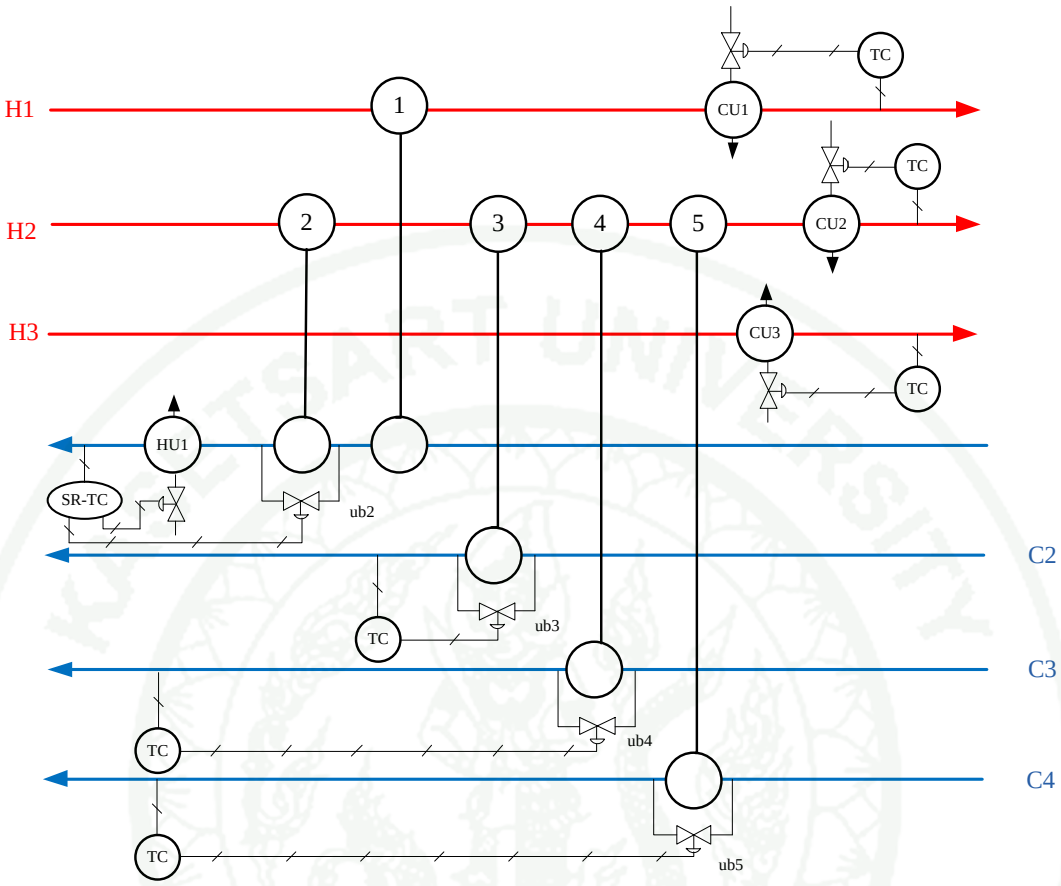

Figure 11 The control structure for the case study 1

Figure 11 shows that the split-range signal of the pair of Q_{h1} and u_{b2} switch alternately to their lower constraints (SR-TC is split-range temperature control).

Table 11 Disturbances and active constraints in the HENs

Time (sec)	Disturbance of Temperature							Active constraint	
	ΔTH_1^{in}	ΔTH_2^{in}	ΔTH_3^{in}	ΔTC_1^{in}	ΔTC_2^{in}	ΔTC_3^{in}	ΔTC_4^{in}	Q_{h1}	u_{b2}
<5	0	0	0	0	0	0	0	S_U	U
5-15	-10	-10	-10	+5	+5	0	0	S_U	U
15-25	-10	-10	+10	-5	-5	0	0	U	S_L
25-35	0	0	0	0	0	0	0	S_U	U

U - Unsaturated manipulated variable (inactive constraint)

S_L - Saturated manipulated variable (active constraint) at the lower bound

S_U - Saturated manipulated variable (active constraint) at the upper bound

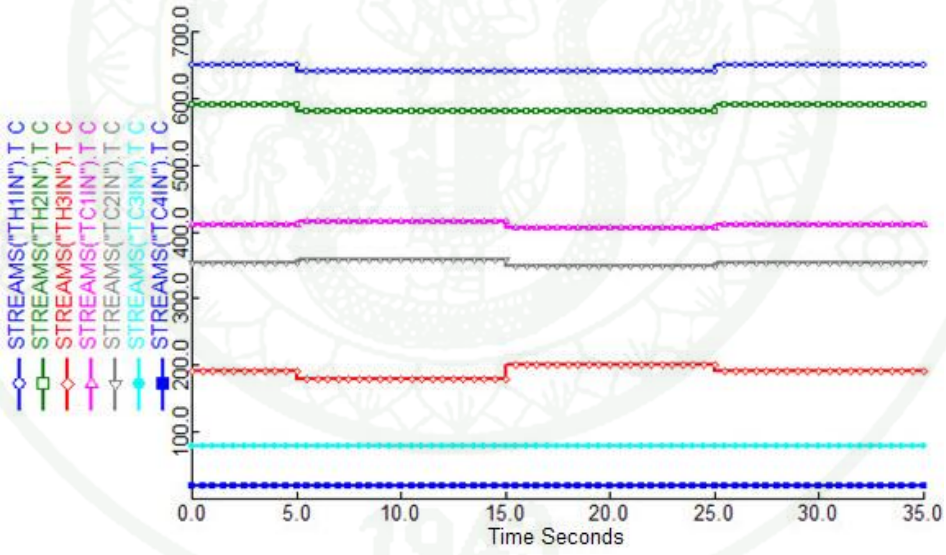

(a) Inlet temperatures

Figure 12 Dynamics simulation of the HENs in case study 1 (a) Inlet temperatures, (b) Hot stream target temperatures, (c) Cold stream target temperatures and (d) Manipulated variables (Q_{h1} and u_{b2})

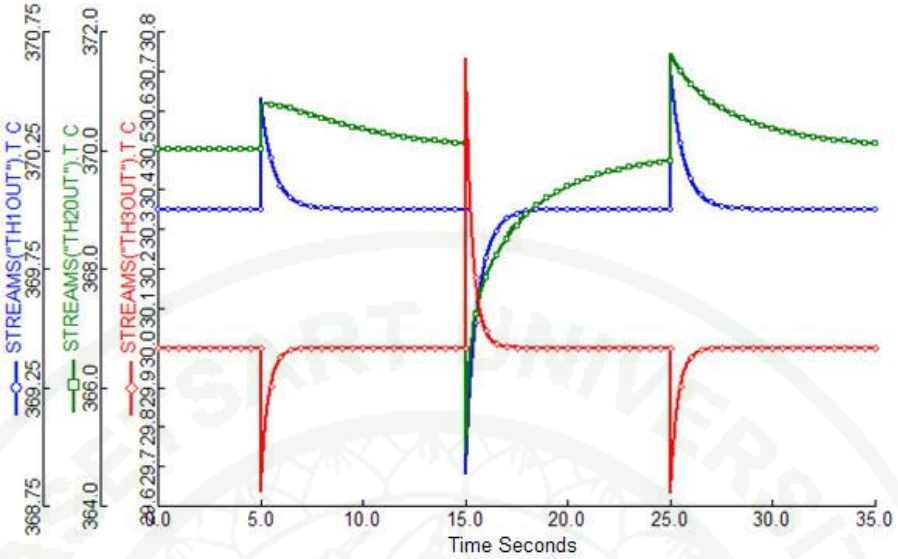

(b) Hot stream target temperatures

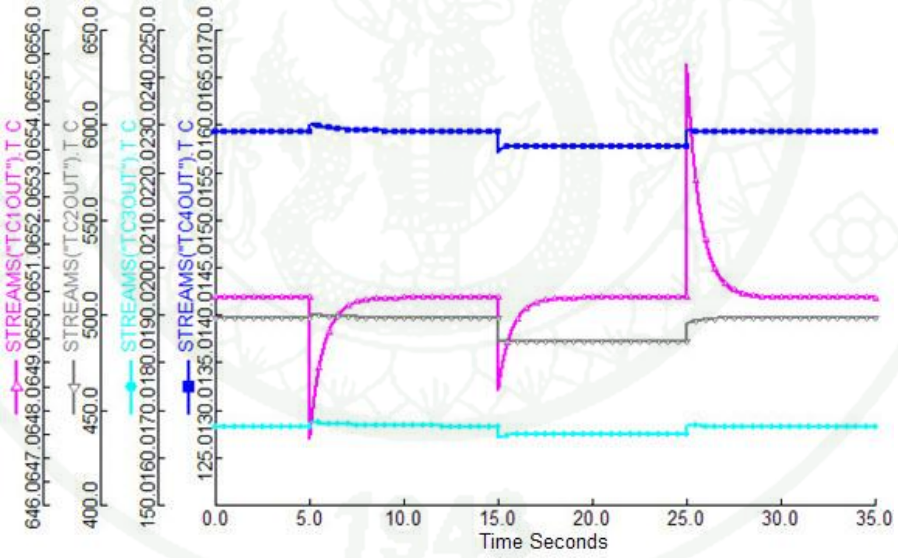

(c) Cold stream target temperatures

Figure 12 (Continued)

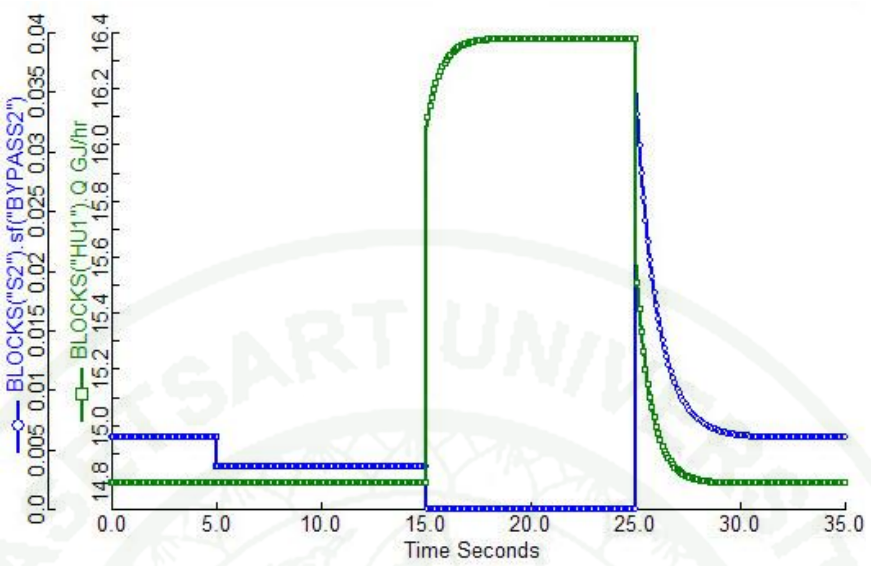

(d) Manipulated variables (Q_{h1} and u_{b2})

Figure 12 (Continued)

The results of control structures in HENs for this case are tested by performing dynamics simulation on Aspen Dynamics. The information regarding the disturbances and active constraints of the system is shown in Table 11. The dynamic results show that the control structures can provide optimality. Figure 12 shows the dynamic result of the HENs with the control structure. Figure 12b and 12c show the controllability of the control structure to keep all target temperatures. Figure 12d shows the response of split-range control that u_{b2} is primary manipulated variable and Q_{h1} is secondary manipulated variable to keep temperature of TC_1^{out}.

Case study 2: Sweetening of COG process

This case study was introduced by El-Halwagi and Manousiouthakis (1989) as shown in Figure 13. The MENs problem of Coke-Oven Gas (COG) sweetening is to remove acidic impurities, especially hydrogen sulfide (H_2S), from COG - a mixture of H_2, CH_4, CO, N_2, NH_3, CO_2, and H_2S. Hydrogen sulfide is an impurity that should be removed because of its corrosive. The two solvents used are aqueous ammonia (L1) and chilled methanol (L2) to absorb required amounts of H_2S in the sour COG (R1). The acid gases are then stripped out from solvents in a solvent regeneration unit and the regenerated MSAs are recirculated. The stripped acid gases are fed to a Claus unit where sulfur is recovered from hydrogen sulfide. The tail gases leaving the Claus unit, R2, is concerned in the view of air-pollution control and should be treated to remove hydrogen sulfide.

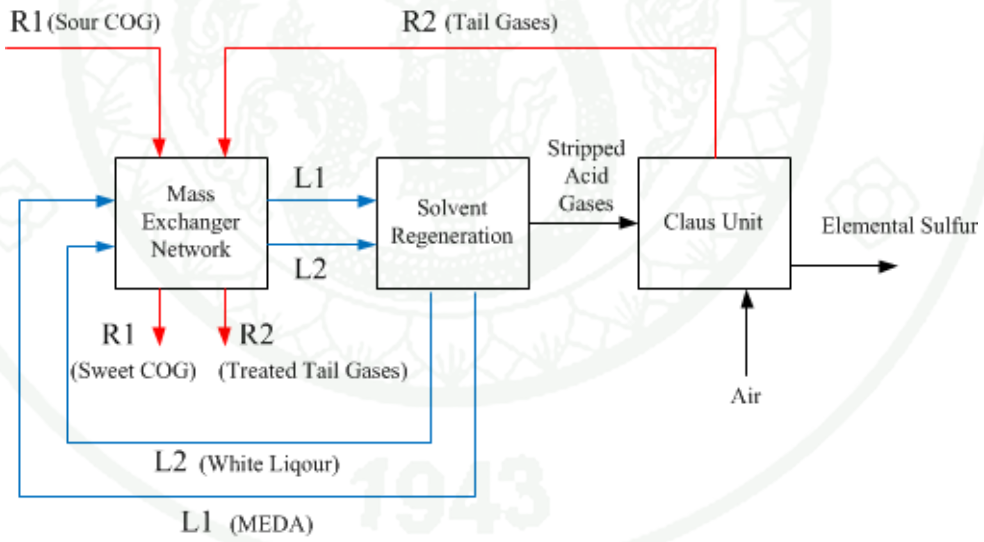

Figure 13 MENs for the COG sweetening

Source: El-Halwagi and Manousiouthakis (1989)

The stream data for this case study is shown in Table 12. The equilibrium solubility data for H_2S in 15 %wt Methyl-Di-Methanol-Amide (MDEA) and White Liquor can be correlated by the following relation, respectively.

For 15 %wt MDEA: $y^{H_2S} = 1.168x_1^{H_2S}$ at 330 °C

White Liquor: $y^{H_2S} = 0.344x_2^{H_2S}$ at 368 °C

Table 12 Problem data for the case study 2

Rich streams	Description	G_i (kg/s)	Mass fraction	
			YIN	*YOUT*
R1	Sour COG)	4.3	0.070	0.0003
R2	Tail gases	1.6	0.051	0.0001

MSA	Description	L_j^{up} (kg/s)	Mass fraction		Annual cost ($/kg-yr)
			XIN	*XOUT*	
L1	MDEA	11.8	0.0006	0.0310	117,360
L2	White Liquor	∞	0.0002	0.0035	174,060

Results for case study 2 are illustrated in Table 13 and Figure 14. We find that in addition to the five periods uncertain parameters. The disturbances, mass fraction, are between ±0.02%w/w for R_1 and ±0.01%w/w for R_2 in five periods. There are three mass exchangers and the total annual cost is 2,911,101 $/year. The cost of MSAs is 2,758,814 $/year.

Table 13 Result data (Multi-period) for the case study 2

Period	streams	Flowrate (kg/s)	Mass fraction	
			IN	*OUT*
1	R1	4.3	0.07	0.0003
	R2	1.6	0.051	0.0001
	L1	9.79	0.0006	0.031
	L2	23.315	0.0002	0.0035
2	R1	4.3	0.05	0.0003
	R2	1.6	0.052	0.0001
	L1	9.79	0.0006	0.031
	L2	23.315	0.0002	0.0035
3	R1	4.3	0.06	0.0003
	R2	1.6	0.061	0.0001
	L1	9.79	0.0006	0.031
	L2	23.315	0.0002	0.0035
4	R1	4.3	0.084	0.0003
	R2	1.6	0.048	0.0001
	L1	9.79	0.0006	0.031
	L2	23.315	0.0002	0.0035
5	R1	4.3	0.09	0.0003
	R2	1.6	0.041	0.0001
	L1	9.79	0.0006	0.031
	L2	23.315	0.0002	0.0035

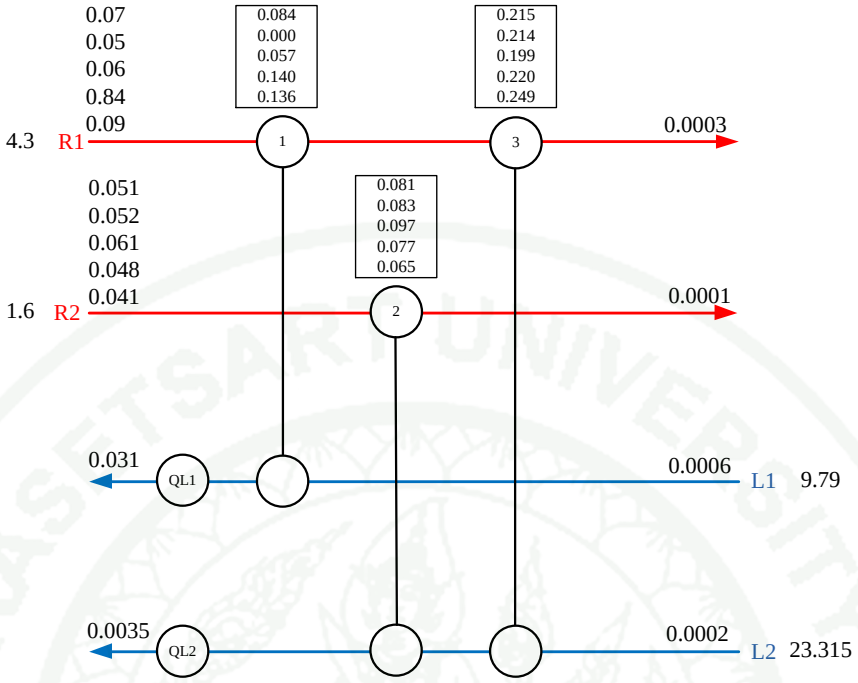

Figure 14 Optimal network configurations for case study 2

After that, Aspen Plus was used as shown in Figure 15 to ensure the overall mass balance and the mass fraction of H_2S of the synthesized. The result is shown in Table 14 which indicates that the outlet mass fraction of H_2S is corresponding to the target of the process. From the result, we can conclude that the optimal MENs obtained from GAMS acceptable. In addition, the total annual cost obtained from this work is better than the result from Thunyawart (2010).

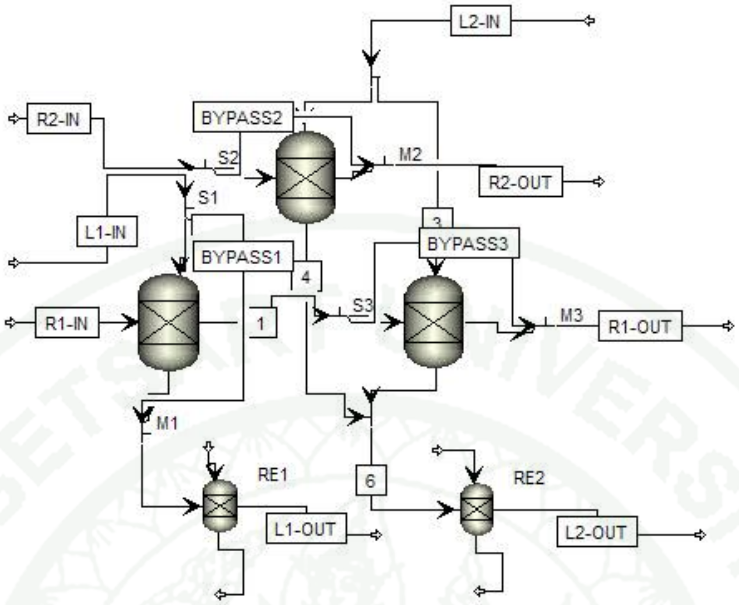

Figure 15 Optimal MENs for COG process on Aspen Plus

Table 14 Targets verification on Aspen Plus for case study 2

Targets	GAMS result	Aspen result	% Relative difference
Flowrate of L1 (kg/s)	9.79	9.79	-
Flowrate of L2 (kg/s)	25.315	25.315	-
Mass fraction of H_2S in R1	0.0003	0.00032	6.25
Mass fraction of H_2S in R2	0.0001	0.0001	-
Mass fraction of H_2S in L1	0.031	0.032	3.23
Mass fraction of H_2S in L2	0.0035	0.0034	2.86

In the next step, the degrees of freedom of the optimal MENs are checked. In this case, the $N_{DOF,U}$ = 3+2-4 = 1. There is one degree of freedom for utility optimization. Because of this, a strategy for optimal operation is needed.

Then, the information set of active constraints are required to design the optimal split-range control structure. The multi-parametric toolbox (Kvasnica *et al.*,

2004) is used to find active constraint regions. In this case study, we generate two active constraint regions as shown in Table 15.

Table 15 Set of active constraints in case study 2

Region	Manipulated variables				
	Q_{L1}	Q_{L2}	u_{b1}	u_{b2}	u_{b3}
1	S_L	U	U	U	U
2	U	U	S_L	U	U

U - Unsaturated manipulated variable (inactive constraint)

S_L - Saturated manipulated variable (active constraint) at the lower bound

This table indicates that the manipulated variable Q_{L1} and u_{b1} switch alternately to become active constraints and should be combined as a split-range pair. Q_{L2}, u_{b2} and u_{b3} are never saturated; hence, there are no needs for secondary manipulated variable. And Table 16 shows the relationship between manipulated variables and controller outputs by relative order.

Table 16 Relative orders of the MENs in the case study 2

MV / CV	Q_{L1}	Q_{L2}	u_{b1}	u_{b2}	u_{b3}
R_1^{out}	∞	∞	2	1	∞
R_2^{out}	∞	∞	∞	∞	1
L_1^{out}	1	∞	2	∞	∞
L_2^{out}	∞	1	∞	∞	2

The optimal split-range control structure can obtain by solving an ILP with GAMs software. The values of binary variables $x_{i,j}$ shown in Tables 17, there are primary manipulated variables (Q_{L2}, u_{b1}, u_{b2} and u_{b3}) and the secondary manipulated variable (Q_{L1} for u_{b1}). If the primary manipulated variable, u_{b1}, is saturated, the secondary manipulated variable, Q_{L1}, is used to control output. And Table 18, $z_{k,j}$ from

solving problem shows the control pairing, the direct effect, which are R_1^{out} - u_{b3}, R_2^{out} - u_{b2}, L_1^{out} - u_{b1} and L_2^{out} - Q_{L2}. The resulting control structure is shown in Figure 16.

Table 17 The value of $x_{i,j}$ after solving problem for the case study 2

Pri MV \ Sec MV	Q_{L1}	Q_{L2}	u_{b1}	gu_{b2}	u_{b3}
Q_{L2}		1			
u_{b1}	1		1		
u_{b2}				1	
u_{b3}					1

(the remaining entries are zero)

Table 18 The value of $z_{k,j}$ after solving problem for the case study 2

CV \ MV	Q_{L2}	u_{b1}	u_{b2}	u_{b3}
R_1^{out}				1
R_2^{out}			1	
L_1^{out}		1		
L_2^{out}	1			

(the remaining entries are zero)

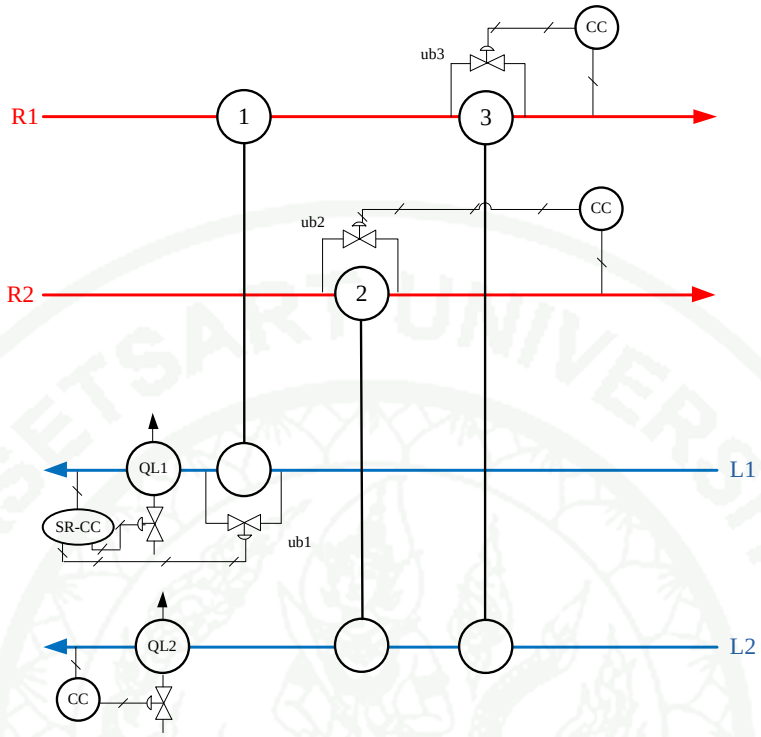

Figure 16 The control structure for the case study 2

The split-range signal of the pair of Q_{L1} and u_{b1} switch alternately to their lower constraints (SR-CC is split-range composition control) as shown in Figure 16.

Table 19 Disturbances and active constraints in the MENs

Time (sec)	Disturbance of mass fraction				Active constraint	
	ΔR_1^{in}	ΔR_2^{in}	ΔL_1^{in}	ΔL_2^{in}	Q_{L1}	u_{b1}
<5	0.07	0.051	0.0006	0.0002	S_L	U
5-15	0.06	0.041	0.0006	0.0002	S_L	U
15-25	0.09	0.061	0.0006	0.0002	U	S_L
25-35	0.07	0.041	0.0006	0.0002	S_L	U

U - Unsaturated manipulated variable (inactive constraint)

S_L - Saturated manipulated variable (active constraint) at the lower bound

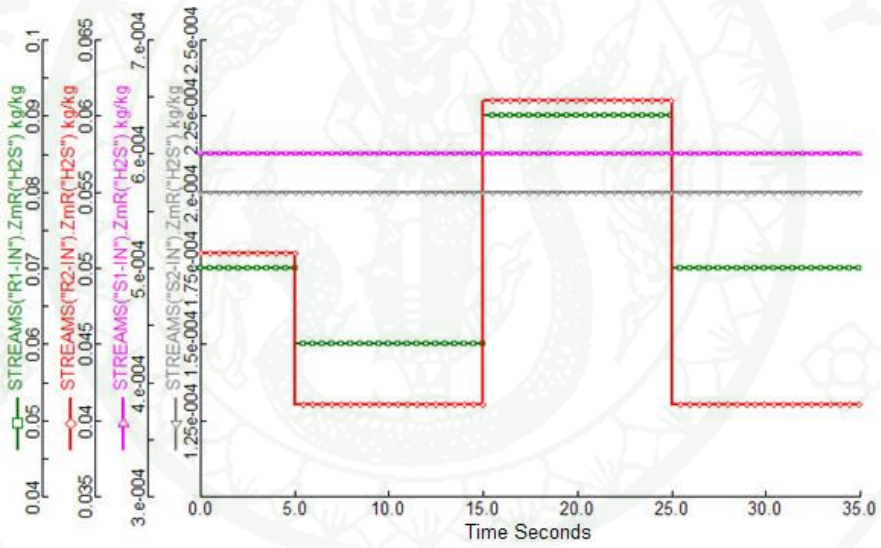

(a) Inlet mass fraction

Figure 17 Dynamics simulation of the MENs in case study 2 (a) Inlet mass fraction, (b) Rich stream target mass fraction, (c) Lean stream target mass fraction and (d) Manipulated variables (Q_{L1} and u_{b1})

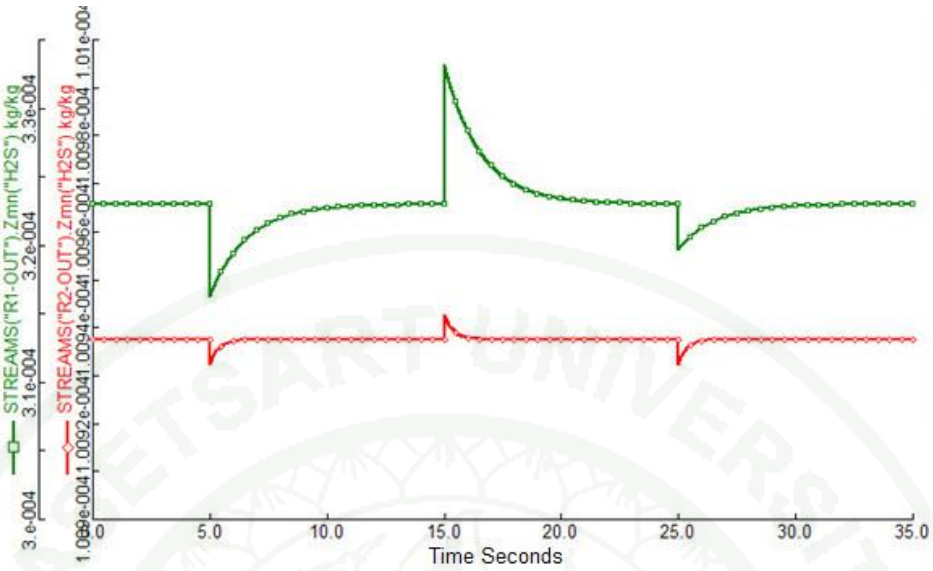

(b) Rich stream target mass fraction

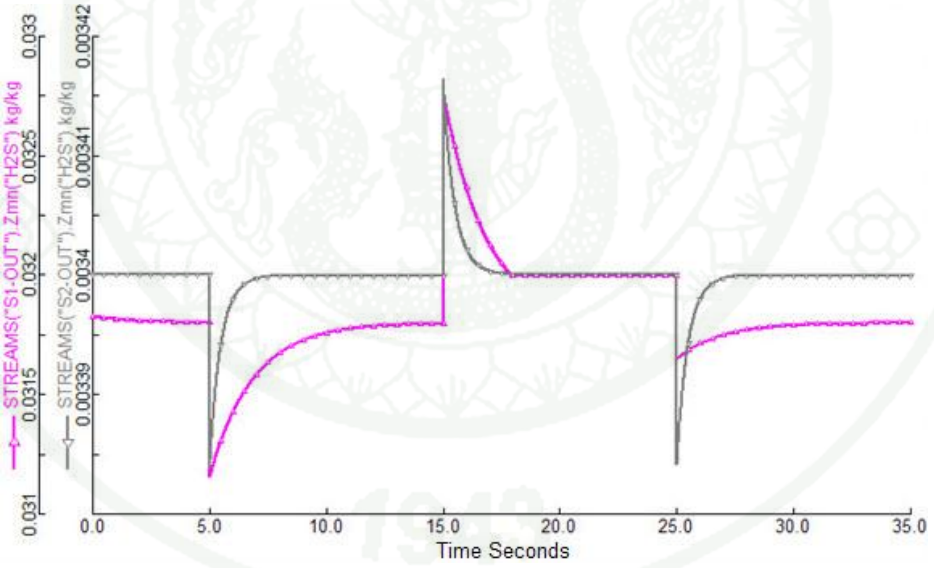

(c) Lean stream target mass fraction

Figure 17 (Continued)

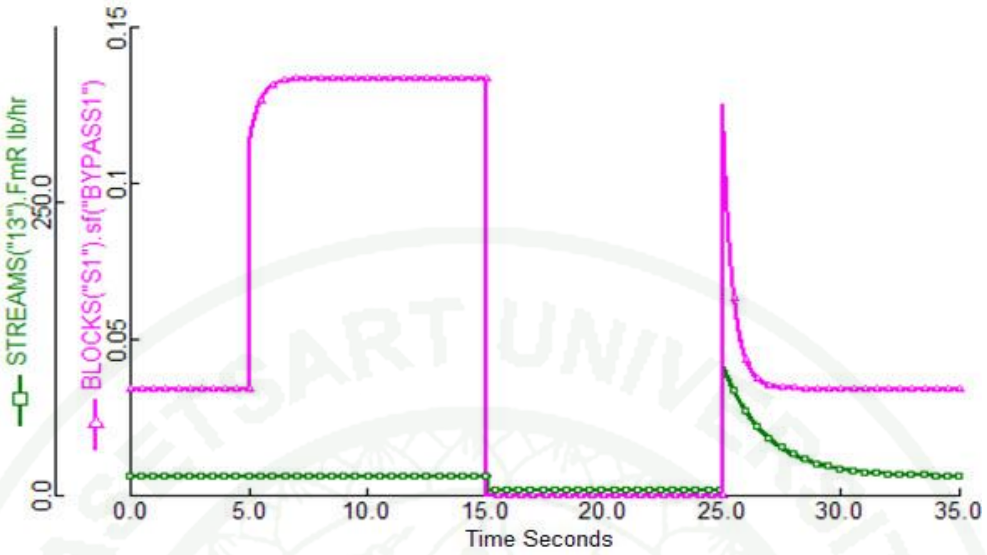

(d) Manipulated variables (Q_{L1} and u_{b1})

Figure 17 (Continued)

The results of control structures in MENs case study 2 are tested by performing dynamics simulation on Aspen Dynamics. The information of the disturbances and active constraints of the MENs in this case study is shown in Table 19. The dynamic results indicate that the control structures can provide optimality. Figure 17 shows the dynamic result of the MENs with the control structure. Figure 17b and 17c show the controllability of the control structure to keep all target mass fraction. Figure 17d shows the response of split-range control that u_{b1} is primary manipulated variable and Q_{L1} is secondary manipulated variable to keep mass fraction of H_2S in L_1^{out}.

Case study 3: Heat integration system for 15 process streams

This case study of large scale HENs is taken from Fieg *et al.* (2009). The problem data are given in Table 20 that consists of eight hot and seven cold process streams, with one hot and one cold utility. The costs equation for exchangers is \$8000 + 500 (Area) $^{0.7}$ (Area unit in m^2) and the minimum approach temperature equal to 10 °C. The disturbances are all inlet temperatures of hot streams with the expected temperatures variation ±10% °C.

Table 20 Problem data for the case study 3

Stream	*TIN* (°C)	*TOUT* (°C)	*FCp* (kW/K)	*h* (kW/m^2K)	Cost (\$/kW-yr)
H1	180	75	30	2	-
H2	280	120	60	1	-
H3	180	75	30	2	-
H4	140	40	30	1	-
H5	220	120	50	1	-
H6	180	55	35	2	-
H7	200	60	30	0.4	-
H8	120	40	100	0.5	-
C1	40	230	20	1	-
C2	100	220	60	1	-
C3	40	190	35	2	-
C4	50	190	30	2	-
C5	50	250	60	2	-
C6	90	190	50	1	-
C7	160	250	60	3	-

Table 20 (Continued)

Stream	*TIN* (°C)	*TOUT* (°C)	*FCp* (kW/K)	*h* (kW/m^{2}K)	Cost ($/kW-yr)
S1	325	325	-	1	80
W1	25	40	-	2	10

Results for this case are shown in Table 21 and Figure 18. We find that in addition to the four periods uncertain parameters, the disturbances are the inlet temperature to change ±10% in four periods. It has five heat exchangers in eight stages and the total annual cost is 1,666,379 $/year, which included the cost for cooling and heating utilities is 1,581,450 $/year. The optimal network configuration as shown in Figure 18 that there are twenty-two units which of eleven heat exchangers, five cold and six hot utilities.

Table 21 Result data (Multi-period) for the case study 3

Period	Stream	*TIN* (°C)	*TOUT* (°C)	FC_p (kW/K)	*h* ($kW/m^2 K$)	Cost ($/kW-yr)
1	H1	180	75	30	2	-
	H2	280	120	60	1	-
	H3	180	75	30	2	-
	H4	140	40	30	1	-
	H5	220	120	50	1	-
	H6	180	55	35	2	-
	H7	200	60	30	0.4	-
	H8	120	40	100	0.5	-
	C1	40	230	20	1	-
	C2	100	220	60	1	-
	C3	40	190	35	2	-
	C4	50	190	30	2	-
	C5	50	250	60	2	-
	C6	90	190	50	1	-
	C7	160	250	60	3	-
2	H1	190	75	30	2	-
	H2	290	120	60	1	-
	H3	175	75	30	2	-
	H4	145	40	30	1	-
	H5	210	120	50	1	-
	H6	190	55	35	2	-
	H7	196	60	30	0.4	-
	H8	130	40	100	0.5	-

Table 21 (Continued)

Period	Stream	*TIN* (°C)	*TOUT* (°C)	FC_p (kW/K)	*h* (kW/m^2 K)	*Cost* ($/kW-yr)
	C1	40	230	20	1	-
	C2	100	220	60	1	-
	C3	40	190	35	2	-
	C4	50	190	30	2	-
	C5	50	250	60	2	-
	C6	90	190	50	1	-
	C7	160	250	60	3	-
3	H1	170	75	30	2	-
	H2	270	120	60	1	-
	H3	183	75	30	2	-
	H4	150	40	30	1	-
	H5	218	120	50	1	-
	H6	170	55	35	2	-
	H7	204	60	30	0.4	-
	H8	122	40	100	0.5	-
	C1	40	230	20	1	-
	C2	100	220	60	1	-
	C3	40	190	35	2	-
	C4	50	190	30	2	-
	C5	50	250	60	2	-
	C6	90	190	50	1	-
	C7	160	250	60	3	-

Table 21 (Continued)

Period	Stream	*TIN* (°C)	*TOUT* (°C)	FC_p (kW/K)	*h* (kW/m^2 K)	*Cost* ($/kW-yr)
4	H1	174	75	30	2	-
	H2	278	120	60	1	-
	H3	190	75	30	2	-
	H4	130	40	30	1	-
	H5	230	120	50	1	-
	H6	175	55	35	2	-
	H7	210	60	30	0.4	-
	H8	120	40	100	0.5	-
	C1	40	230	20	1	-
	C2	100	220	60	1	-
	C3	40	190	35	2	-
	C4	50	190	30	2	-
	C5	50	250	60	2	-
	C6	90	190	50	1	-
	C7	160	250	60	3	-
	S1	325	325	-	1	80
	W1	25	40	-	2	10

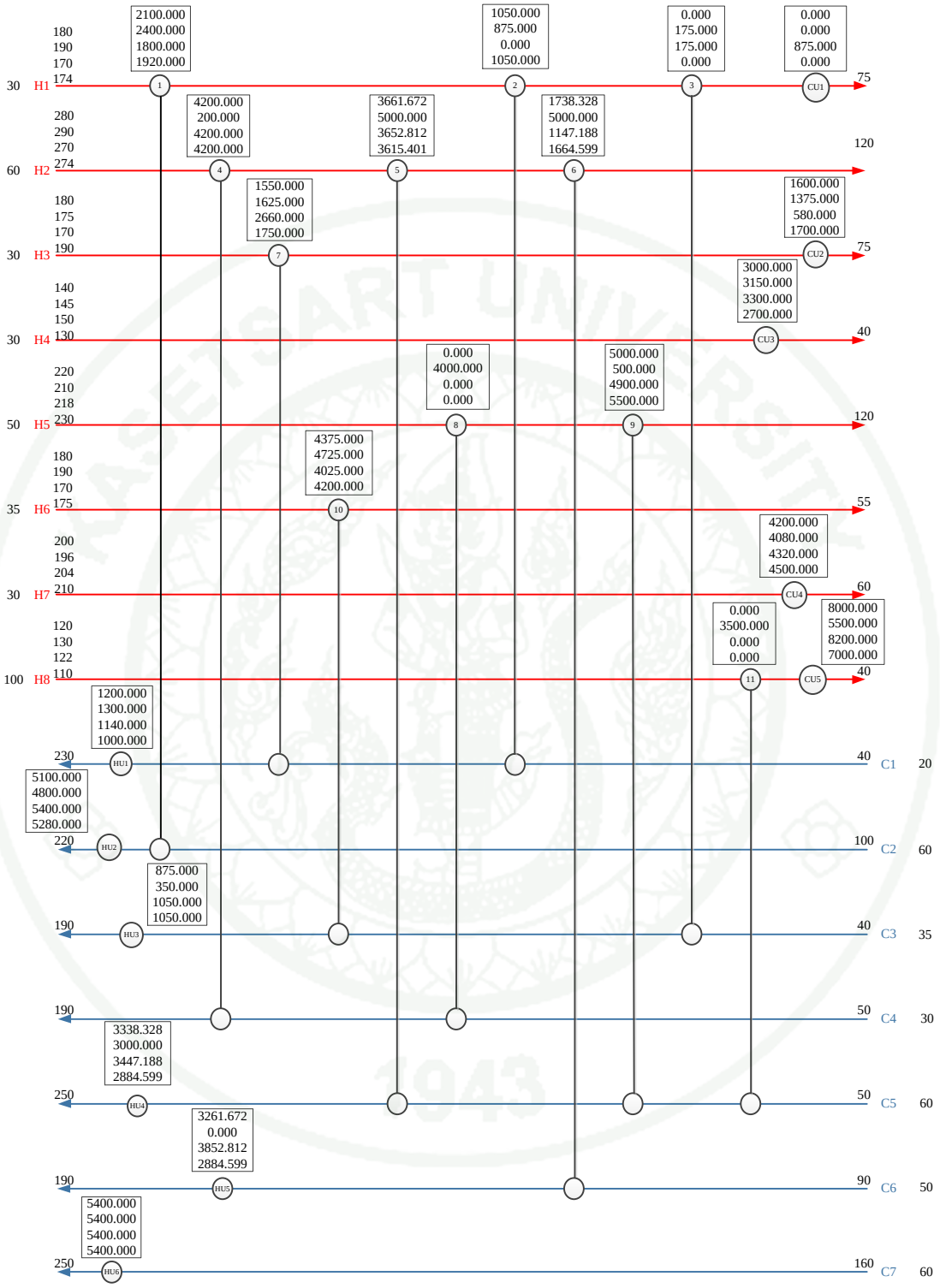

Figure 18 Optimal network configurations for case study 3

After that, the synthesized HENs is simulated using Aspen Plus as shown in Figure 19 to ensure the overall heat balance and the thermal specification. Table 22 shows the results indicate the heat duty of utilities and area of heat exchanger. We found that the results given by GAMS and Aspen Plus are not much difference. From the result, we can conclude that the optimal HENs obtained from GAMS is acceptable.

Table 22 Targets verification on Aspen Plus for case study 3

Targets	GAMS result	ASPEN result	% Relative Difference
Heating utility (kW)	20450.00	21466.70	4.73
Cooling utility (kW)	18575.00	17846.30	3.92
Total Area (m^2)	2293.03	2314.08	0.91

Then, the degrees of freedom (DOFs) are checked. We obtain $N_{DOF,U}$ = 11+11-15 = 7. This case gives degree of freedom at seven for utility cost optimization. Therefore, a strategy for optimal operation is needed.

The information set of active constraints will be used to design optimal split-range control structure. The multi-parametric toolbox (Kvasnica *et al.*, 2004) is used to find active constraint regions as shown in Table 23.

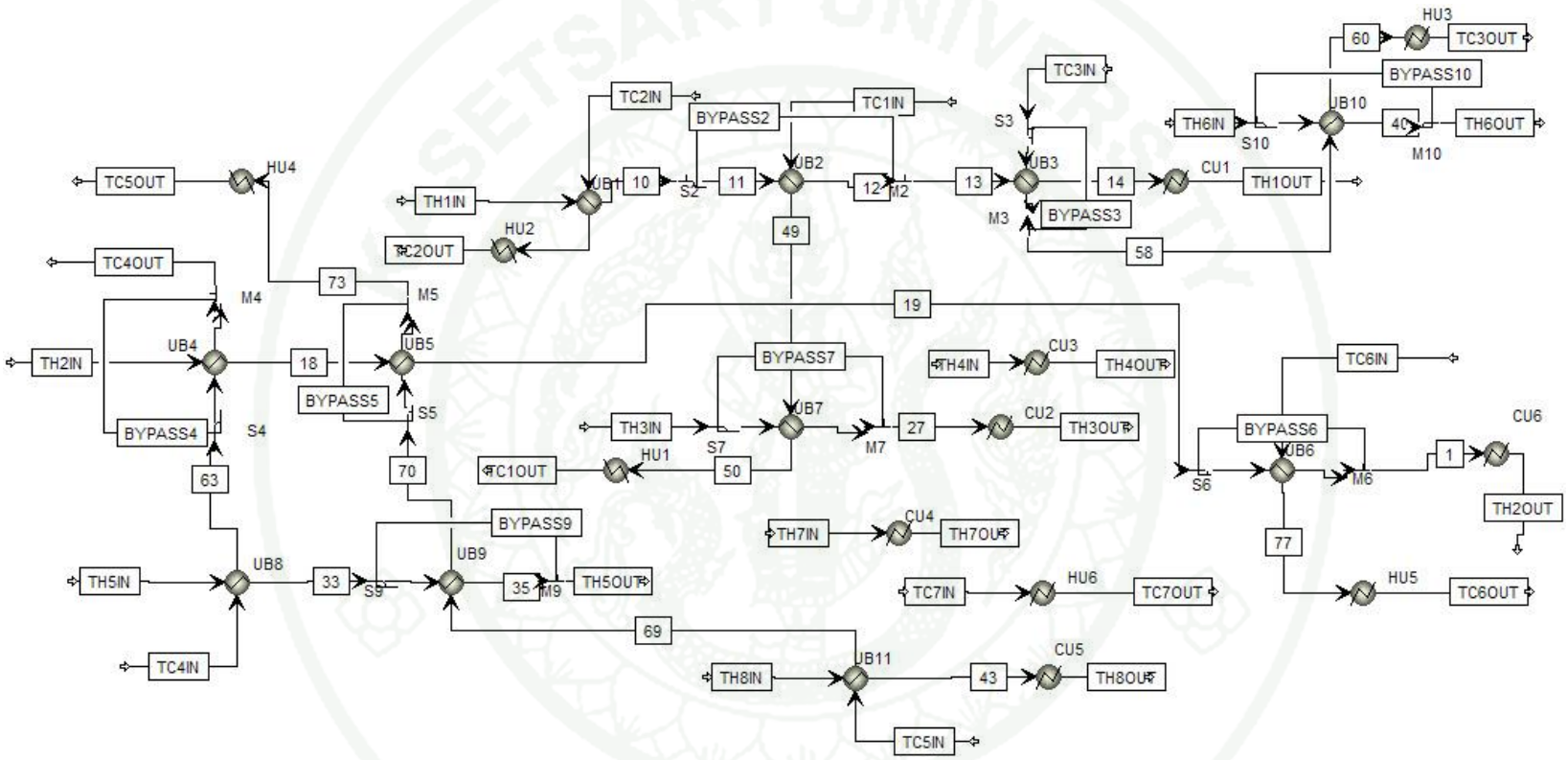

Figure 19 Optimal network configurations for case study 3 on Aspen Plus

Table 23 Set of active constraints in case study 3

Region	Manipulated variables										
	Q_{c1}	Q_{c2}	Q_{c3}	Q_{c4}	Q_{c5}	Q_{h1}	Q_{h2}	Q_{h3}	Q_{h4}	Q_{h5}	Q_{h6}
1	S_L	U	U	U	U	U	U	S_L	S_L	U	U
2	S_L	U	U	U	U	U	U	S_L	U	U	U
3	S_L	U	U	U	U	U	U	U	U	U	U
Region	Manipulated variables										
	u_{b1}	u_{b2}	u_{b3}	u_{b4}	u_{b5}	u_{b6}	u_{b7}	u_{b8}	u_{b9}	u_{b10}	u_{b11}
1	S_L	U	U	U	U	U	S_L	S_L	U	U	S_L
2	S_L	U	U	U	S_U	U	S_L	S_L	U	U	S_L
3	S_L	U	S_L	U	S_U	U	S_L	S_L	U	U	S_L

U - Unsaturated manipulated variable (inactive constraint)

S_L - Saturated manipulated variable (active constraint) at the lower bound

S_U - Saturated manipulated variable (active constraint) at the upper bound

In Table 23 shows the manipulated variable Q_{h3}, Q_{h4}, u_{b3} and u_{b5} can become active constraints when they are combined as a split-range pair. Since the manipulated variables Q_{c1}, u_{b1}, u_{b7}, u_{b8} and u_{b11} are always saturated; therefore, it is not used for control. Furthermore, the manipulated variable Q_{c2}, Q_{c3}, Q_{c4}, Q_{c5}, Q_{h1}, Q_{h2}, Q_{h5}, Q_{h6}, u_{b2}, u_{b4}, u_{b6}, u_{b9} and u_{b10} have never saturated, so there is no need of split-range combinations.

The optimal split-range control structure is obtained by solving an ILP with CPLEX solver of GAMS software. The additional information of relative orders is shown in Table 24. The values of binary variables $x_{i,j}$ shown in Tables 25, there are primary manipulated variables (Q_{c2}, Q_{c3}, Q_{c4}, Q_{c5}, Q_{h1}, Q_{h2}, Q_{h5}, Q_{h6}, u_{b2}, u_{b3}, u_{b4}, u_{b5}, u_{b6}, u_{b9} and u_{b10}) and the secondary manipulated variable (Q_{h3} for u_{b3} and Q_{h4} for u_{b5}). If the primary manipulated variable is saturated, the secondary manipulated variable is used to control output. And Table 26 shows $z_{k,j}$ from solving problem shows the control pairing, the direct effect, which are TH_1^{out} - u_{b2}, TH_2^{out} - u_{b6}, TH_3^{out} - Q_{c2}, TH_4^{out} - Q_{c3}, TH_5^{out} - u_{b9}, TH_6^{out} - u_{b10}, TH_7^{out} - Q_{c4}, TH_8^{out} - Q_{c5}, TC_1^{out} - Q_{h1}, TC_2^{out} - Q_{h2},

TC_3^{out} - u_{b3}, TC_4^{out} - u_{b4}, TC_5^{out} - u_{b5}, TC_6^{out} - Q_{h5} and TC_7^{out} - Q_{h6}. The result of control structure is shown in Figure 20.

Table 24 Relative orders of the HENs in the case study 3

CV \ MV	Q_{c1}	Q_{c2}	Q_{c3}	Q_{c4}	Q_{c5}	Q_{h1}	Q_{h2}	Q_{h3}	Q_{h4}	Q_{h5}	Q_{h6}	u_{b1}	u_{b2}	u_{b3}	u_{b4}	u_{b5}	u_{b6}	u_{b7}	u_{b8}	u_{b9}	u_{b10}	u_{b11}
TH_1^{out}	1	∞	∞	∞	∞	∞	∞	∞	∞	∞	∞	4	3	2	∞	∞	∞	∞	∞	∞	∞	∞
TH_2^{out}	∞	∞	∞	∞	∞	∞	∞	∞	∞	∞	∞	∞	∞	∞	3	2	1	∞	∞	∞	∞	∞
TH_3^{out}	∞	1	∞	∞	∞	∞	∞	∞	∞	∞	∞	∞	∞	∞	∞	∞	∞	2	∞	∞	∞	∞
TH_4^{out}	∞	∞	1	∞	∞	∞	∞	∞	∞	∞	∞	∞	∞	∞	∞	∞	∞	∞	∞	∞	∞	∞
TH_5^{out}	∞	∞	∞	∞	∞	∞	∞	∞	∞	∞	∞	∞	∞	∞	∞	∞	∞	∞	2	1	∞	∞
TH_6^{out}	∞	∞	∞	∞	∞	∞	∞	∞	∞	∞	∞	∞	∞	∞	∞	∞	∞	∞	∞	∞	1	∞
TH_7^{out}	∞	∞	∞	1	∞	∞	∞	∞	∞	∞	∞	∞	∞	∞	∞	∞	∞	∞	∞	∞	∞	∞
TH_8^{out}	∞	∞	∞	∞	1	∞	∞	∞	∞	∞	∞	∞	∞	∞	∞	∞	∞	∞	∞	∞	∞	2
TC_1^{out}	∞	∞	∞	∞	∞	1	∞	∞	∞	∞	∞	∞	∞	∞	∞	∞	3	2	∞	∞	∞	∞
TC_2^{out}	∞	∞	∞	∞	∞	∞	1	∞	∞	∞	∞	2	∞	∞	∞	∞	∞	∞	∞	∞	∞	∞
TC_3^{out}	∞	∞	∞	∞	∞	∞	∞	1	∞	∞	∞	∞	∞	3	∞	∞	∞	∞	∞	∞	2	∞
TC_4^{out}	∞	∞	∞	∞	∞	∞	∞	∞	∞	∞	∞	∞	∞	∞	∞	∞	∞	∞	∞	2	∞	∞
TC_5^{out}	∞	∞	∞	∞	∞	∞	∞	∞	1	∞	∞	∞	∞	∞	∞	2	∞	∞	∞	3	∞	4
TC_6^{out}	∞	∞	∞	∞	∞	∞	∞	∞	∞	1	∞	∞	∞	∞	∞	∞	2	∞	∞	∞	∞	∞
TC_7^{out}	∞	∞	∞	∞	∞	∞	∞	∞	∞	∞	1	∞	∞	∞	∞	∞	∞	∞	∞	∞	∞	∞

(the remaining entries are zero)

Table 25 The value of $x_{i,j}$ after solving problem for the case study 3

Pri MV \ Sec MV	Q_{c2}	Q_{c3}	Q_{c4}	Q_{c5}	Q_{h1}	Q_{h2}	Q_{h3}	Q_{h4}	Q_{h5}	Q_{h6}	u_{b2}	u_{b3}	u_{b4}	u_{b5}	u_{b6}	u_{b9}	u_{b10}
Q_{c2}	1																
Q_{c3}		1															
Q_{c4}			1														
Q_{c5}				1													
Q_{h1}					1												
Q_{h2}						1											
Q_{h5}									1								
Q_{h6}										1							
u_{b2}											1						
u_{b3}							1					1					
u_{b4}													1				
u_{b5}								1						1			
u_{b6}															1		
u_{b9}																1	
u_{b10}																	1

(the remaining entries are zero)

Table 26 The value of $z_{k,j}$ after solving problem for the case study 3

CV \ MV	Q_{c2}	Q_{c3}	Q_{c4}	Q_{c5}	Q_{h1}	Q_{h2}	Q_{h5}	Q_{h6}	u_{b2}	u_{b3}	u_{b4}	u_{b5}	u_{b6}	u_{b9}	u_{b10}
TH_1^{out}									1						
TH_2^{out}													1		
TH_3^{out}	1														
TH_4^{out}		1													
TH_5^{out}														1	
TH_6^{out}															1
TH_7^{out}			1												
TH_8^{out}				1											
TC_1^{out}					1										
TC_2^{out}						1									
TC_3^{out}										1					
TC_4^{out}											1				
TC_5^{out}												1			
TC_6^{out}							1								
TC_7^{out}								1							

(the remaining entries are zero)

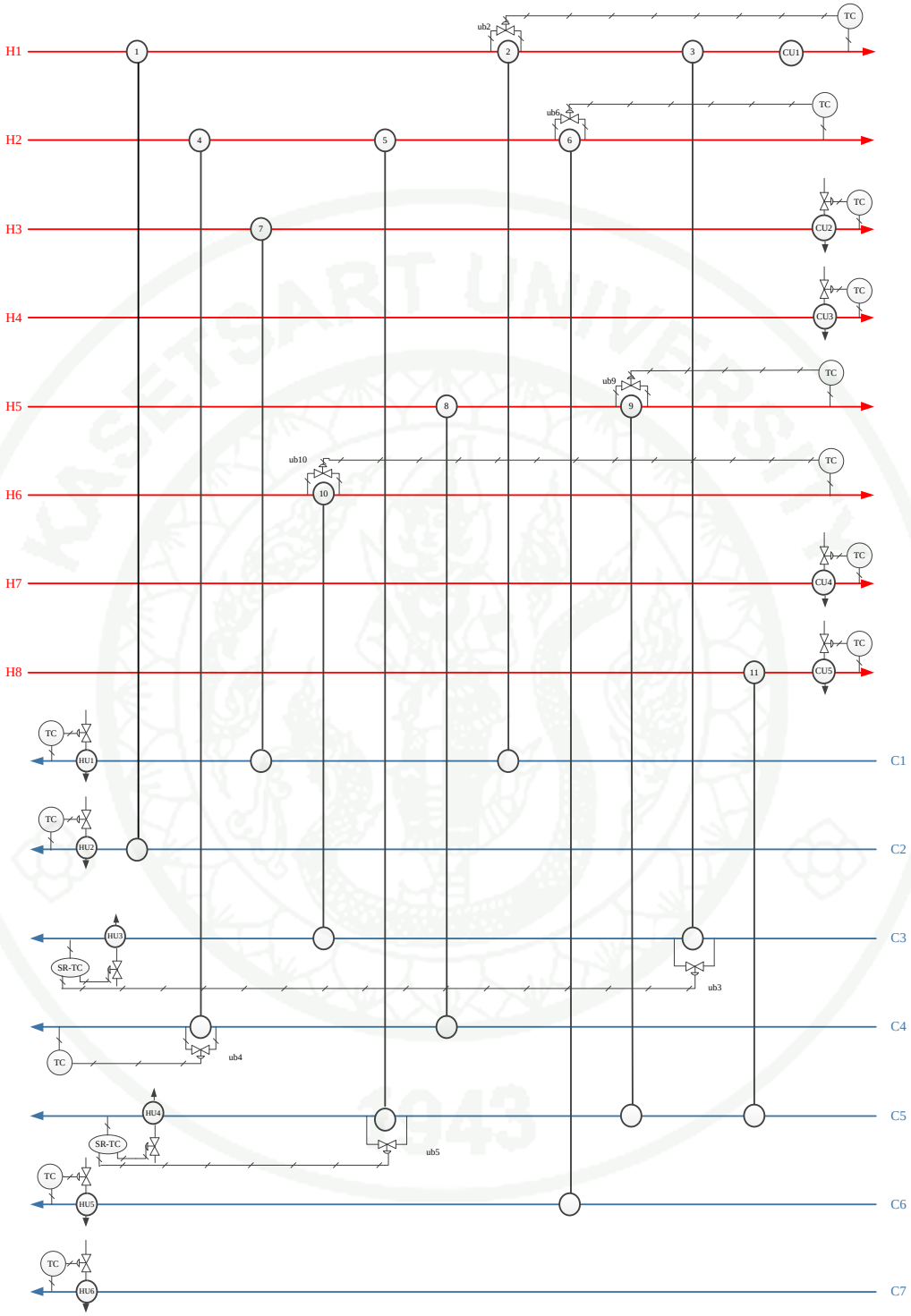

Figure 20 The control structure for the case study 3

Figure 20 show that the split-range signals of the pair of Q_{h3} and u_{b3}, Q_{h4} and u_{b5}; they switch alternately to their lower constraints (SR-TC is split-range temperature control).

The results of control structures in HENs for case study 3 are tested by performing dynamics simulation on Aspen Dynamics. The information regarding the disturbances and active constraints of the system in the case study is shown in Table 27. Figure 21 shows the dynamic results of the HENs for this case. Figure 21c and 21d show the ability of the control structure to keep all target temperatures. And Figure 21e and 21f show the response of split-range control that u_{b3} is primary manipulate variable and Q_{h3} is secondary manipulated variable to keep temperature of $TC_3^{\,out}$ and u_{b5} is primary manipulated variable and Q_{h4} is secondary manipulated variable to keep temperature of $TC_5^{\,out}$.

Table 27 Disturbances and active constraints in the large scale HENs

Time	Disturbance of Temperature								Active constraint			
(sec)	ΔTH_1^{in}	ΔTH_2^{in}	ΔTH_3^{in}	ΔTH_4^{in}	ΔTH_5^{in}	ΔTH_6^{in}	ΔTH_7^{in}	ΔTH_8^{in}	Q_{h3}	u_{b3}	Q_{h4}	u_{b5}
<5	0	0	0	0	0	0	0	0	S_L	U	S_L	U
5-15	-10	-10	-10	-10	0	0	-10	-10	S_L	U	U	S_U
15-25	+10	-10	+10	+10	-10	+10	+10	+10	U	S_L	U	S_U

U - Unsaturated manipulated variable (inactive constraint)

S_L - Saturated manipulated variable (active constraint) at the lower bound

S_U - Saturated manipulated variable (active constraint) at the upper bound

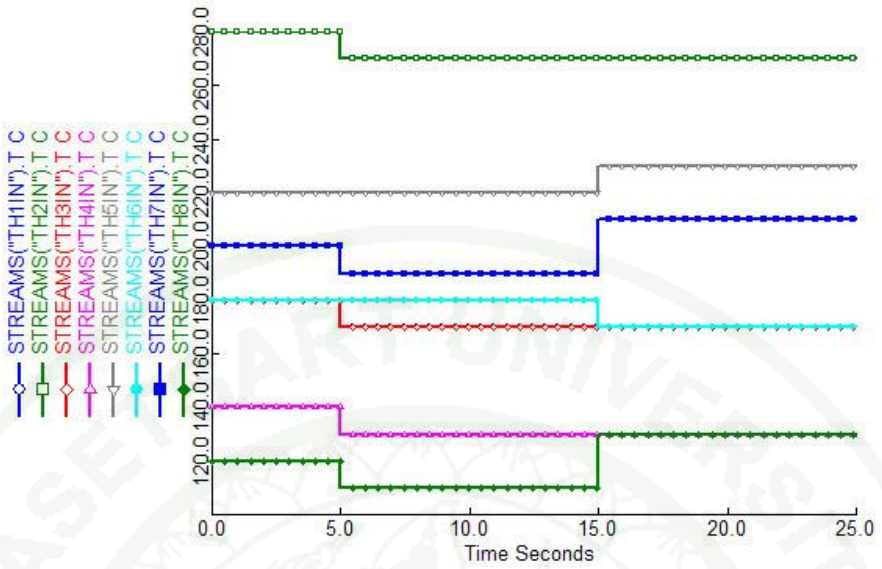

(a) Hot stream inlet temperatures

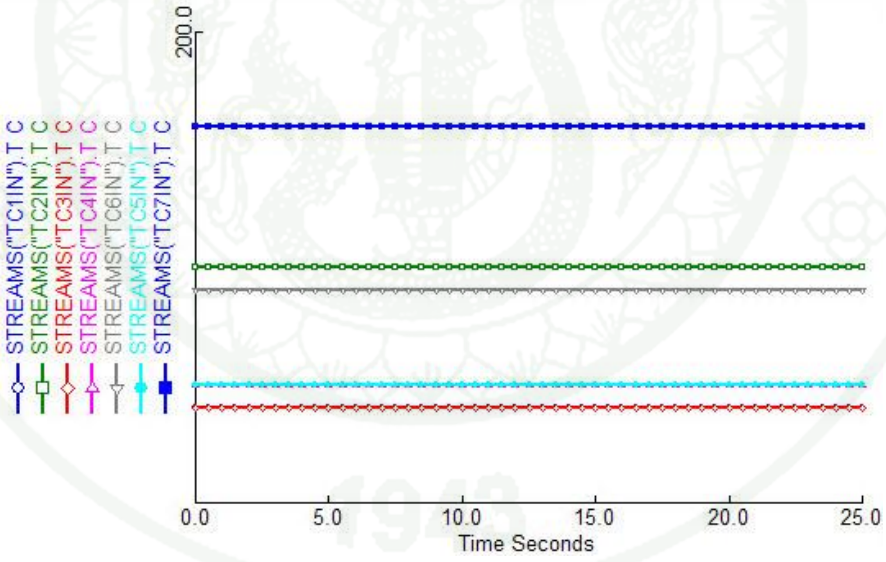

(b) Cold stream inlet temperatures

Figure 21 Dynamics simulation of the HENs in case study 3 (a) Hot stream inlet temperatures, (b) Cold stream inlet temperatures, (c) Hot stream Target temperatures, (d) Cold stream Target temperatures, (e) Manipulated variables (Q_{h3} and u_{b3}) and (f) Manipulated variables (Q_{h4} and u_{b5})

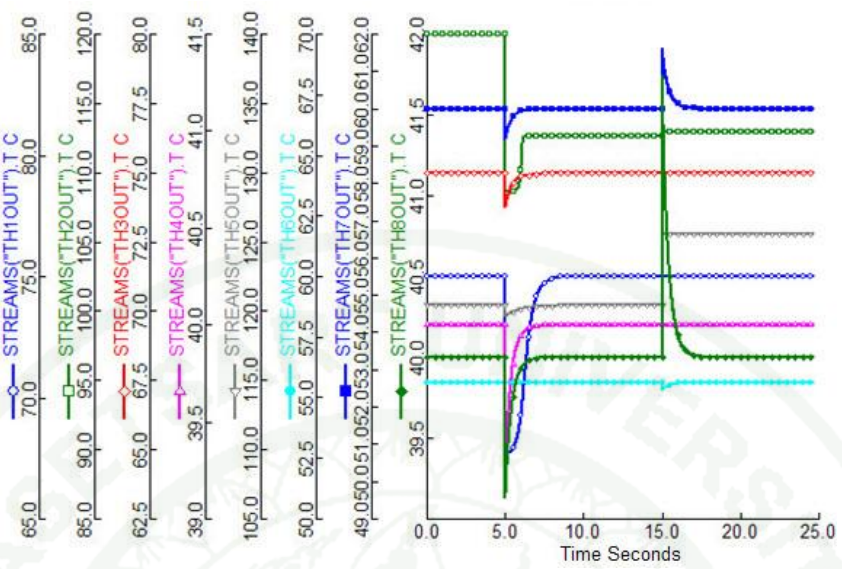

(c) Hot stream Target temperatures

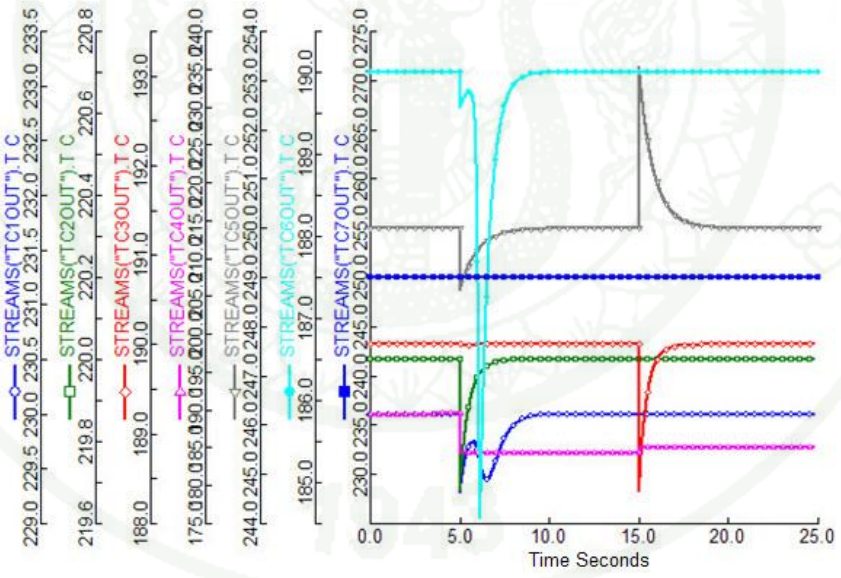

(d) Cold stream Target temperatures

Figure 21 (Continued)

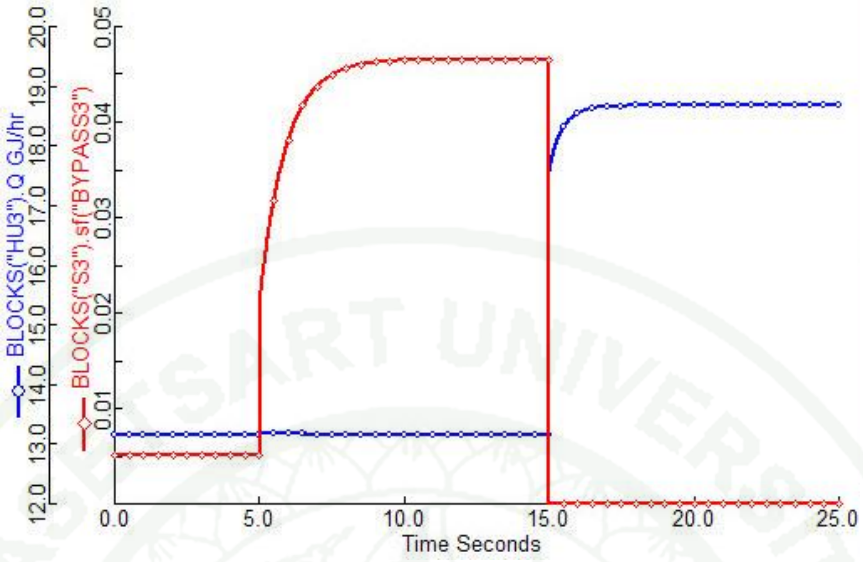

(e) Manipulated variables (Q_{h3} and u_{b3})

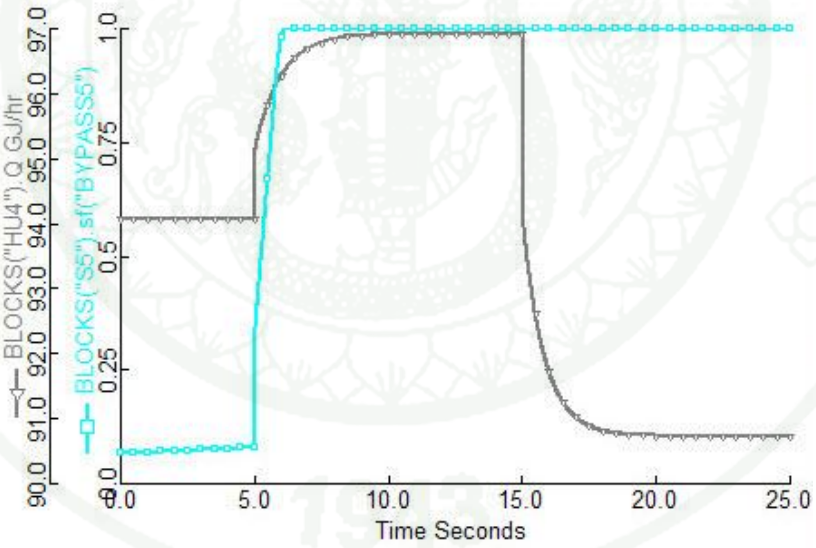

(f) Manipulated variables (Q_{h4} and u_{b5})

Figure 21 (Continued)

Case study 4: Sweetening of COG process with external utilities

This case study shows the synthesizing of CHAMENs. There is hot and cold utilities are added to the process that affects the network configuration and the total annual cost of MENs. The sweetening of COG process is selected to simulate of the CHAMENs. For this case, the hot and cold utilities are added to heat up and cool down the solvent streams (MSAs). The aim of CHAMENs synthesis can be transfered H_2S in the waste water to MSAs. The problem data is shown in Tables 12 and 28. The cost equation for an exchanger is \$700 + 175 (Area) $^{0.8}$ (Area unit in m^2).

Table 28 Thermal data for the streams in the sweetening of COG process

Stream	*TIN* (°C)	*TOUT* (°C)	LB. Temp. (°C)	UB. Temp. (°C)	*Cp* (kJ/kg °C)	*h* (kW/m^2 °C)
L1	330	330	280	330	2.4	2
L2	368	368	368	368	2.5	1
Utility	*TIN* (°C)		*TOUT* (°C)		Cost ($/kW-yr)	*h* (kW/m^2 °C)
HU	800		800		80	3.4
CU	20		30		15	1.7

Thermodynamic feasibility for heat exchange is ensured by a minimum temperature approach equal to 10 °C. In the considered range of operation, the equilibrium solubility data for H_2S in 15 %wt MDEA and White Liquor are changed that depend on temperature. The following relations are correlated as follow:

For 15 wt% MDEA: $y = (9.38600\times10^{-8}\times10^{(0.02150\,T_1)}) \times x_1$

White liquor: $y = (5.86807\times10^{-5}\times10^{(0.01024\,T_2)}) \times x_2$

Table 29 Result data (Multi-period) for the case study 4

Period	streams	Flowrate (kg/s)	Mass fraction	
			IN	*OUT*
1	R1	4.3	0.07	0.0003
	R2	1.6	0.051	0.0001
	L1	11.8	0.0006	0.031
	L2	6.797	0.0002	0.0035
2	R1	4.3	0.068	0.0003
	R2	1.6	0.051	0.0001
	L1	11.8	0.0006	0.031
	L2	6.797	0.0002	0.0035
3	R1	4.3	0.067	0.0003
	R2	1.6	0.051	0.0001
	L1	11.8	0.0006	0.031
	L2	6.797	0.0002	0.0035

Results for case study 4 are illustrated in Table 29 and Figure 22. We find that in addition to the three periods uncertain parameters. The disturbances, mass fraction, are between ±0.002%w/w for R_1 in three periods. The total annual cost of this CHAMENs is 2,631,193 $/year and the cost of MSAs is decreased to 2,477,980 $/year. The cost for additional utilities is 9,936 $/year. Table 30 shows the comparison of cost detail between MENs (case study 2) and CHAMENs that indicate the total annual cost for sweetening of COG process using CHAMENs is cheaper than synthesizing with MENs.

Table 30 The comparison of cost detail for MENs and CHAMENs for case study 4

Detail	MENs	CHAMENs
Load of S1 (kg/s)	9.79	11.8
Load of S2 (kg/s)	25.315	6.797
MSAs cost ($/yr)	2,758,814	2,477,980
Utilities cost ($/yr)	-	6,875
Mass exchangers cost ($/yr)	152,287	143,277
Heat exchangers cost ($/yr)	-	3,062
Total annualized cost ($/yr)	2,911,101	2,631,193
% TAC reduction		9.62

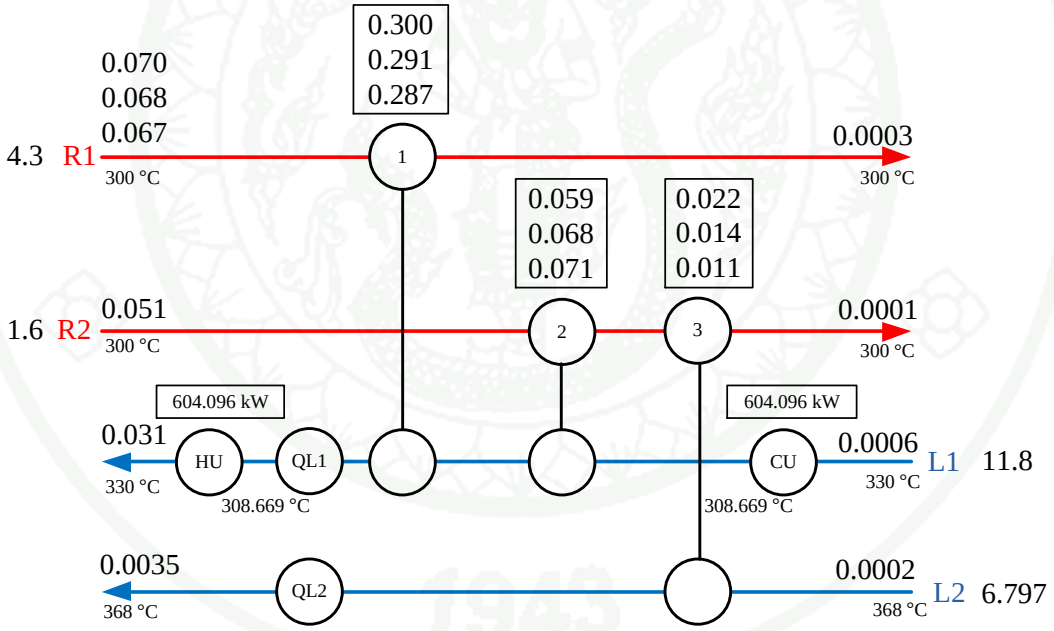

Figure 22 Optimal network configurations for case study 4

To guarantee the overall mass and energy balance of the synthesized CHAMENs, we simulate using Aspen Plus as shown in Figure 23. The result is shown in Table 31 which indicates the outlet mass fraction of H2S is following the target of process. We found that the results given by GAMS and Aspen Plus are not much difference. From the result, we can conclude that the optimal CHAMENs obtained from GAMS is acceptable. In addition, the total annual cost from this work is lower than the result of Thunyawart's (2010).

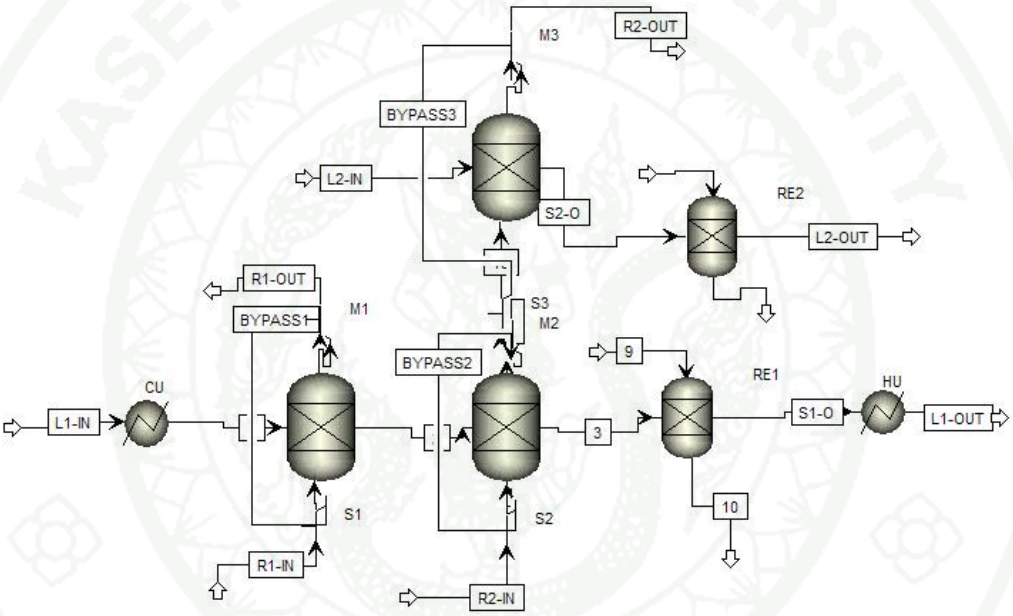

Figure 23 Optimal CHAMENs for COG process on Aspen Plus

Table 31 Targets verification on Aspen Plus for case study 4

Targets	GAMS result	Aspen result	% Relative difference
Flowrate of L1 (kg/s)	11.8	11.8	-
Flowrate of L2 (kg/s)	6.797	6.797	-
Mass fraction of H_2S in R1	0.0003	0.00036	16.67
Mass fraction of H_2S in R2	0.0001	0.0001	-
Mass fraction of H_2S in L1	0.031	0.031	-
Mass fraction of H_2S in L2	0.0035	0.0035	-

After that, the degrees of freedom of the optimal CHAMENs are checked. For this case, we can obtain the $N_{DOF,U}$ = 3+2-4 = 1. There is one degree of freedom for utility optimization, so a strategy for optimal operation is needed.

Then, the information set of active constraints are required that will be used to design optimal split-range control structure. The multi-parametric toolbox (Kvasnica *et al.*, 2004) is used to find active constraint regions as shown in Table 32.

Table 32 Set of active constraints in case study 4

Region	Manipulated variables				
	Q_{L1}	Q_{L2}	u_{b1}	u_{b2}	u_{b3}
1	U	U	U	S_L	U
2	U	S_L	U	U	U

U - Unsaturated manipulated variable (inactive constraint)

S_L - Saturated manipulated variable (active constraint) at the lower bound

Table 32 demonstrates the manipulated variable Q_{L2} and u_{b2} switch alternately to become active constraints and should be combined as a split-range pair. Q_{L1}, u_{b1} and u_{b3} are never saturated, so, there are no needs for secondary manipulated variable.

In the next step, the optimal split-range control structure is obtained by solving an ILP with CPLEX solver of GAMS software. The additional information of relative orders is shown in Table 33. Tables 34 shows the values of binary variables $x_{i,j}$, there are primary manipulated variables (Q_{L1}, u_{b1}, u_{b2} and u_{b3}) and the secondary manipulated variable (Q_{L2} for u_{b2}). If the primary manipulated variable, u_{b2}, is saturated, the secondary manipulated variable, Q_{L2}, is used to control output. And Table 35 shows the values of binary variables $z_{k,j}$ from solving problem shows the control pairing, the direct effect, which are which are R_1^{out} - u_{b1}, R_2^{out} - u_{b3}, L_1^{out} - Q_{L1} and L_2^{out} - u_{b2}. The result of control structure is shown in Figure 24.

Table 33 Relative orders of the CHAMENs in the case study 4

CV \ MV	Q_{L1}	Q_{L2}	u_{b1}	u_{b2}	u_{b3}
R_1^{out}	∞	∞	1	2	3
R_2^{out}	∞	∞	∞	2	1
L_1^{out}	1	∞	2	3	∞
L_2^{out}	∞	1	∞	∞	2

Table 34 The value of $x_{i,j}$ after solving problem for the case study 4

Pri MV \ Sec MV	Q_{L1}	Q_{L2}	u_{b1}	u_{b2}	u_{b3}
Q_{L1}	1				
u_{b1}			1		
u_{b2}		1		1	
u_{b3}					1

(the remaining entries are zero)

Table 35 The value of $z_{k,j}$ after solving problem for the case study 4

CV \ MV	Q_{L1}	u_{b1}	u_{b2}	u_{b3}
R_1^{out}		1		
R_2^{out}				1
L_1^{out}	1			
L_2^{out}			1	

(the remaining entries are zero)

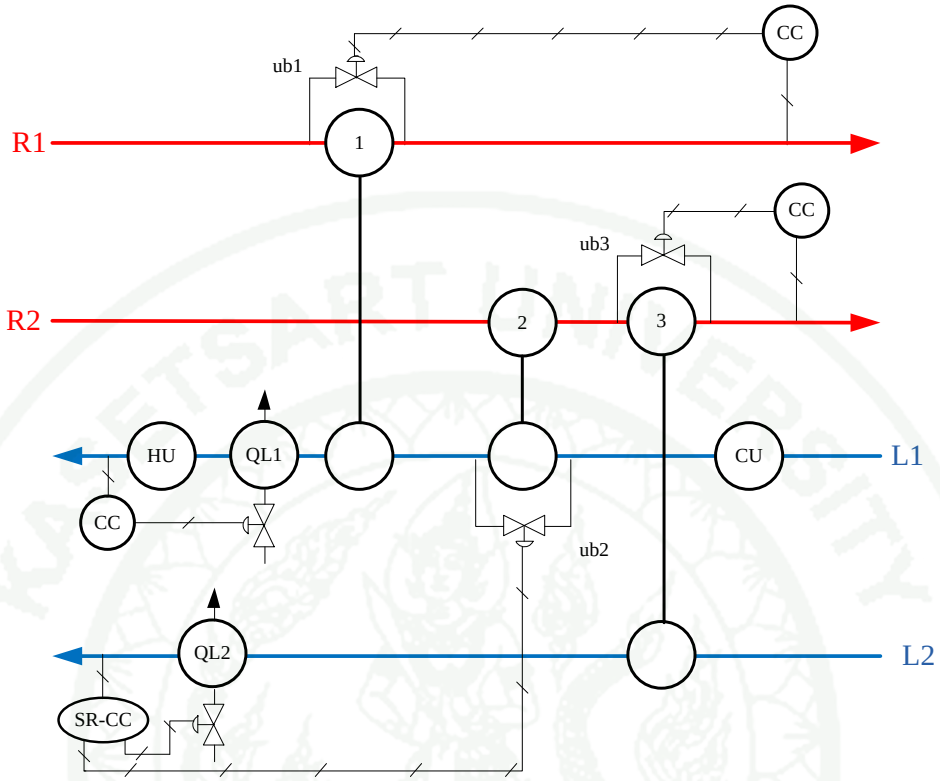

Figure 24 The control structure for the case study 4

The split-range signal of the pair of Q_{L2} and u_{b2} switch alternately to their lower constraints (SR-CC is split-range composition control) as show in Figure 24.

Table 36 Disturbances and active constraints in the CHAMENs

Time	Disturbance of mass fraction				Active constraint	
(sec)	ΔR_1^{in}	ΔR_2^{in}	ΔL_1^{in}	ΔL_2^{in}	Q_{L2}	u_{b2}
<5	0.07	0.051	0.0006	0.0002	U	S_L
5-15	0.09	0.061	0.0006	0.0004	U	S_L
15-25	0.05	0.041	0.0006	0.0002	S_L	U
25-35	0.07	0.051	0.0006	0.0002	U	S_L

U - Unsaturated manipulated variable (inactive constraint)

S_L - Saturated manipulated variable (active constraint) at the lower bound

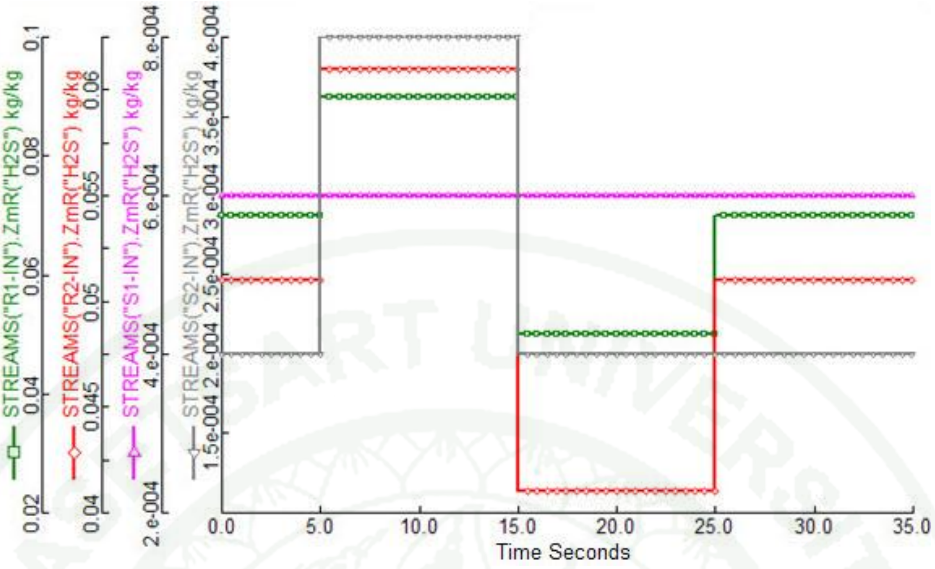

(a) Inlet mass fraction

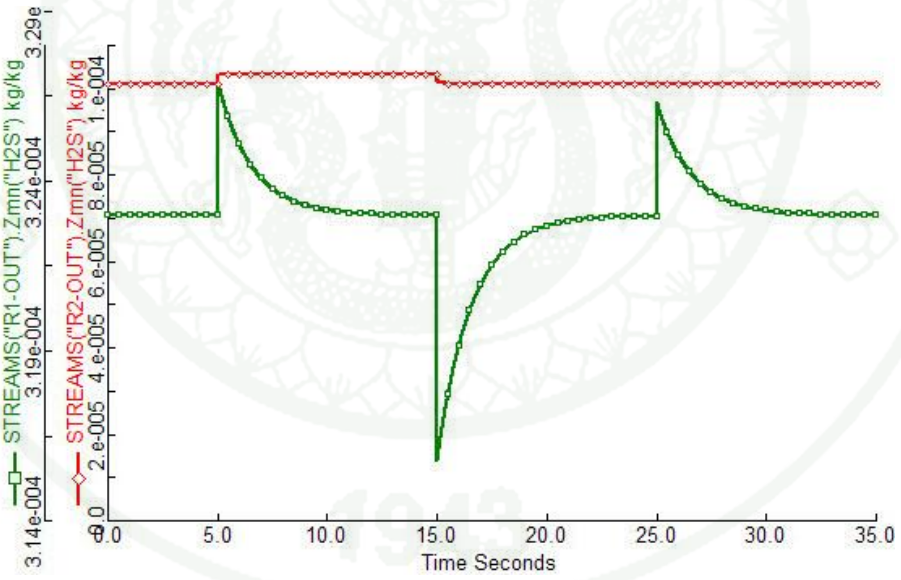

(b) Rich stream target mass fraction

Figure 25 Disturbances and active constraint in the CHAMENs in case study 4 (a) Inlet mass fraction, (b) Rich stream target mass fraction, (c) Lean stream target mass fraction and (d) Manipulated variables (Q_{L2} and u_{b2})

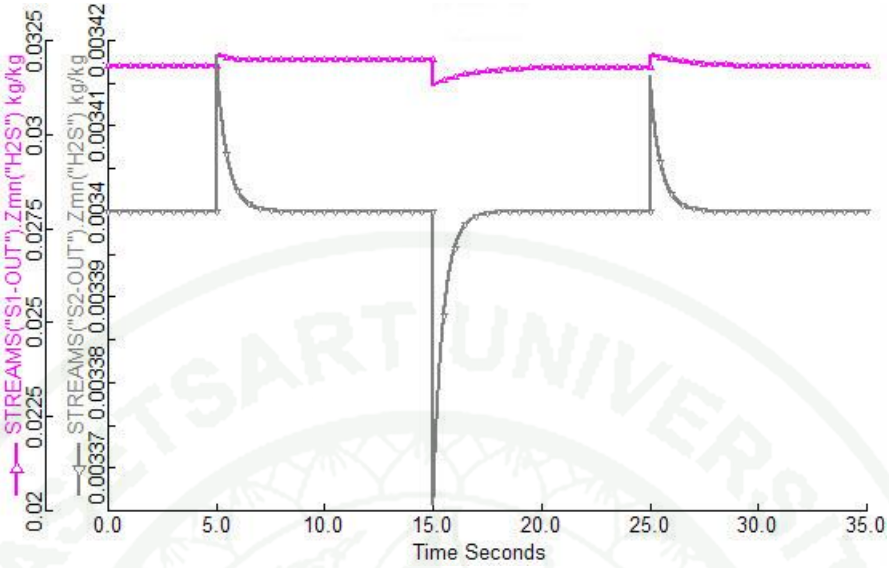

(c) Lean stream target mass fraction

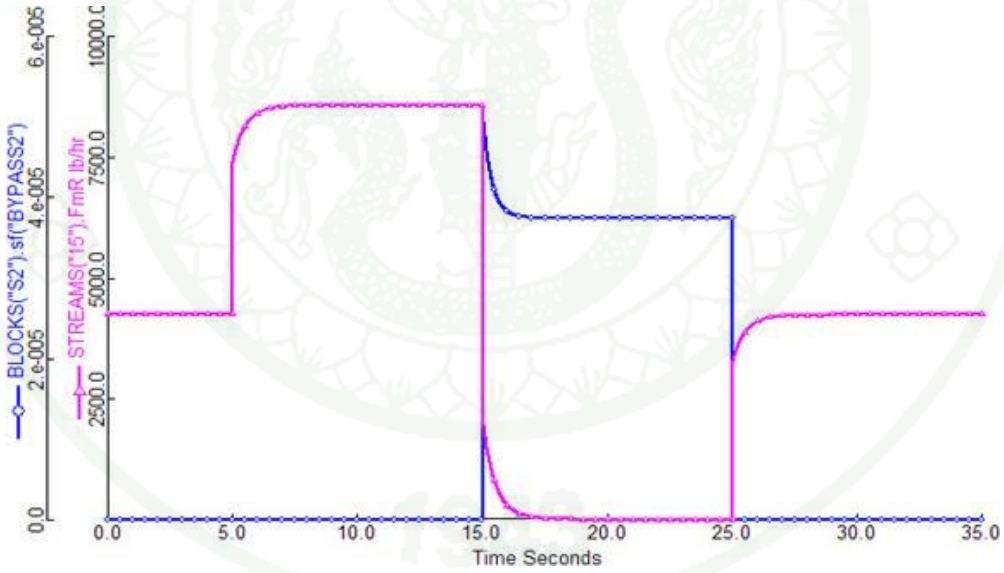

(d) Manipulated variables (Q_{L2} and u_{b2})

Figure 25 (Continuted)

In this case study, the results of control structures in CHAMENs are tested by performing dynamics simulation on Aspen Dynamics. The information of the disturbances and active constraints of the CHAMENs is shown in Table 36. The

dynamic results indicate that the control structures can provide optimality. Figure 25 shows the dynamic result of the CHAMENs with the control structure. Figure 25b and 25c show the controllability of the control structure to keep all target mass fraction. Figure 25d shows the response of split-range control that Q_{L2} is primary manipulated variable and u_{b2} is secondary manipulated variable to keep mass fraction of H_2S in L_2^{out}.

Case study 5: Sweetening of COG process with simultaneous heat integration

This case study is the special example that to verify the capability in synthesizing simultaneously HENs and MENs. The CHAMENs in this case consists of the heat integration system of case 1 is combined with the COG process of case 2. The problem data for the synthesizing of CHAMENs as shown in Table 4, 12 and 28.

Table 37 Result data for the case study 5

Period	Stream	*TIN* (°C)	*TOUT* (°C)	*FCp* (kW/°C)	*h* (kW/m^2°C)	Cost ($/kW-yr)
1	H1	650	370	10	1	-
	H2	590	370	20	1	-
	H3	190	30	15	1	-
	C1	410	650	15	1	-
	C2	353	500	13	1	-
	C3	80	167	5	1	-
	C4	20	160	5	1	-
2	H1	645	370	10	1	-
	H2	587	370	20	1	-
	H3	200	30	15	1	-
	C1	410	650	15	1	-
	C2	353	500	13	1	-
	C3	80	167	5	1	-
	C4	20	160	5	1	-
3	H1	660	370	10	1	-
	H2	580	370	20	1	-
	H3	180	30	15	1	-

Table 37 (Continued)

Period	Stream	*TIN* (°C)	*TOUT* (°C)	*FCp* (kW/°C)	*h* (kW/m^2 °C)	Cost ($/kW-yr)
	C1	410	650	15	1	-
	C2	353	500	13	1	-
	C3	80	167	5	1	-
	C4	20	160	5	1	-
4	H1	648	370	10	1	-
	H2	595	370	20	1	-
	H3	196	30	15	1	-
	C1	410	650	15	1	-
	C2	353	500	13	1	-
	C3	80	167	5	1	-
	C4	20	160	5	1	-
5	H1	640	370	10	1	-
	H2	600	370	20	1	-
	H3	184	30	15	1	-
	C1	410	650	15	1	-
	C2	353	500	13	1	-
	C3	80	167	5	1	-
	C4	20	160	5	1	-
	S1	800	800	-	3.4	80
	W1	20	30	-	1.7	15

Table 37 (Continued)

Period	streams	Flowrate (kg/s)	Mass fraction	
			IN	OUT
1	R_1	4.3	0.07	0.0003
	R_2	1.6	0.051	0.0001
	L_1	11.8	0.0006	0.031
	L_2	∞	0.0002	0.0035
2	R_1	4.3	0.068	0.0003
	R_2	1.6	0.051	0.0001
	L_1	11.8	0.0006	0.031
	L_2	∞	0.0002	0.0035
3	R_1	4.3	0.067	0.0003
	R_2	1.6	0.051	0.0001
	L_1	11.8	0.0006	0.031
	L_2	∞	0.0002	0.0035

Results for case study 5 are illustrated in Table 37 and Figure 26. The heat of hot stream, H2, can use to heat the solvent, L1, in sweetening of COG process. And there using the cold utility to cooling the solvent, L1. The optimal CHAMENs represent the total annual cost is 2,700,670 $/year that 14.89 % reduction when compare with the total annual cost of case study 1 and case study 2 as shown in Table 38.

The optimal CHAMENs with heat integration configuration is shown Figure 26 that there are fifteen units consist of six heat exchangers, three mass exchangers, two hot utilities, three cold utilities and one MSAs utility.

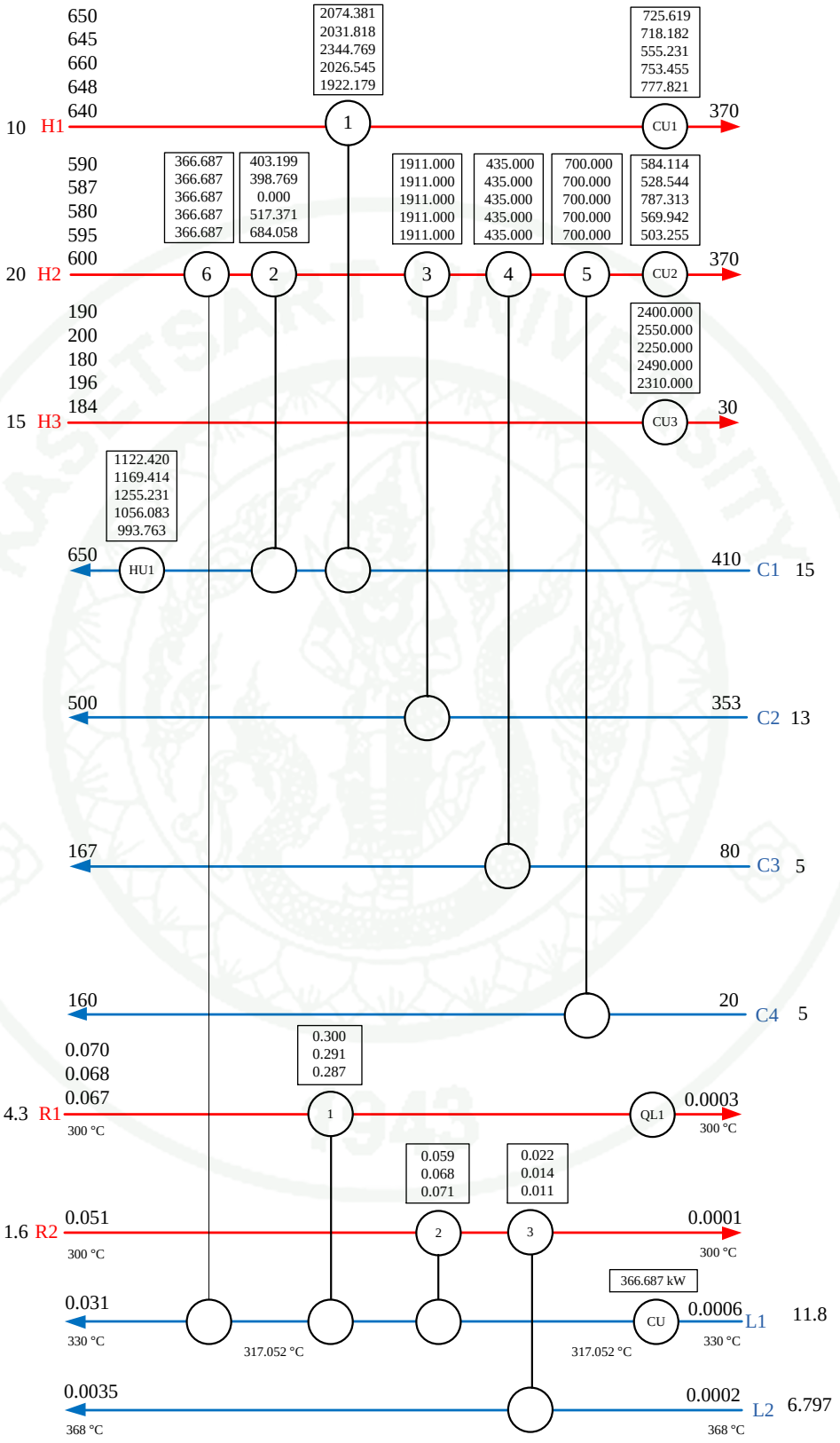

Figure 26 Optimal network configurations for case study 5

Table 38 Comparison on cost detail for HENs, MENs, and CHAMENs for case study 5

Detail	HENs	MENs	CHAMENs
Load of S1 (kg/s)	-	9.79	11.8
Load of S2 (kg/s)	-	25.315	6.797
MSAs cost ($/yr)	-	2,758,814	2,567,929
Utilities cost ($/yr)	111,664	-	70,910
Mass exchangers cost ($/yr)	-	152,287	38,656
Heat exchangers cost ($/yr)	150,561	-	23,176
Total annualized cost ($/yr)	3,173,325		2,700,670
% TAC reduction		14.89	

Table 38 shows the comparison of cost detail in case study 1 and 2 with cost detail in case study that are different. Because of the configuration of HENs and MENs are differently designed that may cause from the change in feasible search space, the more optional in stream matching, the more constraints involving in the optimization model, and the compromise in adding the utilities load and the number of heat transfer equipment to increase the mass exchanger equilibrium performance. In detail, the utilities cost increase to 70,910 $/year, the MSAs cost is 2,567,929 $/year, mass exchangers cost decrease to 38,656 $/year, and heat exchangers cost decrease to 23,176 $/year and the total annual cost decrease to 2,700,670 $/year. The result indicate that the synthesis of simultaneous heat and mass exchanger networks might obtain more advantageous network than individually synthesis of HENs and MENs in which lowering the total annual cost of the network.

To ensure the overall mass balance, the overall heat balance and the mass fraction of H_2S of the synthesized, we simulate using Aspen Plus as shown in Figure 27. The result is shown in Table 39 which indicates that the results given by GAMS and Aspen Plus are not much difference. From the result, we can conclude that the optimal CHAMENs obtained from GAMS is acceptable. In addition, the total annual cost obtained from this work is lower than the result of Thunyawart (2010).

Table 39 Targets verification on Aspen Plus for case study 4

Targets	GAMS result	Aspen result	% Relative difference
Flowrate of L1 (kg/s)	11.8	11.8	-
Flowrate of L2 (kg/s)	6.797	6.797	-
Mass fraction of H_2S in R1	0.0003	0.0003	-
Mass fraction of H_2S in R2	0.0001	0.0001	-
Mass fraction of H_2S in L1	0.031	0.031	-
Mass fraction of H_2S in L2	0.0035	0.0035	-
Heating utility (kW)	1255.231	1434.363	12.48
Cooling utility (kW)	4481.821	4618.219	2.95
Total Area of heat exchanger (m^2)	265.576	244.736	7.84

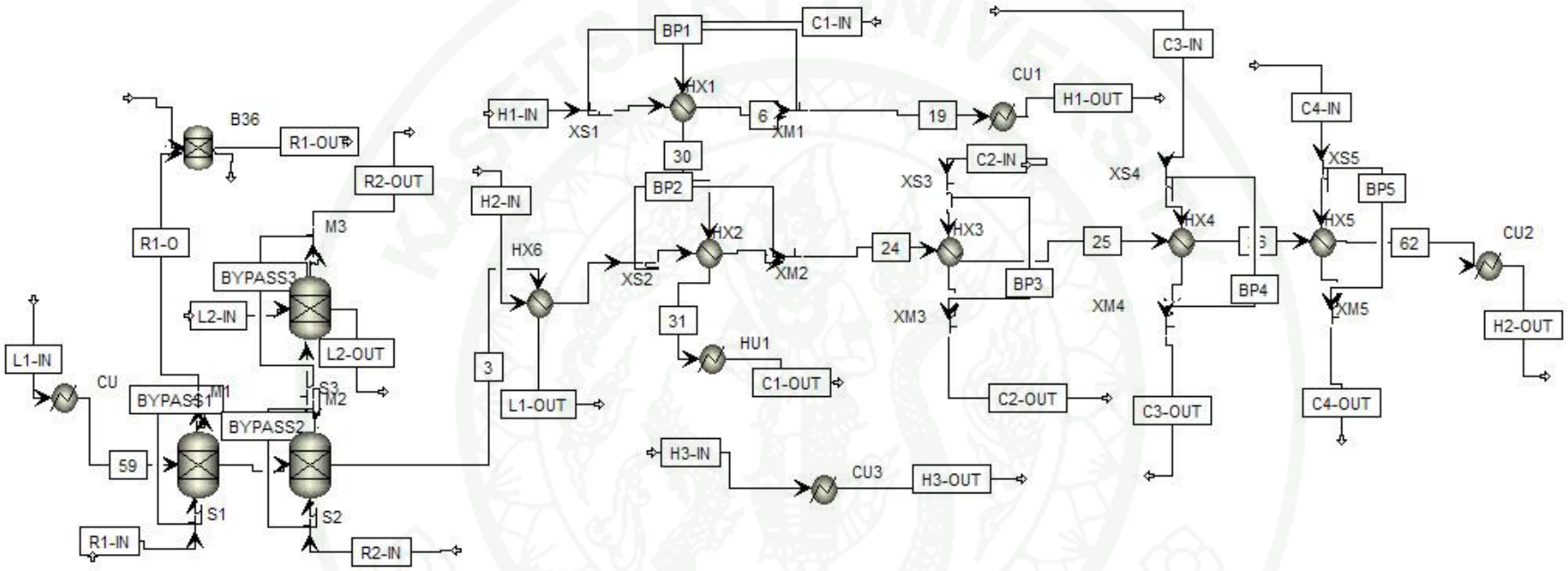

Figure 27 Optimal CHAMENs with heat integration on Aspen Plus

After that, the degrees of freedom are checked. In this case, the $N_{DOF,U}$ = 6+4-7 = 3 for HENs and the $N_{DOF,U}$ = 3+1-4 = 0 for MENs. The degrees of freedom for HENs are two, so, a strategy for optimal operation is needed. Then, the information set of active constraints are required that will be used to design optimal split-range control structure. In this case study generate two active constraint regions as shown in Table 40.

Table 40 Set of active constraints in case study 5

Region	Manipulated variables								
	Q_{c1}	Q_{c2}	Q_{c3}	Q_{h1}	u_{b1}	u_{b2}	u_{b3}	u_{b4}	u_{b5}
1	U	U	U	S_L	S_L	U	U	U	U
2	U	U	U	U	S_L	S_L	U	U	U

U - Unsaturated manipulated variable (inactive constraint)

S_L - Saturated manipulated variable (active constraint) at the lower bound

In Table 40 shows the manipulated variables Q_{h1} and u_{b2} switch alternately to become active constraints and should be combined as a split-range pair. Q_{c1}, Q_{c2}, Q_{c3}, u_{b3}, u_{b4} and u_{b5} are never saturated; hence, there are no needs for secondary manipulated variable.

Then, the additional information of relative orders is shown in Table 41. The optimal split-range control structure is obtained by solving an ILP with CPLEX solver of GAMS software. Tables 42 shows the values of binary variables $x_{i,j}$, there are primary manipulated variables (Q_{h1}) and the secondary manipulated variable (Q_{h2} for u_{b2}). If the primary manipulated variable, u_{b2}, is saturated, the secondary manipulated variable, Q_{h2}, is used to control output. And Table 43 shows the values of binary variables $z_{k,j}$ from solving problem shows the control pairing, the direct effect, which are which are TH_1^{out} - Q_{c1}, TH_2^{out} - Q_{c2} , TH_3^{out} - Q_{c3} , TC_1^{out} - u_{b2}, TC_2^{out} - u_{b3} , TC_3^{out} - u_{b4} and TC_4^{out} - u_{b5}. The result of control structure is shown in Figure 28.

Table 41 Relative orders of the CHAMENs in the case study 5

MV / CV	Q_{c1}	Q_{c2}	Q_{c3}	Q_{h1}	u_{b1}	u_{b2}	u_{b3}	u_{b4}	u_{b5}
TH_1^{out}	1	∞	∞	∞	2	∞	∞	∞	∞
TH_2^{out}	∞	1	∞	∞	∞	5	4	3	2
TH_3^{out}	∞	∞	1	∞	∞	∞	∞	∞	∞
TC_1^{out}	∞	∞	∞	1	3	2	∞	∞	∞
TC_2^{out}	∞	∞	∞	∞	∞	2	1	∞	∞
TC_3^{out}	∞	∞	∞	∞	∞	3	2	1	∞
TC_4^{out}	∞	∞	∞	∞	∞	∞	∞	2	1

Table 42 The value of $x_{i,j}$ after solving problem for the case study 5

Pri MV / Sec MV	Q_{c1}	Q_{c2}	Q_{c3}	Q_{h1}	u_{b2}	u_{b3}	u_{b4}	u_{b5}
Q_{c1}	1							
Q_{c2}		1						
Q_{c3}			1					
u_{b2}				1	1			
u_{b3}						1		
u_{b4}							1	
u_{b5}								1

(the remaining entries are zero)

Table 43 The value of $z_{k,j}$ after solving problem for the case study 5

CV \ MV	Q_{c1}	Q_{c2}	Q_{c3}	u_{b2}	u_{b3}	u_{b4}	u_{b5}
TH_1^{out}	1						
TH_2^{out}		1					
TH_3^{out}			1				
TC_1^{out}				1			
TC_2^{out}					1		
TC_3^{out}						1	
TC_4^{out}							1

(the remaining entries are zero)

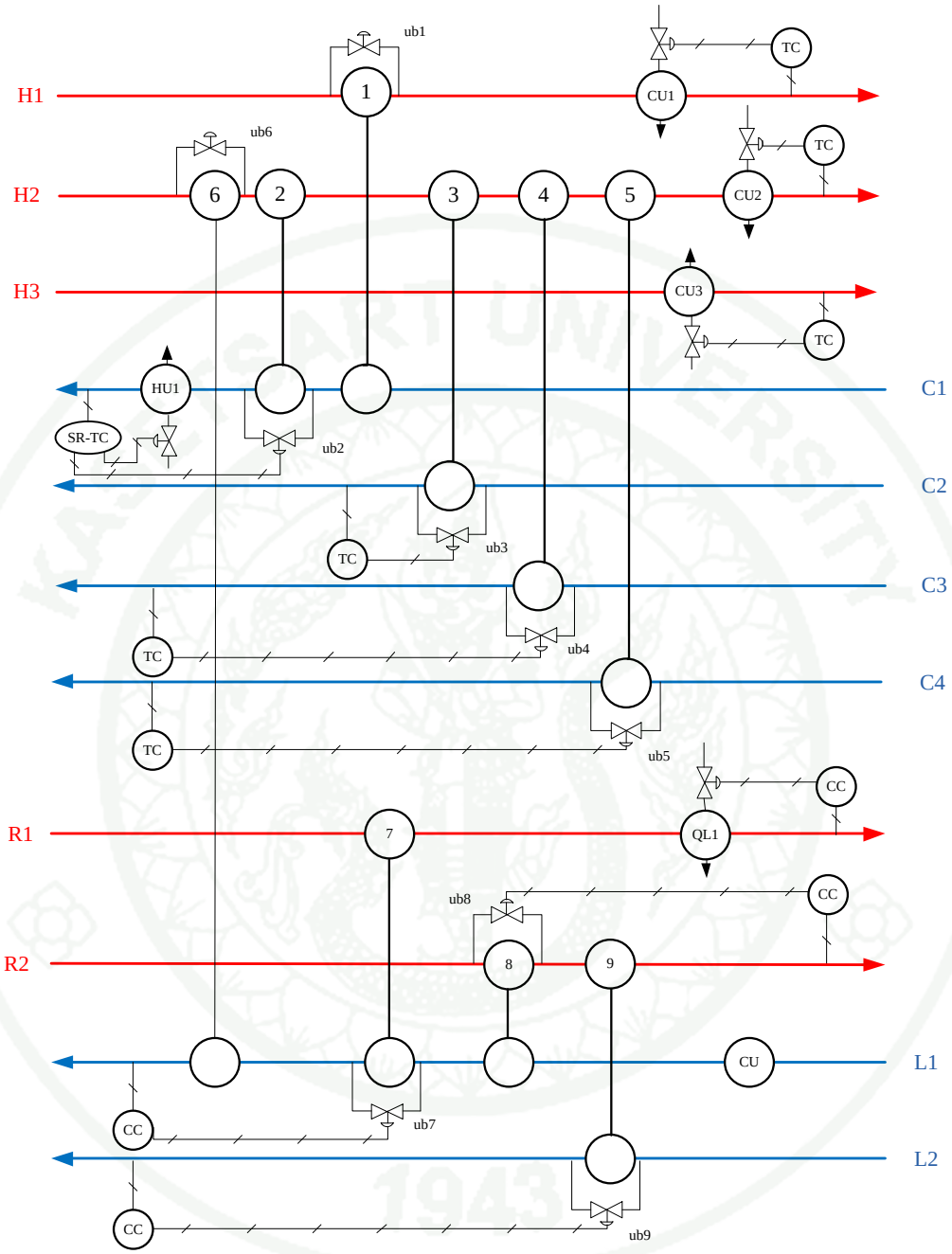

Figure 28 The control structure for the case study 5

Figure 28 shows the split-range signal of the pair of Q_{h1} and u_{b2} switch alternately to their lower constraints (SR-TC is split-range temperature control).

Table 44 Disturbances and active constraints for HENs in the CHAMENs with heat integration

Time	Disturbance of Temperature							Active constraint	
(hour)	ΔTH_1^{in}	ΔTH_2^{in}	ΔTH_3^{in}	ΔTC_1^{in}	ΔTC_2^{in}	ΔTC_3^{in}	ΔTC_4^{in}	Q_{h1}	u_{b2}
<5	0	0	0	0	0	0	0	S_L	U
5-15	+10	+10	+10	-5	-5	0	0	U	S_L
15-25	+10	-10	-10	+5	+5	0	0	U	S_L
25-35	0	0	0	0	0	0	0	S_L	U

U - Unsaturated manipulated variable (inactive constraint)

S_L - Saturated manipulated variable (active constraint) at the lower bound

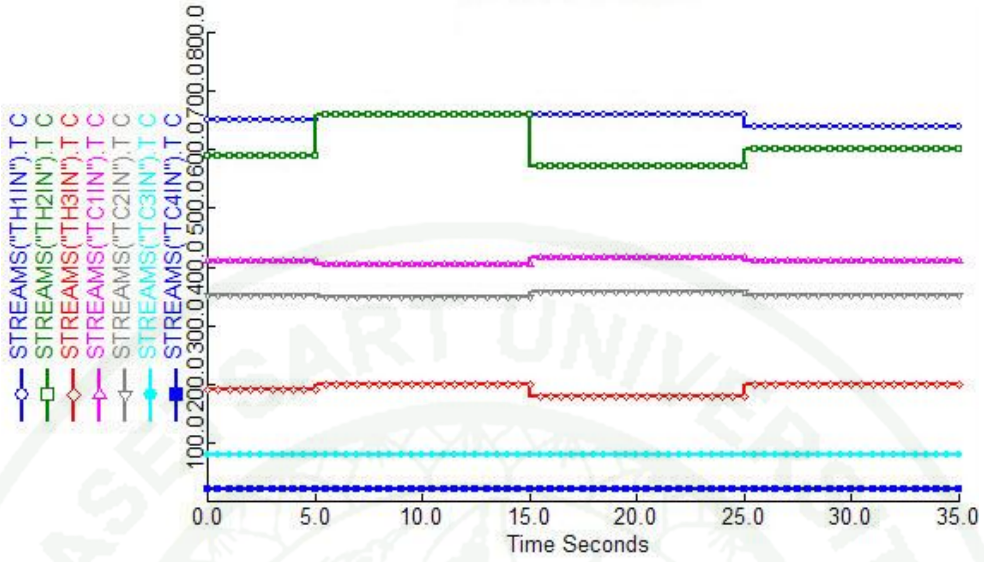

(a) Inlet temperatures

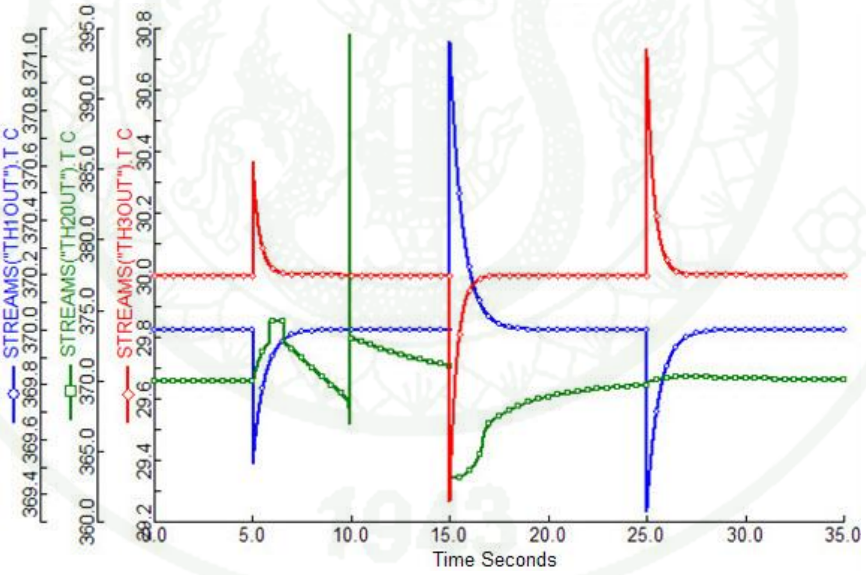

(b) Hot stream target temperatures

Figure 29 Dynamics simulation of the HENs in the CHAMENs with heat integration (a) Inlet temperatures, (b) Hot stream target temperatures, (c) Cold stream target temperatures and (d) Manipulated variables (Q_{h1} and u_{b2})

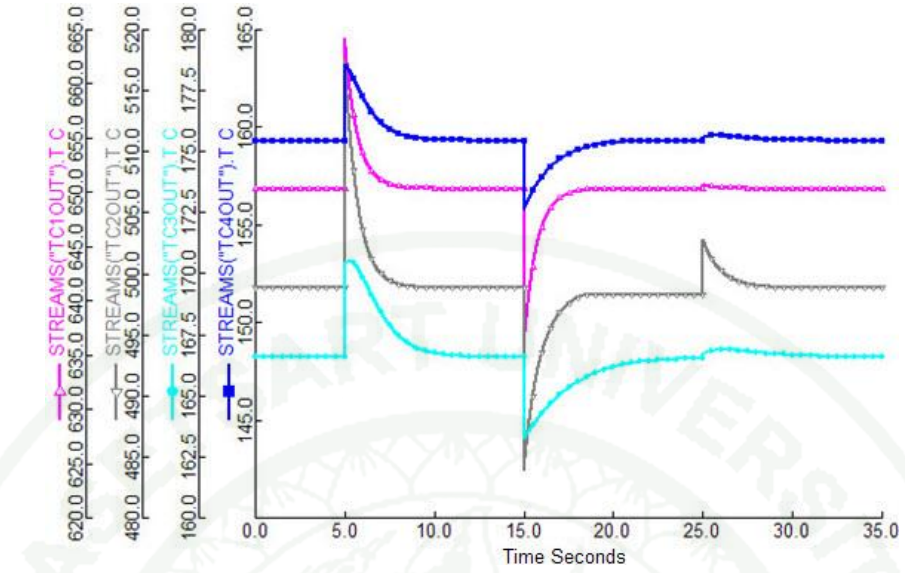

(c) Cold stream target temperatures

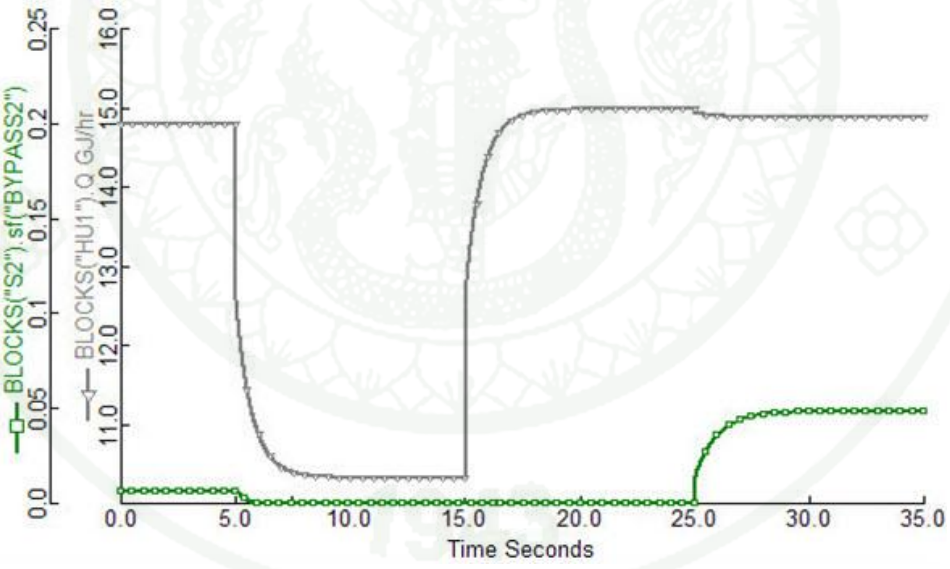

(d) Manipulated variables (Q_{h1} and u_{b2})

Figure 28 (Continued)

Table 45 Disturbances and active constraints for MENs in the CHAMENs with heat integration

Time (sec)	Disturbance of mass fraction			
	ΔR_1^{in}	ΔR_2^{in}	ΔL_1^{in}	ΔL_2^{in}
<5	0.07	0.051	0.0006	0.0002
5-15	0.09	0.061	0.0006	0.0002
15-25	0.05	0.041	0.0006	0.0002
25-35	0.07	0.051	0.0006	0.0002

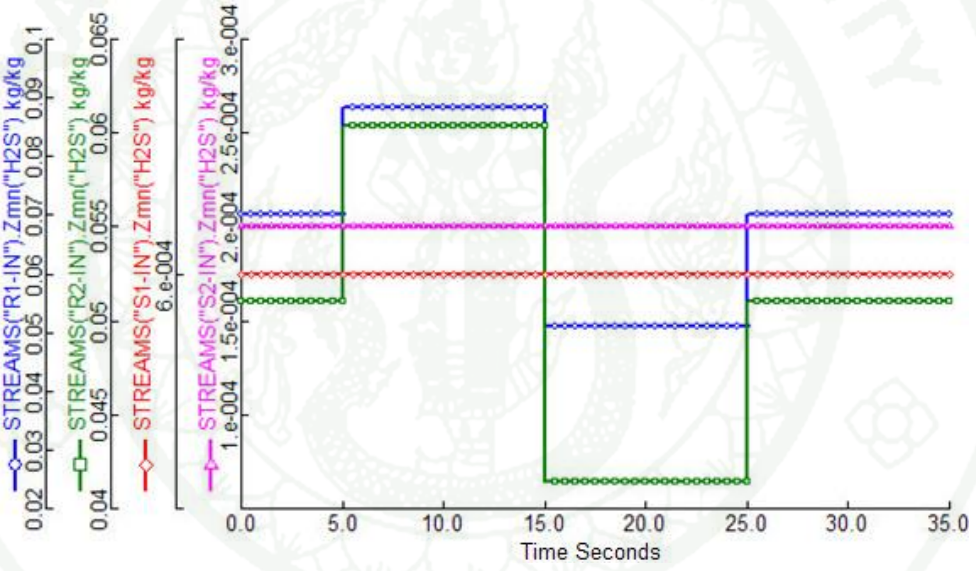

(a) Inlet mass fraction

Figure 30 Dynamics simulation of the MENs in the CHAMENs with heat Integration (a) Inlet mass fraction and (b) Rich stream target mass fraction

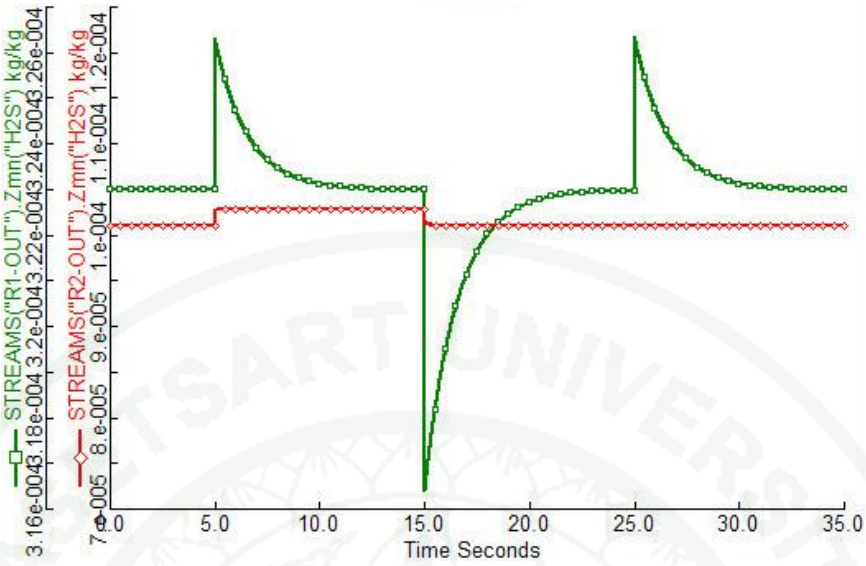

(b) Rich stream target mass fraction

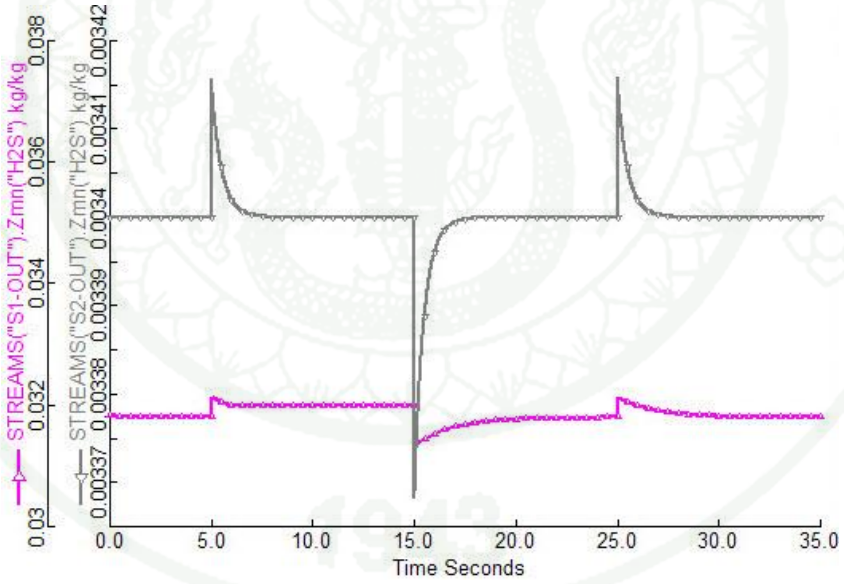

(c) Lean stream target mass fraction

Figure 29 (Continuted)

The results of control structures in HENs for this case are tested by performing dynamics simulation on Aspen Dynamics. The information regarding the disturbances and active constraints of the system in the case study is shown in Table 44. The dynamic results show that the control structures can provide optimality. Figure 29 shows the dynamic result of the HENs with the control structure. Figure 29b and 29c show the ability of the control structure to keep all target temperatures. Figure 29d shows the response of split-range control that Q_{h1} is primary manipulated variable and u_{b2} is secondary manipulated variable to keep temperature of TC_1^{out}. The results of control structures in MENs are tested that the information of the disturbances and active constraints of the MENs in this case study is shown in Table 45. The dynamic results indicate that the control structures can provide optimality. Figure 30 shows the dynamic result of the MENs with the control structure. Figure 30b and 30c show the controllability of the control structure to keep all target mass fraction.

CONCLUSION AND RECOMMENDATION

Conclusion

Most research uses individual mixed-integer nonlinear programming (MINLP) for generating the optimal configuration and nonlinear programming (NLP) for feasibility test. In this research, flexible heat exchanger networks (HENs), mass exchanger networks (MENs), and combined heat and mass exchanger networks (CHAMENs) MINLP synthesis combining with NLP feasibility test as a single optimization problem are presented. First, the optimal configuration is synthesized with a minimum total annual cost (TAC) and minimum slack variable. Then the optimal configuration is simulated in Aspen Plus to ensure the optimal target of the synthesized networks. After that, the active constraint regions can be formulated using parametric programming. Next, the optimal split-range control structure can be determined by integer linear program (ILP). Finally, the control structure is dynamically tested to ensure that the target can be controlled.

Five cases studies are proposed in this work. Case study 1 from Thunyawart (2010), heat integration system for 7 process streams, has the total annual costs of 262,225 $/year distributed among 9 units of heat exchangers. Two active constraint regions are found. There are two remaining degree of freedom for utility cost optimization and the design optimal split-range control structure are determined by ILP. Case study 2 information from El-Halwagi and Manousiouthakis (1989), sweetening of COG process, has the total annual costs of 2,911,101 $/year for 5 units of mass exchangers operating with 2 active constraint regions. There are one remaining degree of freedom for utility cost optimization, used ILP to determine an optimal split-range control structure. Case study 3 from Fieg *et al.* (2009), heat integration system for 15 process streams, has the total annual costs of 1,666,379 $/year distributed among the 22 units of heat exchangers. Two active constraint regions are found. There are two seven remaining degree of freedom for utility cost optimization and the design optimal split-range control structure are determined by

ILP. Case study 4 as sweetening of COG process with external utilities, it has the total annual costs at 2,631,193 $/year for 5 unit of mass exchangers operating and one hot utility and one cold utility with 2 active constraint regions. There are one remaining degree of freedom for utility cost optimization, used ILP to determine an optimal split-range control structure. Case study 5 as sweetening of COG process with simultaneous heat integration has the total annual cost of 2,700,670 $/year for 11 units of heat exchangers and 4 units of mass exchangers with 2 active constraint regions. If has three degree of freedom for HENs for utility cost optimization, used ILP to determine an optimal split-range control structure. The dynamic tests of all case studies show the control structures can keep the target. In addition, the comparison of the total annual cost is obtained in this work is lower than the result from literatures. So, we can conclude that this approach can solve the problem and decrease total annual cost as well.

Recommendations

1. In this work, we adjusted only inlet temperature of HENs, only inlet mass fraction of MENs but in practical we can have several ways to disturb the system of HENs and MENs such as the changing of flowrate.

2. Advance control would be of interest instead of only split-range control e.g. Predictive Control.

3. The GAMS software in this work cannot solve the large system problem, so, another algorithm should be used to solve e.g. Genetics Algorithm (GA).

LITERATURE CITED

Aaltola, J. 2003. **Simultaneous Synthesis of Flexible Heat Exchanger Network.** Ph.D Thesis, Helsinki University of Technology.

Aguilera, N. and J.L. Marchetti. 1998. Optimizing and controlling the operation of heat exchanger networks. **AIChE J.** 44: 1090-1104.

Acevedo, J., and E.N. Pistikopoulos. 1996. A parametric MINLP algorithm for process synthesis problems under uncertainty. **Ind. Eng. Chem. Res.** 35: 147–158.

Acevedo, J., and E.N. Pistikopoulos. 1997. A multi parametric programming approach for linear process engineering problems under uncertainty. **Ind. Eng. Chem. Res.** 36: 717–728.

Acevedo, J., and E.N. Pistikopoulos. 1999. An algorithm for multi parametric mixed integer linear programming problems. **Operation Research Letters** 24: 139-148.

Biegler, L.T., E.I. Grossman and A.W. Westerberg. 1997. **Systematic Methods of Chemical Process Design.** Prentice Hall, Upper Saddle River, New Jersey.

Chen, C.L., and P.S. Hung. 2004. Simultaneous synthesis of flexible heat exchange networks with uncertain source-stream temperatures and flow rates. **Ind. Eng. Chem. Res.** 43: 5916–5928.

Chen, C.L. and S.H. Ping. 2005, Simultaneous synthesis of mass exchange networks for waste minimization, **Comput. Chem. Eng.** 29: 1561-1576

Chen, C.L. and S.H. Ping. 2007. Synthesis of flexible heat exchange networks and mass exchange networks. **Comput. Chem. Eng.** 31: 1619-1632

El-Halwagi, M.M. 1997. **Pollution Prevention through Process Integration**, Alabama, Auburn University.

El-Halwagi, M.M. and V. Manousiouthakis. 1989. Synthesis of Mass Exchange Networks. **AIChE J.** 35: 1233.

El-Halwagi, M.M. and V. Manousiouthakis. 1990. Automatic Synthesis of Mass Exchange Networks with Single-Component Targets. **Chem. Engr. Sci.** 45: 2813.

Fieg, G., X. Luo and I.E. Grossmann. 1986. A monogenetic algorithm for optimal design of large-scale heat exchanger networks. **Chem. Eng. Process.** 48: 1506–1516.

Floudas, C.A. and I.E. Grossmann. 1986. Synthesis of flexible heat exchanger networks for multi-period operation. **Comput. Chem. Eng.** 10: 153–168.

Giovanini, L.L. and J.L. Marchetti. 2003. Low-level flexible-structure control applied to heat exchanger networks. **Comput. Chem. Eng.** 27: 1129-/1142.

Glemmestad, B. 1997. **Optimal Operation of Integrated Processes: Studies on Heat Recovery Systems**. PhD Thesis, Norwegian University of Science and Technology.

Glemmestad, B., S. Skogestad and T. Gundersen. 1999. Optimal operation of heat exchanger networks. **Comput. Chem. Eng.** 23: 509-522.

Kvasnica, M., P. Grieder and M. Baotic. 2004. **Multi-parametric toolbox (MPT).** Available Source: http://control.ee.ethz.ch/~mpt, 1 March 2007.

Lersbamrungsuk, V. 2008. **Development of Control Structure Design and Structural Controllability for Heat Exchanger Networks.** Ph.D Thesis, Kasetsart University.

Lersbamrungsuk, V., S. Skogestad and T. Srinophakun. 2006. A simple strategy for optimal operation of heat exchanger networks. In: **International Conference on Modeling in Chemical and Biological Engineering Sciences**, Bangkok, Thailand.

Lersbamrungsuk, V., T. Srinophakun, S. Skogestad and S. Narasimhan. 2008. Control structure design for optimal operation of heat exchanger networks. **AIChE J.** 54: 150-162.

Marselle, DF, M. Morari and D.F. Rudd. 1982. Design of resilient processing plants-II Design and control of energy management systems. **Chem. Engr. Sci.** 37: 259-270.

Mathisen, K.W. 1994. **Integrated Design and Control of Heat Exchanger Networks.** PhD Thesis, Norwegian University of Science and Technology.

Papalexandri, K.P. and E.N. Pistikopoulos. 1994. Synthesis and retrofit design of operable heat exchanger networks. 1. Flexibility and structural controllability aspects. **Ind. Eng. Chem. Res.** 33: 1718-1737.

Papalexandri, K.P. and E.N. Pistikopoulos. 1994. Synthesis and retrofit design of operable heat exchanger networks. 2. Dynamics and control structure considerations. **Ind. Eng. Chem. Res.** 33: 1738-1755.

Pistikopoulos, E.N., V. Dua, N.A. Bozinis, A. Bemporad and M. Morari. 2002. On-line optimization via off-line parametric optimization tools. **Comput. Chem. Eng.** 26:175-185.

Porsom, S. 2008. **Systematic Approach of Simulation and Control of Heat Exchanger Networks using Parametric Programming and Split-Range Control.** Master of Engineering Thesis, Chemical Engineering Program, Kasetsart University.

Saboo, A.K., and M. Morari. 1984. Design of Resilient Processing Plants–IV. Some New Results on Heat Exchanger Network Synthesis. **Chem. Eng. Sci.** 39: 579–592.

Saboo, A.K., M. Morari. and D.C. Woodcock. 1985. Design of resilient processing plants-VIII, a resilience index for heat exchanger networks. **Comput. Chem. Eng.** 40: 1553–1565.

Srinivas, B.K. and M.M. El-Halvagi. 1994. Synthesis of Combined Heat and Reactive Mass Exchange Networks. **Comp. Chem. Eng.** 49: 2059-2074.

Thunyawart, J. 2010. **Design of Control Structure for Combined Heat and Reactive Mass Exchanger Networks.** Master of Engineering Thesis, Chemical Engineering Program, Kasetsart University.

Turnprakiat, K. 2007. **Development of Simultaneous Heat and Mass Exchanger Networks Module for ASPEN PLUS.** Master of Engineering Thesis, Chemical Engineering Program, King Mongkut's University of Technology Thonburi.

Yee, T.F. and I.E. Grossman. 1990. Simultaneous optimization models for heat integration – II. Heat exchanger network synthesis. **Comput. Chem. Eng.** 14: 1165-1184.

Zamora, J. M., and I.E. Grossmann. 1998. A global MINLP optimization algorithm for the synthesis of heat exchanger networks with no stream splits. **Comput. Chem. Eng.** 22: 367–384.

APPENDIX

Case study 1: Heat integration system for 7 process streams

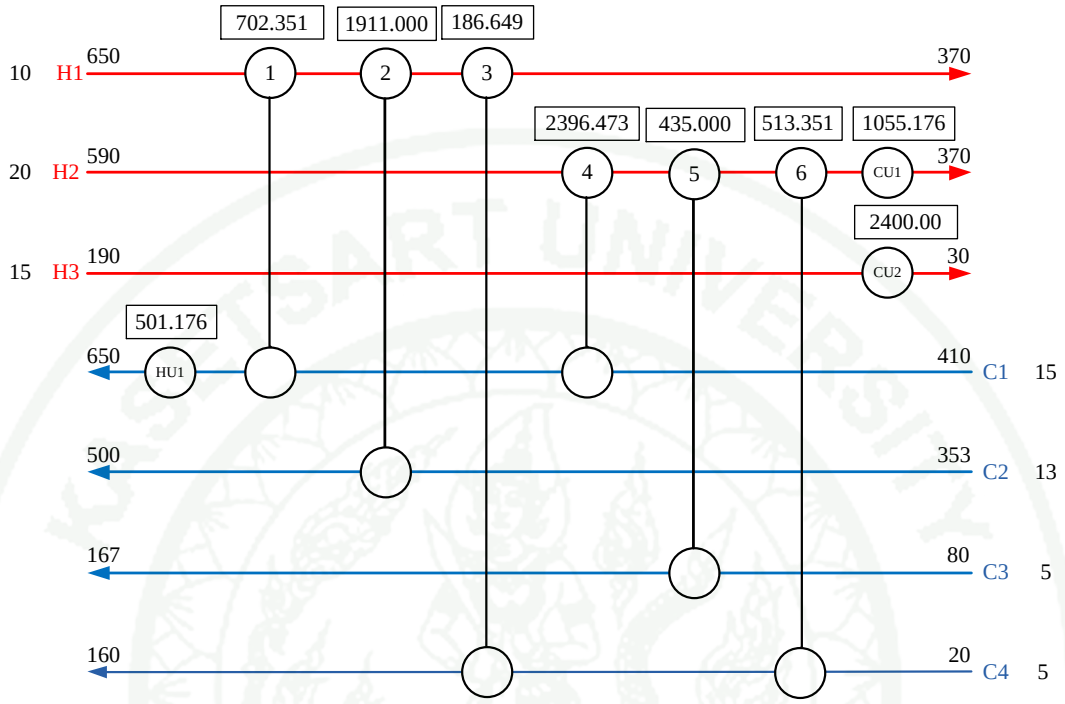

Appendix Figure 1 Heat exchanger networks for case study 1 under normal condition

Case study 2: Sweetening of COG process

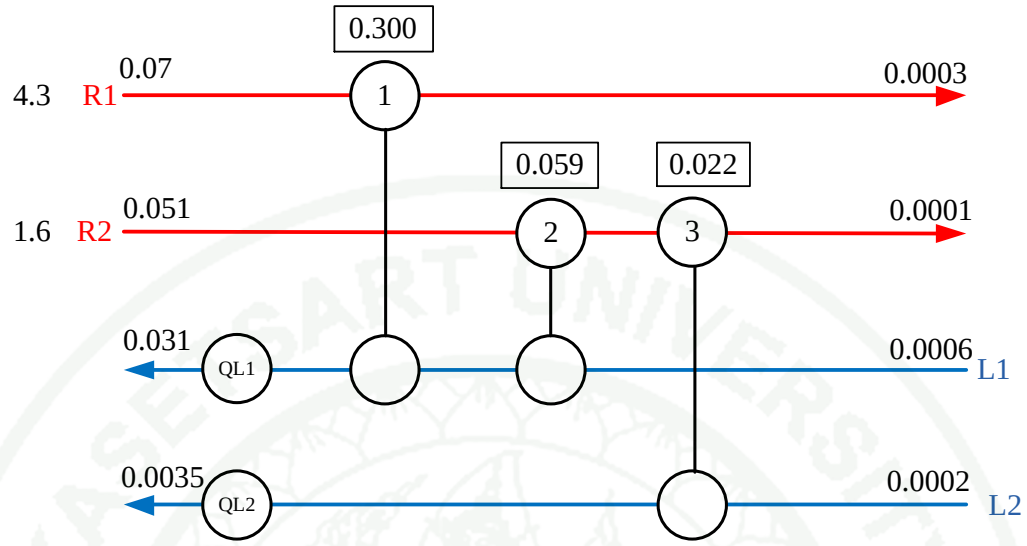

Appendix Figure 2 Mass exchanger networks for case study 2 under normal condition

Case study 3: Heat integration system for 15 process streams

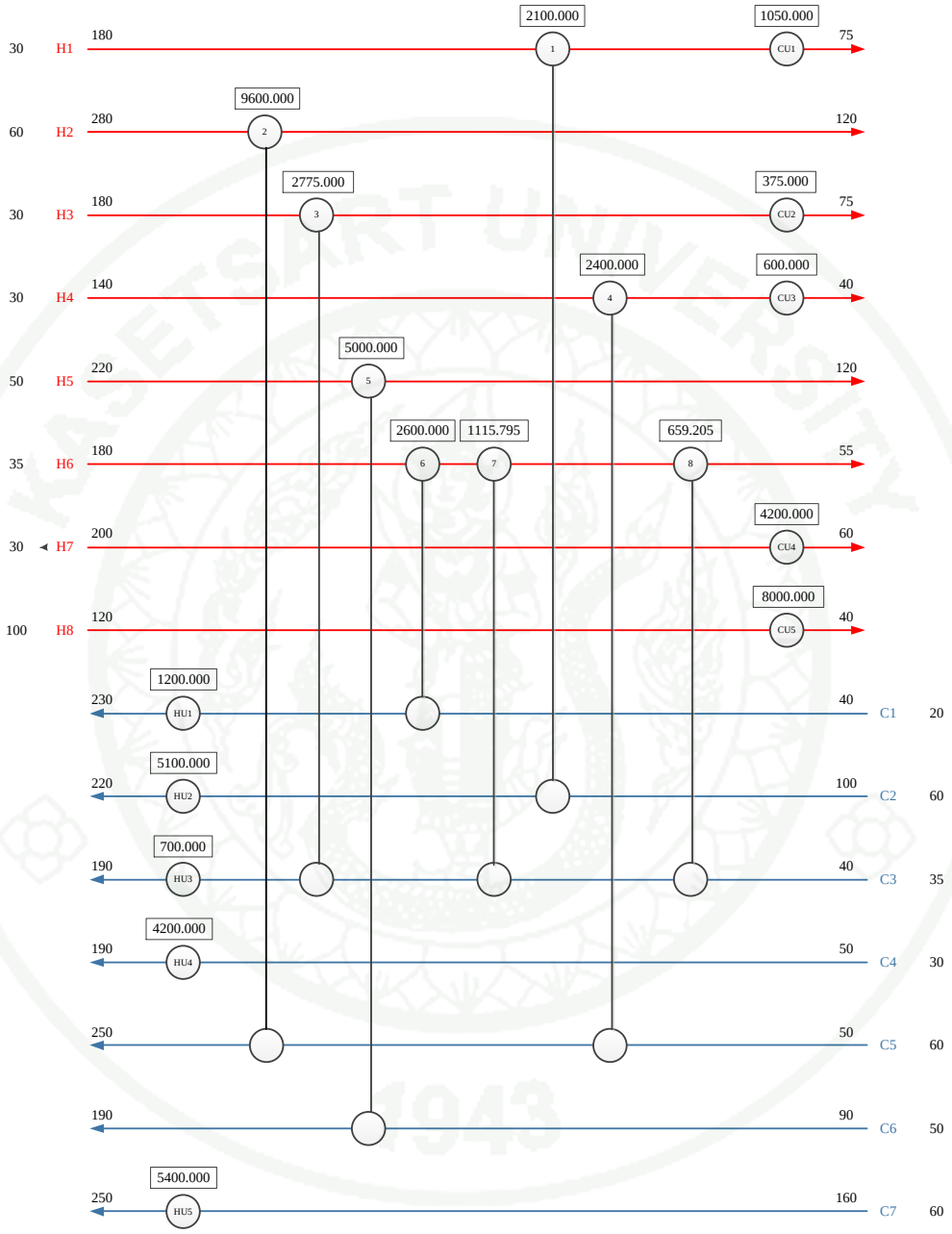

Appendix Figure 3 Large scale heat exchanger networks for case study 3 under normal condition

Case study 4: Sweetening of COG process with external utilities

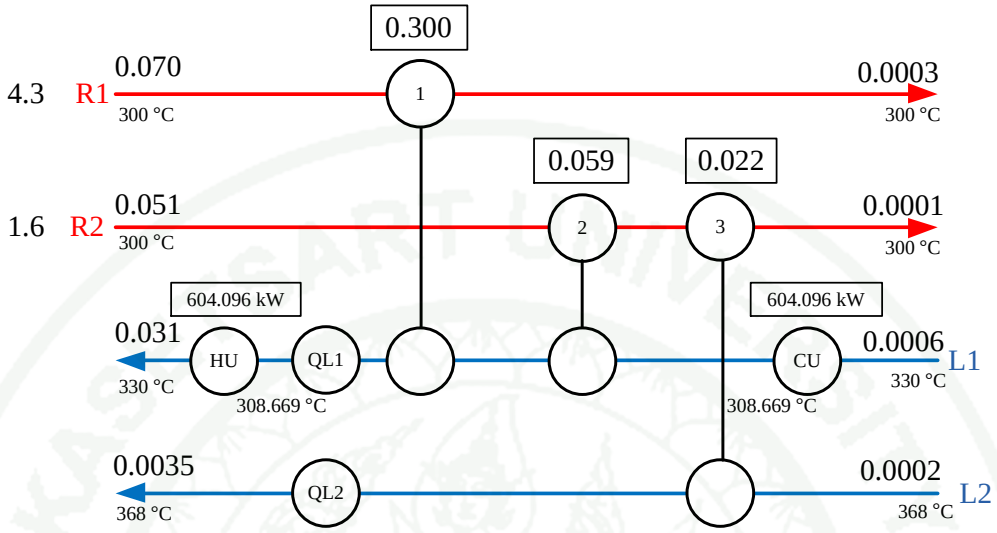

Appendix Figure 4 Combined heat and mass exchanger networks with external utilities under normal condition

Case study 5: Sweetening of COG process with simultaneous heat integration

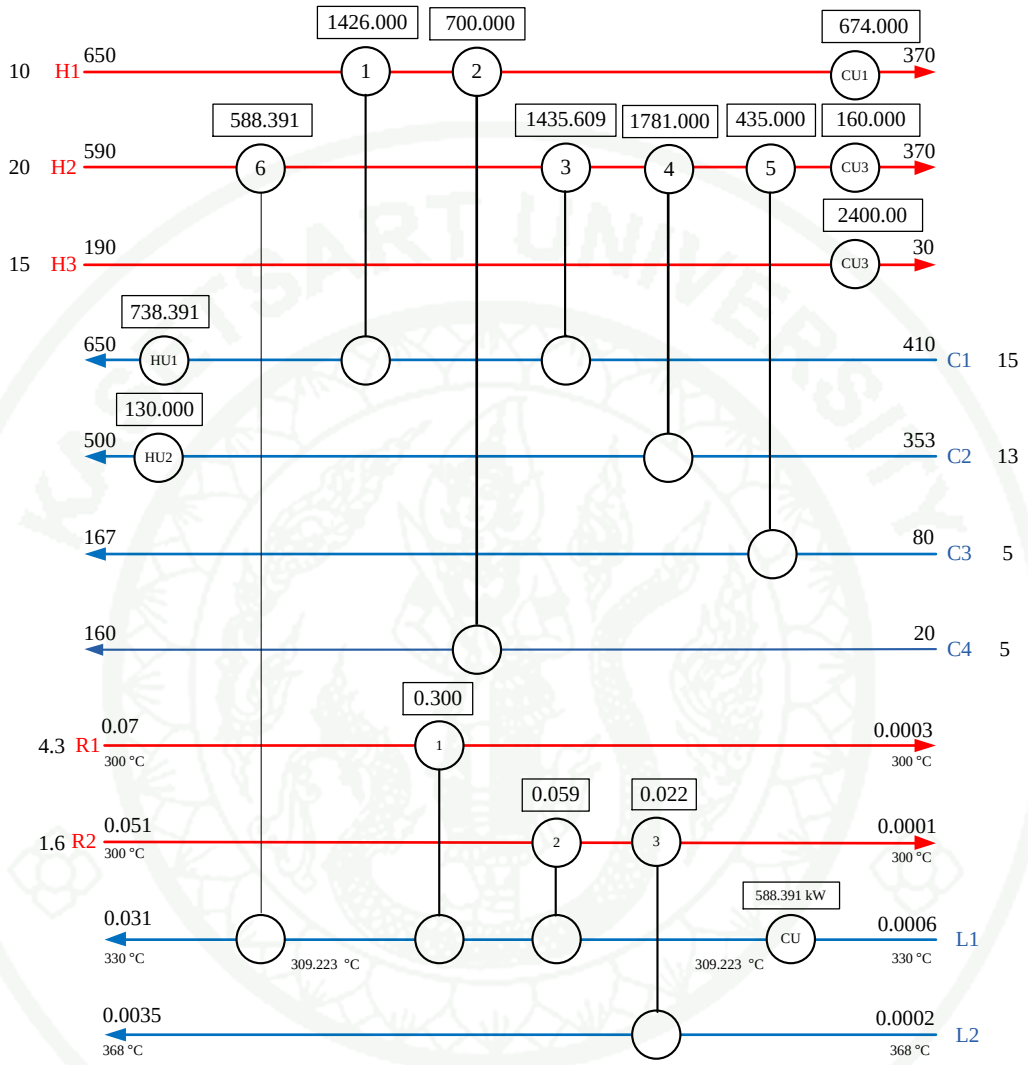

Appendix Figure 5 Combined heat and mass exchanger networks with simultaneous heat integration under normal condition

CIRRICULUM VITAE

NAME : Miss Kanokkan Boontom

BIRTH DATE : June 13, 1986

BIRTH PLACE : Ratchaburi, Thailand

EDUCATION :

YEAR	**INSTITUTE**	**DEGREE**
2009	King Mongkut's University of Technology North Bangkok	B.Eng (Chem Eng)